Available online at www.sciencedirect.com
ScienceDirect
Icarus 196 (2008) 318–358
ICARUS
www.elsevier.com/locate/icarus

North polar region of Mars: Advances in stratigraphy, structure, and erosional modification

Kenneth L. Tanaka [a,*], J. Alexis P. Rodriguez [b], James A. Skinner Jr. [a], Mary C. Bourke [b], Corey M. Fortezzo [a,c], Kenneth E. Herkenhoff [a], Eric J. Kolb [d], Chris H. Okubo [e]

[a] *US Geological Survey, Flagstaff, AZ 86001, USA*
[b] *Planetary Science Institute, Tucson, AZ 85719, USA*
[c] *Northern Arizona University, Flagstaff, AZ 86011, USA*
[d] *Google, Inc., Mountain View, CA 94043, USA*
[e] *Lunar and Planetary Laboratory, University of Arizona, Tucson, AZ 85721, USA*

Received 5 June 2007; revised 24 January 2008

Available online 29 February 2008

Abstract

We have remapped the geology of the north polar plateau on Mars, Planum Boreum, and the surrounding plains of Vastitas Borealis using altimetry and image data along with thematic maps resulting from observations made by the Mars Global Surveyor, Mars Odyssey, Mars Express, and Mars Reconnaissance Orbiter spacecraft. New and revised geographic and geologic terminologies assist with effectively discussing the various features of this region. We identify 7 geologic units making up Planum Boreum and at least 3 for the circumpolar plains, which collectively span the entire Amazonian Period. The Planum Boreum units resolve at least 6 distinct depositional and 5 erosional episodes. The first major stage of activity includes the Early Amazonian (~3 to 1 Ga) deposition (and subsequent erosion) of the thick (locally exceeding 1000 m) and evenly-layered Rupes Tenuis unit (ABrt), which ultimately formed approximately half of the base of Planum Boreum. As previously suggested, this unit may be sourced by materials derived from the nearby Scandia region, and we interpret that it may correlate with the deposits that regionally underlie pedestal craters in the surrounding lowland plains. The second major episode of activity during the Middle to Late Amazonian (~ <1 Ga) began with a section of dark, sand-rich and light-toned ice-rich irregularly-bedded sequences (Planum Boreum cavi unit, ABb_c) along with deposition of evenly-bedded light-toned ice- and moderate-toned dust-rich layers (Planum Boreum 1 unit, ABb_1). These units have transgressive and gradational stratigraphic relationships. Materials in Olympia Planum underlying the dunes of Olympia Undae are interpreted to consist mostly of the Planum Boreum cavi unit (ABb_c). Planum Boreum materials were then deeply eroded to form spiral troughs, Chasma Boreale, and marginal scarps that define the major aspects of the polar plateau's current regional topography. Locally- to regionally-extensive (though vertically minor) episodes of deposition of evenly-bedded, light- and dark-toned layered materials and subsequent erosion of these materials persisted throughout the Late Amazonian. Sand saltation, including dune migration, is likely to account for much of the erosion of Planum Boreum, particularly at its margin, alluding to the lengthy sedimentological history of the circum-polar dune fields. Such erosion has been controlled largely by topographic effects on wind patterns and the variable resistance to erosion of materials (fresh and altered) and physiographic features. Some present-day dune fields may be hundreds of kilometers removed from possible sources along the margins of Planum Boreum, and dark materials, comprised of sand sheets, extend even farther downwind. These deposits also attest to the lengthy period of erosion following emplacement of the Planum Boreum 1 unit. We find no evidence for extensive glacial flow, topographic relaxation, or basal melting of Planum Boreum materials. However, minor development of normal faults and wrinkle ridges may suggest differential compaction of materials across buried scarps. Timing relations are poorly-defined mostly because resurfacing and other uncertainties prohibit precise determinations of surface impact crater densities. The majority of the stratigraphic record may predate the recent (<20 Ma) part of the orbitally-driven climate record that can be reliably calculated. Given the strong stratigraphic but loose temporal constraints of the north polar geologic record, a comparison of north and south polar stratigraphy permits a speculative scenario in which major Amazonian depositional and erosional episodes driven by global climate activity is plausible.

* Corresponding author. Fax: +1 928 556 7014.
E-mail address: ktanaka@usgs.gov (K.L. Tanaka).

0019-1035/$ – see front matter
doi:10.1016/j.icarus.2008.01.021

Keywords: Mars; Mars, surfaces; Mars, polar caps; Mars, polar geology; Mars, climate

1. Introduction

The north polar plateau, Planum Boreum, and adjacent plains form one of the most geologically intricate and diverse terrains of Mars (Cutts, 1973; Cutts et al., 1976, 1979; Blasius et al., 1982; Howard et al., 1982; Thomas et al., 1992; Fishbaugh and Head, 2000, 2001, 2005; Kolb and Tanaka, 2001; Tanaka, 2005). The stratigraphy of relatively recent layered materials resembles that of ice cores on Earth, which can be used to effectively infer paleoclimate conditions and events (e.g., Carr, 1982; Laskar et al., 2002; Milkovich and Head, 2005). Although many interpretations have been put forth regarding the nature, origin, modification, and climatic implications of martian north polar deposits, many fundamental issues remain unresolved (see Fishbaugh et al., 2008). Some key unanswered questions regarding the geologic history of these materials include: When were north polar materials deposited and by what processes? What are their source materials? What are their compositions and physical characteristics? How and when were the polar deposits deformed and eroded?

A wealth of new spacecraft observations provides data that can address these questions in a more comprehensive fashion than before. Our aim in this manuscript is to reconcile new observations with existing and new hypotheses to converge on what we consider to be a tenable geologic history for the north polar region of Mars. Geologic mapping of the north polar region enables us to integrate various available datasets in order to interpret the more significant aspects of stratigraphy and thereby reconstruct the regional geologic history. These aspects include unit composition and character, unconformities, depositional environments, and deformational and erosional episodes. The pervading geologic context, including relationships with other morphologically, compositionally, spatially, and/or stratigraphically associated units and features, is relied upon heavily in order to produce what we consider to be the most likely interpretive scenario(s). Our observations and interpretations demonstrate a much greater complexity in the stratigraphy and geologic history of Planum Boreum than previously understood.

Major components of the paper include: (1) overview of the increasingly diverse geologic and geographic terminology applied to Planum Boreum region features; (2) the geologic record of Early Amazonian materials (formed between approximately 2 to 3 billion years ago; Hartmann, 2005), which include some of the lower parts of Planum Boreum (commonly referred to as the north polar "basal" unit) and their immediately subjacent plains materials; (3) the composition and detailed stratigraphy of Middle to Late Amazonian polar layered deposits, which also include basal materials (from ∼1 billion years ago until the present); (4) the deformational and especially erosional processes and episodes that led to the modification of north polar deposits; and (5) how these processes and episodes may generally correlate to those of the south polar deposits.

2. Datasets and visualization methods

Post-Viking Orbiter orbiting missions to Mars include Mars Global Surveyor (MGS), Mars Odyssey (ODY), Mars Express (MEX), and Mars Reconnaissance Orbiter (MRO). The near-polar orbits of these spacecraft have yielded the largest concentration of data acquisition at the poles. Topography data acquired by the MGS-borne Mars Orbiter Laser Altimeter (MOLA) instrument yielded the most complete and accurate regional- to global-scale characterization of Mars' complex surface morphology to date (e.g., Smith et al., 2001). MGS in particular resulted in a densely-spaced collection of nadir-view MOLA spot observations between 78° and 87° N latitude. These data were used to produce a 115 m/pixel digital elevation model (DEM), which we use widely in our descriptions and analyses of north polar geology. MOLA tracks become more widely-spaced toward the equator, resulting in progressively lower resolution regional DEMs (231 m/pixel for 68° to 78° N latitude; 463 m/pixel for <68° N latitude). Off-nadir MOLA tracks of lower precision were acquired for >87° N resulting in DEMs of reduced topographic detail. We attempt to observe the geology of Planum Boreum and surrounding terrains by using (where possible) the full extent of available morphology- and composition-based data, including (1) MGS Mars Orbiter Camera (MOC) narrow-angle images (mostly >3 m/pixel), (2) ODY Thermal Emission Imaging System (THEMIS) visual (VIS) images (18–36 m/pixel), (3) MEX High Resolution Stereo Camera (HRSC) images (mostly >20 m/pixel), (4) MRO Context Camera (CTX) images (6 m/pixel; we were only able to process and use those images <∼1 GB in size at the time of this writing), and (5) MRO High Resolution Imaging Science Experiment (HiRISE) images (25 cm/pixel). We also incorporated into our geologic and stratigraphic assessments instrument-derived thematic maps, including water-ice maps produced from spectral data by the teams for the MEX-borne Observatoire pour la Minéralogie, l'Eau, les Glaces, et l'Activité (OMEGA) (Langevin et al., 2005; Rodriguez et al., 2007b) and the MRO-borne Compact Reconnaissance Imaging Spectrometer for Mars (CRISM) (Seelos et al., 2007) and color maps that relate to compositions of surface materials using Mars Color Imager (MARCI) data (Malin et al., 2007). THEMIS infrared (IR) images were also viewed but were not of significant help to our mapping assessments due to their comparatively modest resolution (100 m/pixel) and to the degree of atmospheric haze that commonly reduced their effectiveness in resolving local-scale surface albedo and morphology.

In our descriptions and discussions of north polar materials and features, we comment on landforms, units, and stratigraphic relationships observed in broad spatial ranges. In most cases we simply state the dimensions of the features observed, except when we refer to specific datasets that are particularly revealing. Features hundreds of meters across and

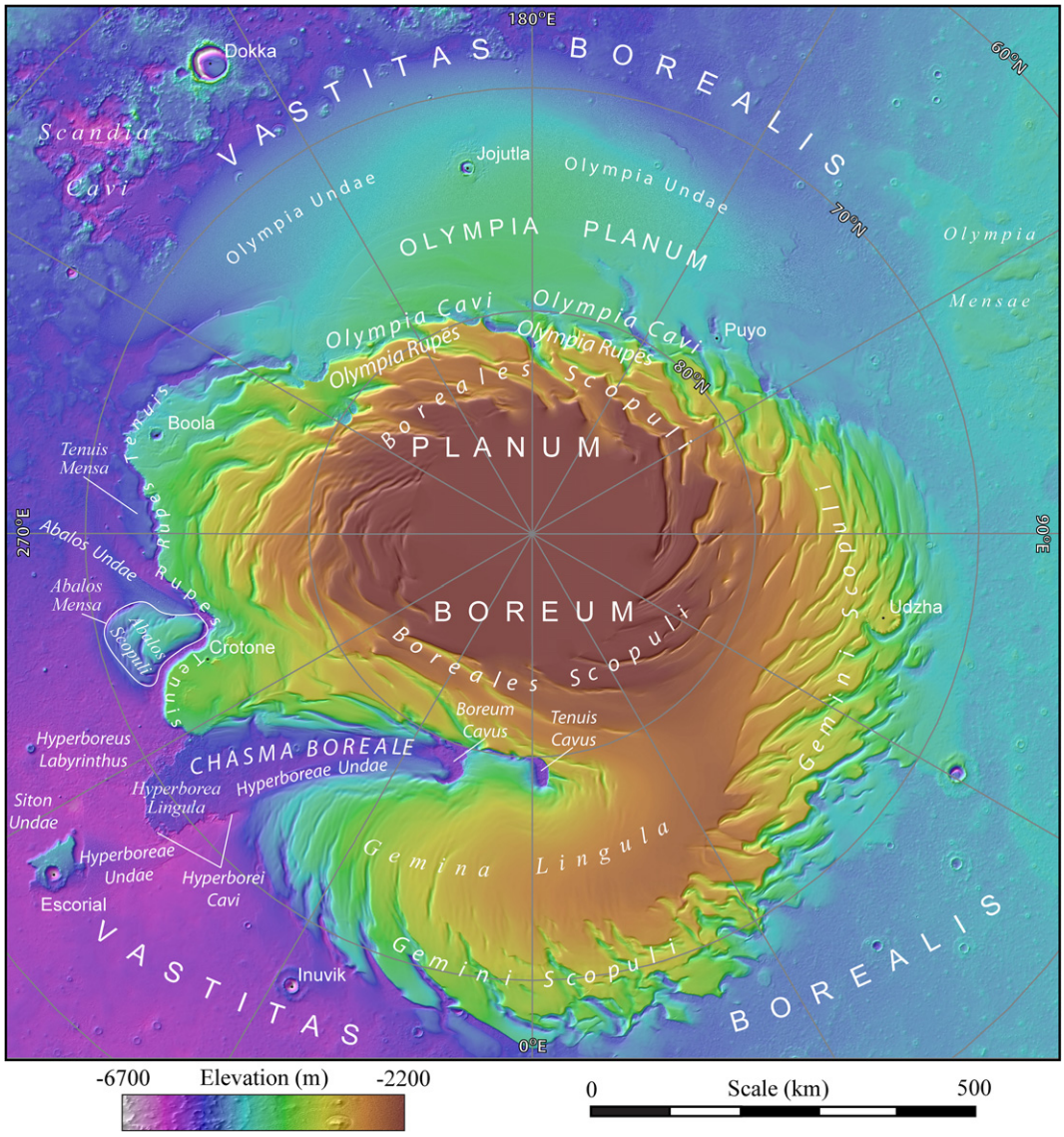

Fig. 1. Regional topography of Planum Boreum, Mars and surrounding lowland plains. Major physiographic features are from the Gazetteer of Planetary Nomenclature and are discussed in the text (see http://planetarynames.wr.usgs.gov). (Image derived from the MOLA DEM (~115 m/pixel) overlain on a topographic hillshade; polar stereographic projection centered at the north pole.)

larger are generally observed in MOLA, THEMIS VIS and IR, HRSC, OMEGA, and/or CRISM datasets, whereas features from sub-kilometer- to decimeter-scales are observed in MOC narrow angle, CTX, and/or HiRISE datasets. In addition to using figures, we commonly provide references and image numbers that document the many observations that we discuss.

Effectively organizing, viewing, and manipulating the sheer volume of these datasets for synoptic observations and mapping (which routinely includes detailed, high-resolution analysis of key locations) is becoming an increasingly complicated data management effort. Our approach, where possible, has been to import the image and topographic datasets as geo-registered raster data into a Geographic Information Systems (GIS), such that multiple datasets can be viewed and used for geologic mapping and analysis within a defined spatial context.

3. Physiography and nomenclature

Formal geographic nomenclature is a critical aspect of planetary research that helps to ensure that key landforms and their spatial relationships are consistently referenced; it has been a continually-developed resource for more than a century (e.g., Schiaparelli, 1879; International Astronomical Union, 1960). MOLA topography and high-resolution image data have facilitated the recent creation of new formal geographic features and/or improvements for existing names and definitions in the north polar region (Fig. 1; see also the Gazetteer of Planetary Nomenclature at http://planetarynames.wr.usgs.gov). In this section, we describe the physiography using the officially-approved geographic nomenclature and avoid informal names cited in the literature if not needed.

The north polar region lies within the northern lowlands of Mars, which include individually-named plains that are gener-

ally adjacent to and north of the highland-lowland boundary scarp (Tanaka and Scott, 1987; Tanaka et al., 2005). Progressing northward, these plains coalesce to form the dominant geographic feature of the northern plains, Vastitas Borealis (Fig. 1). Three regional topographic basins comprise the bulk of Vastitas Borealis. Broad topographic basins are not currently given formal names; the largest of the lowland basins is irregular in shape, contains the north polar region, and is informally referred to as either the "north polar basin" (Head et al., 1999, 2002) or "Borealis basin" (Tanaka et al., 2003, 2005). The surface of Vastitas Borealis displays hummocky textures at subkilometer scales (Kreslavsky and Head, 2000) and crater forms of likely impact origin characterized by crater rims and/or ejecta that are elevated above the surrounding terrain and commonly referred to as "pedestal craters" (e.g., Mouginis-Mark, 1979).

Planum Boreum is defined as the ~1000 km diameter subcircular, north polar plateau that occupies the center of Borealis basin. The planum is not centered on the geographic north pole but is offset along the prime meridian where its margins extend south of 79° N. The opposite side of Planum Boreum is defined by an arcuate set of scarps, Olympia Rupēs (Rupēs is the Latin plural of Rupes) at ~85° N that spans ~120° of longitude. The highest part of Planum Boreum is near the geographic north pole, where the surface elevation is ~−2570 m. The topographic margin of the north polar plateau ranges across ~700 m of elevation, from −5200 m (between 300° and 315° E) to −4500 m (between 60° and 110° E). Using the Vastitas Borealis surface as a proxy for the base of Planum Boreum, the north polar plateau consists of >2500 m thickness of geologic materials.

A variety of features dominate the surface of Vastitas Borealis immediately adjacent to Planum Boreum. Scandia Cavi form irregularly-shaped depressions in the northernmost part of the Scandia region. Between the Scandia region and Planum Boreum, Olympia Planum (formerly "Olympia Planitia" as in Tanaka and Scott, 1987) gently slopes upward from the hummocky plains of Vastitas Borealis and ends against the higher-standing north polar plateau along the Olympia Rupēs scarp system. The bulk of lower Olympia Planum is buried by the broad sand sea of Olympia Undae, which extend into Vastitas Borealis, beyond the eastern and western margins of Olympia Planum, and grade into isolated patches of sand seas (undae) that bury portions of the lowland plains (e.g., Hyperborea, Siton, and Abalos Undae). West of Olympia Planum, low elevation (mostly <200 m high), irregularly-shaped plateaus of Olympia Mensae rise from the plains and extend 180 km north-to-south and 400 km east-to-west. East of Olympia Planum and the Scandia region, Abalos Colles include five prominent, flat-topped or cratered mounds <700 m high and <17 km in diameter (Fig. 2). Escorial crater forms the top of an irregularly-shaped plateau located due south of Chasma Boreale that rises 500–700 m above the surrounding lowland plain and in the lowest part of Borealis basin.

The surface of Planum Boreum has a complex physiographic character. Chasma Boreale forms a 450-km-long, broad canyon that divides part of Planum Boreum into a peninsular lobe from 310° to 10° E, named Gemina Lingula (Fig. 1). This feature is characterized by gently-sloping, arcuate undulations that are tens of meters deep and roughly parallel the trend of nearby spiral troughs, which dominate Planum Boreum. The troughs are generally between 10 and 300 km long, <20 km wide and commonly reach hundreds of meters in depth. The troughs immediately encircling the north pole are named Boreales Scopuli, whereas those that incise Gemina Lingula and the margin of Planum Boreum east of the lingula (to 110° E) are named Gemini Scopuli. Udzha crater is a partly-buried, 45-km-diameter impact crater that is centered at 81.8° N, 77.2° E in eastern Gemini Scopuli.

On the margins of Planum Boreum, the scopuli form overlapping networks of troughs, scarps, and depressions. Olympia Rupēs are marked by a succession of these depressions, locally named Olympia Cavi. These cavi are generally asymmetric in north–south profile, with steeper relief observed on south-facing sides. At their eastern margin, Olympia Cavi gradually deepen, lengthen, and coalesce to form Rupes Tenuis, a slab-like topographic bench and scarp a few hundred meters to a thousand meters high that defines the outer margin of Planum Boreum between 250° and 300° E. Adjacent to and south of Rupes Tenuis is Abalos Mensa, a convex plateau ~180 km across and wedge-shaped in plan view. Abalos Undae comprise the dune field that extends southwestward from the western termination of a narrow trough between Rupes Tenuis and Abalos Mensa. West of Abalos Undae and below and parallel to Rupes Tenuis is an elongate, low-elevation, southward-sloping plateau known as Tenuis Mensa. There are two named impact craters located within this region of Planum Boreum. Boola crater (17 km in diameter and centered at 81.1° N, 254.2° E) occurs near the western termination of Rupes Tenuis. Crotone crater (6.4 km in diameter and centered at 82.2° N, 290.0° E) is along the narrow trough that separates Rupes Tenuis from Abalos Mensa.

Chasma Boreale is a major topographic feature that separates Gemina Lingula from the rest of Planum Boreum proper. The chasma itself has a complex geographic character. On its northeastern end, Chasma Boreale consists of two arcuate depressions named Boreum and Tenuis Cavi, which each have steeply-sloping, high-standing northern and eastern (southwest-facing) walls. Beyond these depressions, the floor of Chasma Boreale transitions into a low plateau named Hyperborea Lingula that rises between 200 and 350 m above Vastitas Borealis. The lingula extends ~100 km beyond the margin of Planum Boreum. Hyperboreae Undae is a dune field that stretches southwest of Boreum Cavus across Chasma Boreale and into Vastitas Borealis. The eastern part of Hyperborea Lingula is cut by several elongate depressions called Hyperborei Cavi. Topographically-pronounced polygonal troughs below the southwest margin of Hyperborea Lingula form Hyperboreus Labyrinthus.

The polar caps of Mars were first observed as bright-albedo features over 300 years ago, and seasonal changes were noted soon thereafter (Kieffer et al., 1992). Early observers recognized that the polar caps do not completely disappear in the summer, leading to the term "residual" cap (Martin et al., 1992). Similarly, the polar caps that wax and wane annually have been

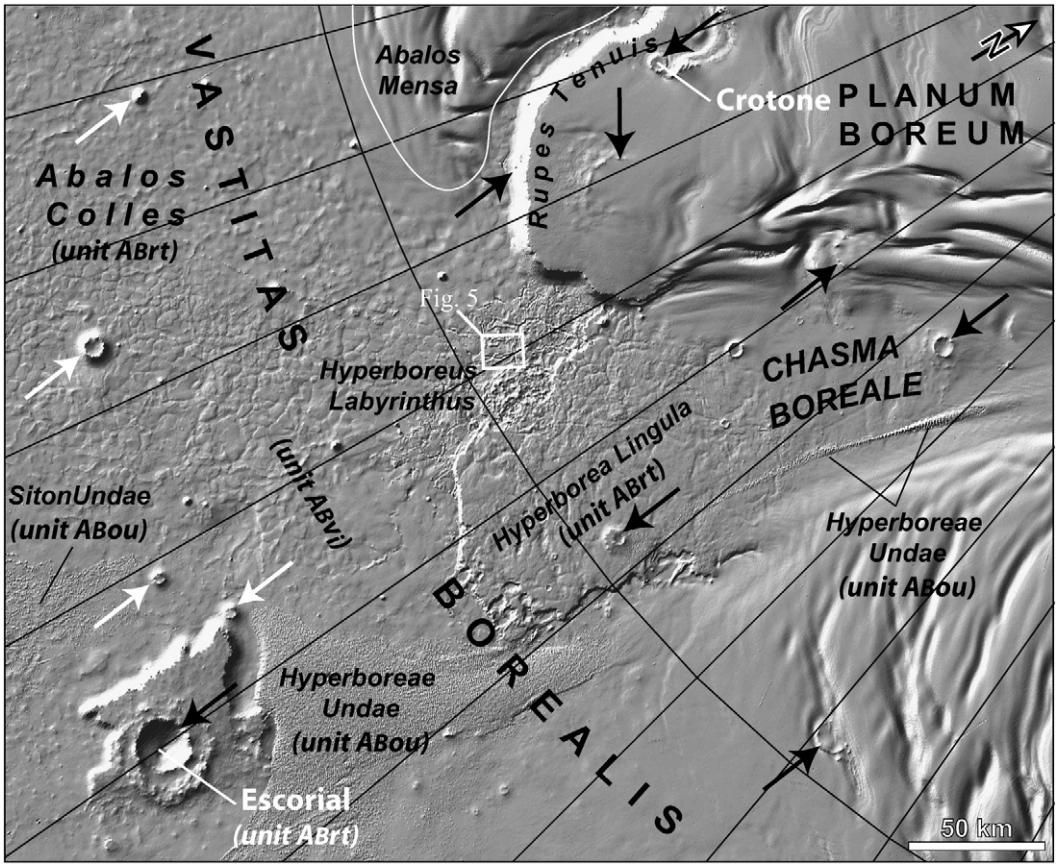

Fig. 2. Local topography of Hyperborea Lingula region, located at the southern termination of Chasma Boreale, Planum Boreum, Mars. Major physiographic features and some map units are denoted (Vastitas Borealis interior unit, ABv$_i$; Rupes Tenuis unit, ABrt; Olympia Undae unit, ABou). Note muted topographic expression of impact craters that superpose (or reside within) unit ABrt. Pedestal-type craters are denoted by black arrows whereas sharp-rimmed cones (interpreted to be eroded craters) are denoted by white arrows. [Image derived from the MOLA hillshade (~115 m/pixel); artificial illumination from the upper left; polar stereographic projection centered at approximately 80.3° N, 302.5° E with 5° longitudinal grid spacing; north toward upper right.]

called the "seasonal" caps. This nomenclature, based on the higher reflectance of the caps, has survived into the modern era of spacecraft observations, when it became clear that seasonal caps are composed of CO_2. Though the simple "cap" terminology defined above is relevant and useful today, the nomenclature used to describe geologic and topographic features in Mars' polar regions varies significantly in the literature. For example, the term "cap" has been used (1) to uniquely refer to *only* the frost and ice that covers the polar regions seasonally and (2) to describe the regional-scale topographic domes that reside at each pole. Within this document, we refer to the north polar topographic dome or plateau as "Planum Boreum" rather than the "north polar cap" to avoid ambiguity and to be consistent with previously-published geologic maps of the polar regions, as suggested by Herkenhoff et al. (2006). As such, the "polar cap" herein refers to the "seasonal cap" or "residual ice cap" that blankets the north polar region during the martian winter.

4. Stratigraphy

The morphology and morphometry of surfaces and features of the north polar region of Mars have been and continue to be used to define and discriminate rock/ice-stratigraphic units at multiple scales in maps (Fig. 3; e.g., Tanaka and Kolb, 2001; Tanaka, 2005; Tanaka et al., 2005; Skinner et al., 2006) as well as other stratigraphic and topical studies (e.g., Fishbaugh and Head, 2005; Milkovich and Head, 2005, 2006). In geologic mapping, the materials are divided into map units that may be grouped based on sets of explicitly-defined and -adhered-to spatial, morphologic, chronologic, and/or genetic relations. The level of detail provided by such mapping is dependent on the resolution of the data, the unit characteristics that the data can resolve, and the scale and objectives of the mapping. Given the regional scope of this study, we describe units of more or less regional significance. In so doing, we may group outcrops that more detailed mapping might have basis to identify as separate, locally-unique units. As a result, to compensate for this observation-scale dependency, our geologic descriptions include the observed range in character of the units. We also attempt to discriminate primary aspects of the units that are related to the origin of the unit from secondary features such as deformational structures, erosional landforms, and surficial deposits that modify the units and their surfaces and reflect later geologic activity.

The primary criterion used in this study to delineate units is the evidence of possible significant hiatus between units. These include (a) unit-wide angular unconformities at the base of or within a particular unit, which we interpret as indicative of ero-

sion of underlying strata followed by deposition of a new unit having a noticeably different bedding attitude (e.g., Skinner and Tanaka, 2003); (b) disconformities (parallel unconformities) where, in the absence of a distinct, observable erosional signature, other indicators of hiatus exist, such as a surface that collected impact craters and/or a major change in material properties and inferred, sustained deviation in emplacement style, and (c) combinations of inferred angular unconformities and disconformities arising from layered materials emplaced by sedimentation over a partly-flat and partly-sloping, eroded surface (see Neuendorf et al., 2005 for formal definitions of unconformity types). The units distinguished in Figs. 3A–3C have observed or inferred lower-bounding unconformities that we describe in this section.

Previous work has determined crater densities and important cross-cutting relationships with adjacent units for some of the polar units described herein, including the Vastitas Borealis interior and Scandia region units (Scott et al., 1986–1987; Tanaka et al., 2005) and what amount to be equivalents to our Planum Boreum 1 and 3 units (Herkenhoff and Plaut, 2000; Tanaka, 2005). These data are valuable for establishing relative ages of the surfaces, and inferring ages of the material units, but

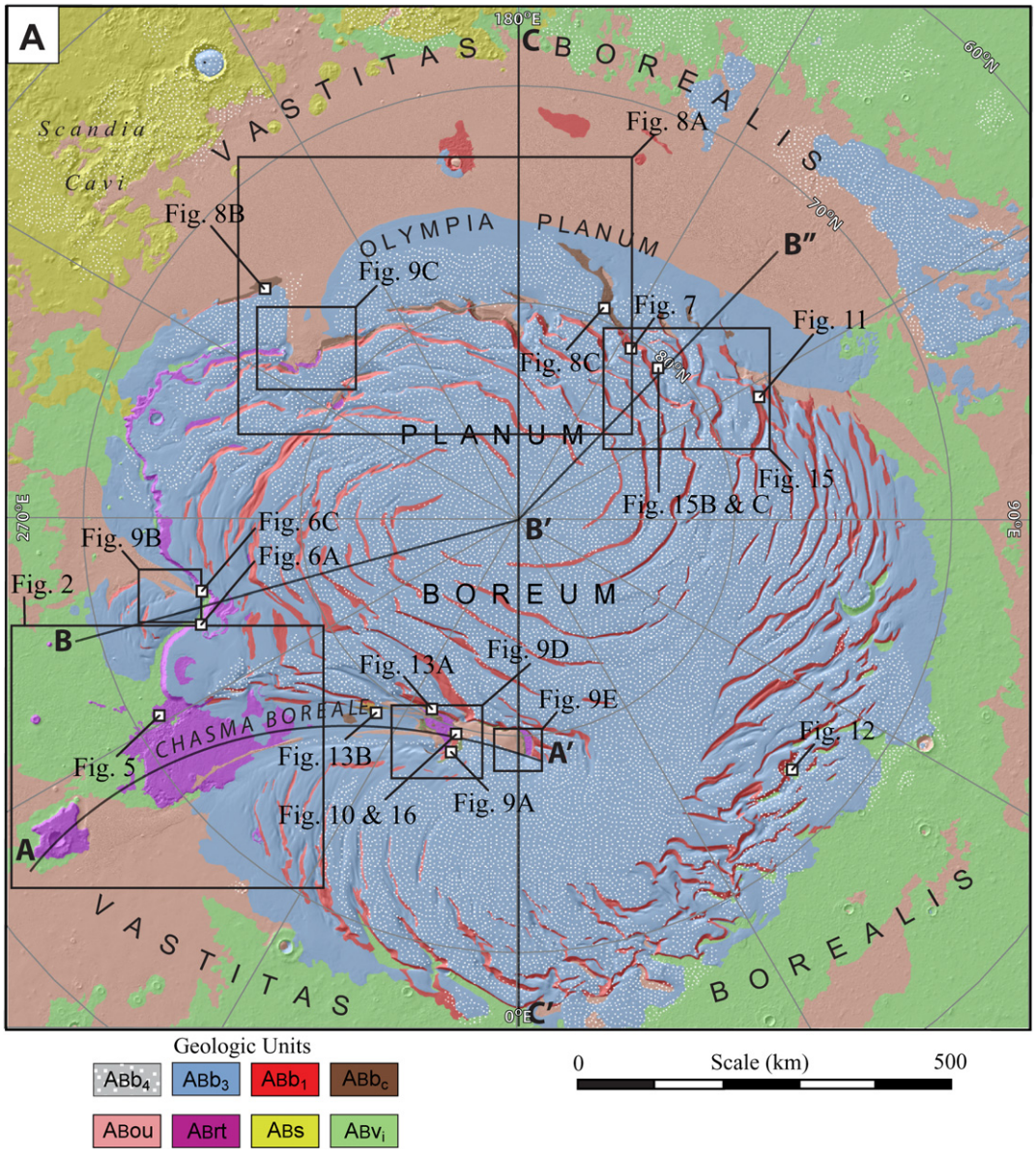

Fig. 3. Geology of Planum Boreum, Mars and surrounding lowland plains (refer to text and Table 1 for discussion). (A) Simplified geologic map showing major units discussed in the text. Locations of Figs. 2 and 5–16 denoted. [Image derived from the geologic map overlain on a MOLA hillshade (~115 m/pixel); polar stereographic projection centered at the north pole.] (B) Correlation of mapped stratigraphic units and their association with interpreted regional geologic events. Dashed boxes denote units that are not represented in the geologic maps or cross-sections due to limited extent, surficial nature, or stratigraphic uncertainty. (C) Schematic stratigraphic column showing the interpreted vertical relationships of the mapped units. Relative thicknesses of units are only approximately shown; those of thinnest geologic units are exaggerated for emphasis. Outcrop forms (on right side of column) depict typical slopes and ledges observed in image and topographic data sets (outcrops widths not related to any physical characteristic). Note uncertain placement of the boundary between the Middle and Late Amazonian relative to Planum Boreum cavi and 1 units (ABb_c and ABb_1).

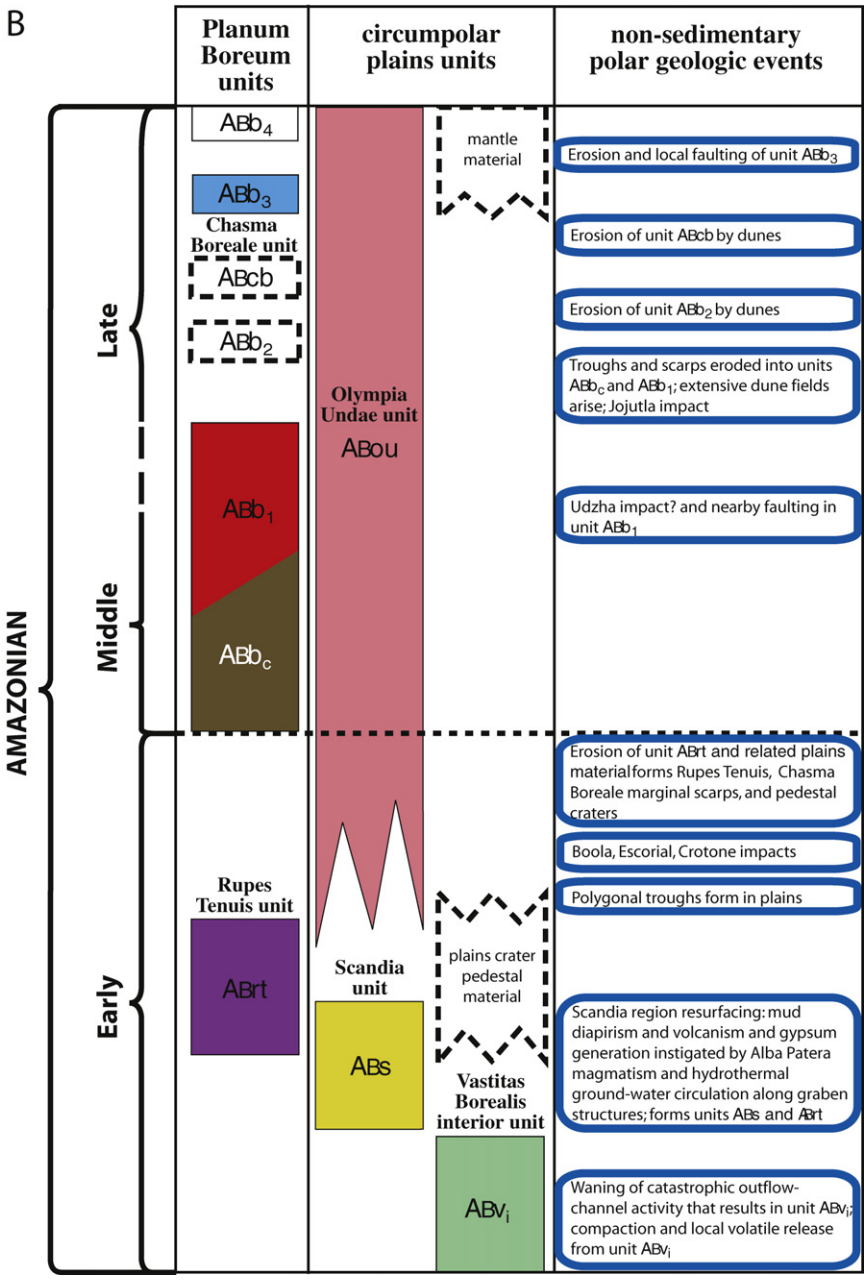

Fig. 3. (*continued*)

mostly at a regional scale. For eroded and/or exhumed units, the crater density provides an upper age limit for emplacement age, which may actually be much older. Model-based absolute ages are not well-constrained for Mars, given uncertainties in interpretation of the crater-density data as well as in the crater production rate, especially for the Amazonian (e.g., Hartmann, 2005). Herein we provide only the most general picture of absolute age ranges in the following description of stratigraphy, based on the suggested ages for martian epoch boundaries by Hartmann (2005).

Table 1 provides a summary of the units portrayed in Fig. 3, including key characteristics, stratigraphic relations, and interpretations. This table also indicates other names applied to these materials in the literature; in some cases, the previous names do not precisely match and may include multiple units and/or parts of units in the definitions provided herein. In particular, "polar layered deposits" was applied to the materials of the north and south polar plateaus on Mars beginning with Mariner 9 observations (e.g., Murray et al., 1972). However, more modern topographic and image data sets have provided recognition of increasing complexity in layer morphology, texture, albedo, and stratigraphy as discussed herein and elsewhere (e.g., Malin and Edgett, 2001; Byrne and Murray, 2002; Fishbaugh and Head, 2005; Tanaka, 2005; Milkovich and Head, 2005, 2006). Thus, "polar layered deposits" now has become overly vague for all but the most general stratigraphic discussions of north polar geology (Herkenhoff et al., 2006). Similarly, we see the need to avoid the term "basal unit" (e.g., Edgett et al., 2003;

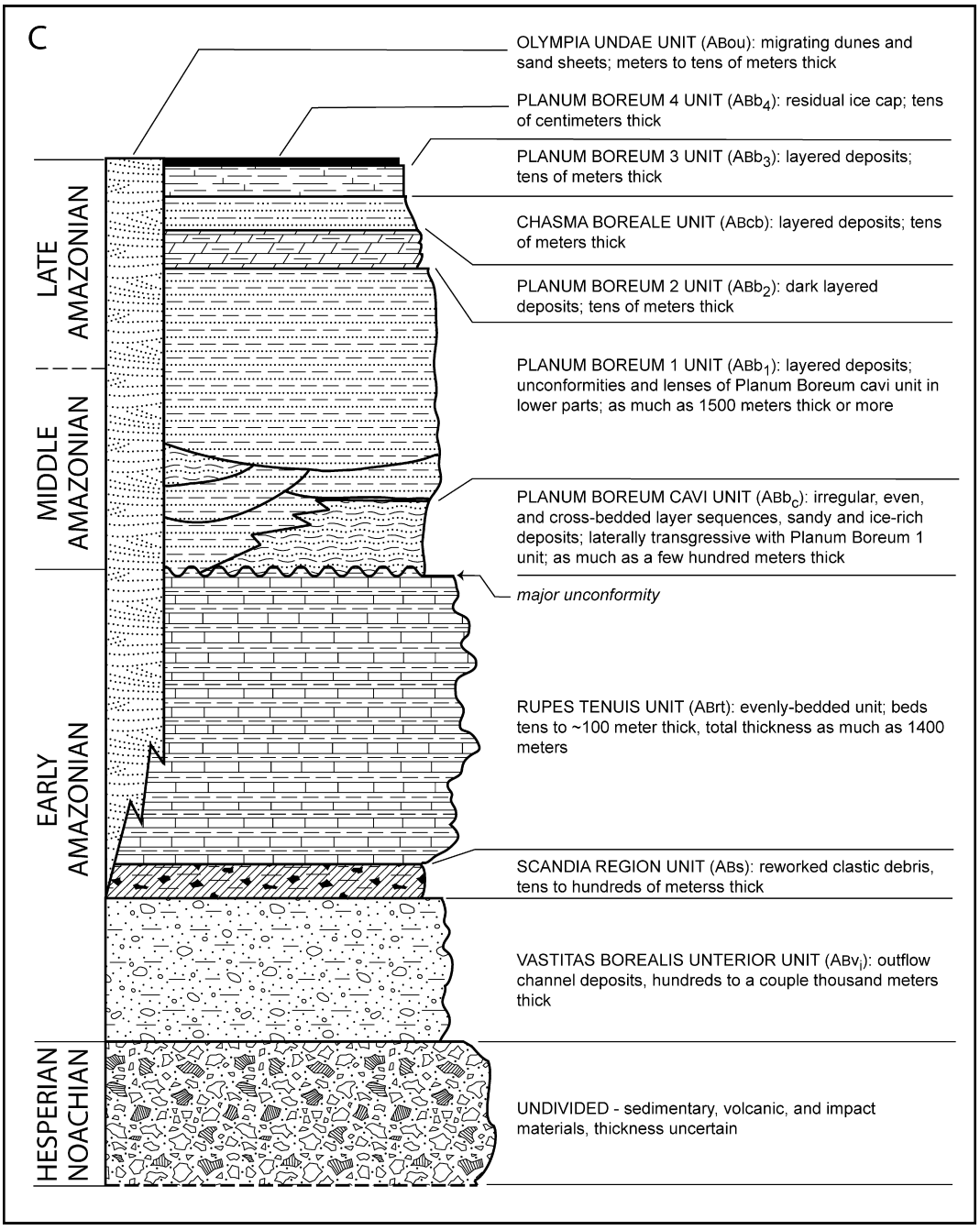

Fig. 3. (*continued*)

Fishbaugh and Head, 2005), because we find that the basal materials of Planum Boreum display widely-varying layer characteristics and ages that justify their discrimination. In other cases, specific geologic names were not previously attached to mappable materials, thereby making reference to them cumbersome.

In the following map-unit descriptions, we focus first on their general stratigraphic relationships that support the renderings shown in Figs. 3A–3C and 4. These aspects form the basis for reconstruction of the broad development of north polar materials and features over time. They also provide context for understanding other stratigraphic aspects of the units discussed in the remainder of the unit descriptions, such as their composition, layering, and modification features. We feel that these map-unit descriptions and inter-relationships provide a generally coherent yet tentative view, which can (and should) be further refined and improved upon through additional scrutiny of existing and newly-acquired data.

4.1. Early Amazonian materials (~3 to 1.0 Ga)

These are the oldest units exposed in the map area (Fig. 3). Underlying these rocks are Hesperian and Noachian materials likely of sedimentary, impact, and volcanic origin that may

be hundreds of meters to kilometers thick (Fig. 3C) (Frey et al., 2002; Tanaka et al., 2003). Impact and tectonic structures and perhaps the dissociation of volatile materials buried within these materials likely contributed to the structure and modifi-

Table 1
Map units, symbols, other published names, primary characteristics and interpretations (in order of youngest to oldest; see text for additional discussion and references)

Unit name	Unit symbol	Other names	Characteristics	Interpretations
Planum Boreum 4 unit	ABb$_4$	Polar ice deposits (Tanaka and Scott, 1987); polar ice cap (Herkenhoff, 2003); upper layered deposits (Tanaka, 2005); Planum Boreum 2 unit (Tanaka et al., 2003)	• Covers most of inner Planum Boreum • Decimeters thick • High albedo • High ice content • Displays pitted, cracked, and ridged surface textures at meter and decameter scales • Overlies mostly unit ABb$_3$ • Unit partly obscures meter-scale surface textures of underlying units	• Surface textures due to eolian and/or sublimation processes • Unit age less than crater age (<15 ka) of underlying surface • May result from period of declining north polar insolation since 21.5 ka
Mantle material (not mapped)	–	Mantling material, etc. (Mustard et al., 2001)	• Regionally covers northern plains at >30–50° N • Meters-scale bumpy texture • Meters thick at margins • High ice content	• Soil of fine lithic particles deposited from atmosphere combined with condensed, interstitial ice • Periglacial processes result in bumpy texture
Planum Boreum 3 unit	ABb$_3$	Banded terrain (Howard et al., 1982); upper layered deposits (Tanaka, 2005); Planum Boreum 2 unit (Tanaka et al., 2003)	• Covers most of Planum Boreum beneath unit ABb$_4$ on inter-trough plateau surfaces and on north-facing slopes • Sequence of <6–8 poorly-defined layers • Moderate surface ice abundance • Overlies units ABb$_c$, ABb$_1$, ABb$_2$, ABcb, and ABou • Meters to decameters thick on margins • Locally appears as relatively bright material covering rippled and hummocky interdune surfaces	• May be pure water ice with thin dust lag or porous dust and some ice • ~<5 Ma (crater age of partly buried Planum Boreum 1 surface) and older than ~15 ka
Olympia Undae unit	ABou	Crescentic dune material, linear dune material, and mantle material (Tanaka and Scott, 1987); dune and mantle material (Tanaka, 2005)	• Forms circum-polar dune fields and associated rippled dark sheets • Strong TES Type 2 signature • Dunes display multiple morphologies and dominantly W and SW migration directions • Subdues underlying landforms • Low surface ice abundance • Strong gypsum signature in eastern Olympia Undae • Superposes multiple older units • Localized dark, downwind streaks • Locally underlies units ABb$_3$, ABb$_4$, and mantle material • Emanates from unit ABb$_c$ outcrops	• Weathered basaltic sand sourced mostly from unit ABb$_c$ • Gypsum may originate from unit ABs • Much of unit may be ice cemented and presently inactive • Dark streaks from dunes may indicate recent, local sand movement (e.g., MOC E04-00846) • May have scoured Olympia Planum and parts of Chasma Boreale • May have developed over most of Amazonian
Chasma Boreale unit	ABcb	Not previously recognized	• Occurs in parts of Chasma Boreale floor • Includes >40 layers but lacks terraces • High albedo • Overlain by units ABou, ABb$_3$; overlies unit ABb$_c$, ABb$_1$ • Wind-sculpted (yardangs) but lacks layer-controlled terraces • Moderate water-ice content	• Ice- and dust-rich deposits • Lack of terraces suggests friable, poorly consolidated material • May have formed after unit ABb$_2$ eroded • ~Late Amazonian; age poorly constrained
Planum Boreum 2 unit	ABb$_2$	Intermediate deposits (Rodriguez et al., 2007b)	• Scattered exposures along some Planum Boreum troughs and margins, in Chasma Boreale, and in some circum-polar craters • Consists of several low-albedo layers • Low water-ice abundance • Thickness ranges from a few to tens of meters • Dark veneers and dust plumes emanate from some exposures • Overlies unit ABb$_1$; buried by units ABb$_3$, ABb$_4$	• Made up of lithic particles, possibly of sand size • Extensively eroded by wind • Source for low-albedo "veneers" • ~Late Amazonian; age poorly constrained

Table 1 (*continued*)

Unit name	Unit symbol	Other names	Characteristics	Interpretations
Planum Boreum 1 unit	ABb_1	Polar layered deposits (Tanaka and Scott, 1987); layered deposits (Herkenhoff, 2003); lower layered deposits (Tanaka, 2005)	• Hundreds of horizontally-extensive, meters-thick layers of alternating albedo and commonly forming terraces; some layers particularly thick and hummocky • Mostly exposed in troughs and scarps of Planum Boreum, surrounding mesas, and some impact craters • Moderate ice content • Thickness may exceed 1500 m near north pole • Lower parts time transgressive with unit ABb_c • Overlies units ABrt and ABvi; underlies several units • Pitted, ridged, and brecciated textures at decimeter to meter scales • Includes hundreds of local unconformities; some make up low-albedo ledges • Rare fault offsets across sequences of layers	• Contrasting and varying layer albedo and color may depend on variation in ice vs dust content as well as surface roughness, illumination, and surficial deposits (e.g., CO_2 frost, dust lags, sandy veneers) • Layering may result from changes in depositional environment relating to insolation-controlled climate cycles • Unconformities relate to locally changing depositional and erosional conditions • Meter-scale ridges may be yardangs produced by down-slope winds • Thick, hummocky layers may be sand rich or indurated lags controlled by non-periodic climate-related events • Middle to Late Amazonian based on >5-km diameter crater density of western Olympia Planum
Planum Boreum cavi unit	ABb_c	Platy unit (Byrne and Murray, 2002); basal unit (Fishbaugh and Head, 2005); Scandia materials (Tanaka, 2005)	• Lines lower, steep walls of Olympia Cavi, northern Olympia Planum, Chasma Boreale, and depression in Abalos Mensa; forms rugged outcrops on floor of upper Chasma Boreale and lens in Planum Boreum • Dark and light even to irregular layering and local cross bedding • Local erosional hollows • Low water ice abundance • Light-toned layers resistant to erosion whereas dark-toned layers friable and disaggregated into dark soils, ripples, and dunes • Light-toned layers form benches marked by polygonal fractures spaced meters apart • Dark dunes emanate mostly from west- to south-facing cavi-wall outcrops and buried surface in eastern Olympia Planum	• Made up of ice-cemented dust (light layers) and weathered basalt fines (dark layers) • Cross-bedding indicates dune accumulations • Irregular bedding and hollows may reflect thicker and/or discontinuous areas of dark layers • Likely underlies most of the main lobe of Planum Boreum except near Rupes Tenuis and perhaps some of Gemina Lingula • May be derived mainly from erosion of units ABs and ABrt • West- and south-facing walls as main dune sources may reflect erosion by dominant circum-polar (westward) and down-slope (southward) winds • Middle to Late Amazonian based on >5-km diameter crater density of western Olympia Planum
Plains crater pedestal material (not mapped)	–	Not previously mapped	• Forms local plateaus that underlie crater ejecta blankets in Vastitas Borealis • Unit margins mostly obscured by slope and mantle materials	• Indicates former presence of plains-mantling dust and ice deposits, perhaps deposited from atmospheric suspension • Preferential preservation beneath craters may result from impact-induced hardening and/or armoring processes • Alternatively, some features may be degraded volcanoes • Poorly constrained Amazonian age range
Rupes Tenuis unit	ABrt	Platy unit (Byrne and Murray, 2002); mantle material (Herkenhoff, 2003); basal unit (Fishbaugh and Head, 2005); Scandia materials (Tanaka, 2005); Scandia region unit (Tanaka et al., 2005)	• Forms Rupes Tenuis, parts of Olympia Cavi floors, and much of Hyperborea Lingula • Evenly-layered; >20 layers observed locally • Some layers locally eroded into rounded plates with concave upward surfaces • Layer surfaces locally fractured at meter scales • Layers ~10 to 100 m thick; margins of thick layers commonly eroded into knobs • Overlies unit ABvi and underlies several units • Marked by several multi-kilometer diameter pedestal craters	• May consist of material eroded mainly from Scandia region unit (ABs) • May originate from aeolian deposition • May form Escorial crater plateau and Abalos Colles • Eroded margins partly obscured by landslide deposits and other slope and mantle materials • Less eroded where impacts hardened and/or armored unit • Superposition relations and crater density suggest Early Amazonian age
Scandia region unit	ABs	Scandia materials (Tanaka, 2005)	• Occurs between Alba Patera and Planum Boreum • Consists of knobby plains (Scandia Colles), knobby, ovoid mesas (Scandia Tholi), and irregularly-shaped depressions (Scandia Cavi) • Superposes unit ABv_i	• Landforms attributed to various processes that may include diapirism of water-saturated sediment, pingo-like hydraulic uplift to form mounds, and phreatic or cryoclastic eruptions • Perhaps related to hydrothermal circulation along fractures systems radial to Alba Patera • Early Amazonian

(*continued on next page*)

Table 1 (*continued*)

Unit name	Unit symbol	Other names	Characteristics	Interpretations
Vastitas Borealis interior unit	ABv_i	Vastitas Borealis Formation (Tanaka and Scott, 1987); Vastitas Borealis interior unit (Tanaka et al., 2005)	• Forms broad, circum-polar plain marked by polygonal troughs spaced kilometers apart • Scattered "ghost craters" and subdued wrinkle ridges • Other features at lower latitudes	• May include deposits resulting from outflow-channel dissection, perhaps within a body of water • Troughs and ghost craters may result from dewatering and compaction • Defines beginning of Amazonian Period

cation of the overlying Early Amazonian deposits that underlie and surround Planum Boreum.

4.1.1. *Vastitas Borealis interior unit (ABv_i)*

The oldest unit mapped in the north polar region is the Vastitas Borealis interior unit (ABv_i), which defines the base of the Early Amazonian Epoch (Tanaka et al., 2005). The ABv_i unit forms a broad plain mostly between −5200 to −4500 m in elevation, which is marked by polygonal troughs that are several kilometers wide and which displays a moderate density of craters $\geqslant$1 km in diameter (Fig. 3A; Tanaka, 1986; Tanaka et al., 2005). Most impact craters <1 km in diameter appear highly degraded (e.g., eroded rim massifs, infilled crater interiors, irregular or partly-untraceable ejecta margins), suggesting that resurfacing generally has modified or removed features tens to hundreds of meters in relief. At decameter scales, most unit surfaces have a characteristic "bumpy" texture, which may result from cryoturbation and volatile deflation of meters-thick sedimentary mantles (Mustard et al., 2001; Tanaka et al., 2003). The unit also includes rimless, flat-floored "stealth" or "ghost" craters that indicate that the unit buries a surface of Early Hesperian or greater age (Head et al., 2002), at depths of hundreds to as much as a couple thousand meters below the Vastitas Borealis surface (Tanaka et al., 2001; Kreslavsky and Head, 2002; Buczkowski and Cooke, 2004; Buczkowski et al., 2005). Along the southern margin of the ABv_i unit in Utopia Planitia, where it does not appear to be mantled, the unit is brighter (i.e., warmer) in THEMIS daytime infrared images than older, adjacent sedimentary materials, suggesting that it is composed of relatively fine-grained material.

The Vastitas Borealis interior unit (ABv_i) is generally interpreted to consist of sedimentary deposits emplaced through outflow channel discharges that may have included catastrophic flooding (e.g., Parker et al., 1989; Baker et al., 1991), pulses of debris flows through outflow channel activity, and/or mass-wasting materials related to the back-wasting of the highland-lowland boundary scarp (Tanaka et al., 2001; Rodriguez et al., 2006a). Reworking by soft-sediment processes such as mud diapir-like upwelling and extrusion (Tanaka et al., 2003; Skinner and Tanaka, 2007) may have provided a bulk material from which fine-grained materials that currently comprise the circum-polar dunes were winnowed. The sands have a spectral signature consistent with that of weathered basalt (Wyatt et al., 2004), which may be indicative of prolonged exposure of the material to water that may have occurred during such soft-sediment-type activity.

4.1.2. *Scandia region unit (ABs)*

The Scandia region unit (ABs) overlies the Vastitas Borealis interior unit (ABv_i) and covers a broad swath of the northern plains from 300 km north of Alba Patera (south of the study area) to the southern margin of Olympia Planum. The region includes irregularly-shaped depressions surrounded by tens- to hundreds-of-meters-high knobby terrain (Scandia Cavi; Fig. 1) as well as scattered knobs and mesas tens of meters high (Scandia Colles) and knobby, ovoid mesas tens of meters high (Scandia Tholi) south of Scandia Cavi and the map region. Ubiquitous burial by a meters-thick, mid- to high-latitude mantle (Mustard et al., 2001) obscures finer-scale (meter to decameter) morphologic and textural characteristics of the ABs unit (e.g., Kreslavsky and Head, 2002).

Tanaka et al. (2003, 2005) proposed that the resurfacing history in the Scandia region may have involved geologic processes analogous to sedimentary diapirism, mud volcanism, pingo-like extrusions, and/or phreatic or cryoclastic eruptions and discharge-related collapse. They suggested that these processes may have been triggered and sustained by regional thermal anomalies produced by magmatic dikes that propagated from Alba Patera or through hydrostatic differences between recharge and discharge regions. Alternatively, Fishbaugh and Head (2001) interpreted the Scandia landforms as related to the movement and melting of a former ice-sheet extension of Planum Boreum.

The resurfacing history of the Scandia region may relate to the discovery of gypsum in dunes north of this region (Langevin et al., 2005) that appear to be eroded from materials underlying the dunes (Roach et al., 2007). These gypsum deposits are proposed to have been produced by volcanically-introduced sulfur and hydrothermal alteration of calcium-bearing volcanic rocks (Tanaka, 2006). Alternatively, Fishbaugh et al. (2007) suggested that the gypsum deposits may have resulted from release of meltwater from beneath the polar layered deposits, which led to alteration of dune material as well as evaporitic deposition of gypsum in dune pore spaces.

At the mouth of Chasma Boreale, below the margin of the Hyperborea Lingula plateau, linear ridges several kilometers long that locally have pitted and grooved summits appear to be cut by (and thus predate) polygonal troughs (Fig. 5). The origin of similar ridges elsewhere on Mars has been attributed by previous workers to be (1) subglacial volcanic hyaloclastic deposits (Chapman, 1994) or (2) extruded mud-volcano-like features induced by underlying magmatism (Skinner et al., 2007), or (3) remnants of magmatic dikes (Rodriguez et al., 2003). Through our geologic mapping, however, we find no

clear evidence for glacier-related processes in the north polar plateau of Mars, as noted previously (Kolb and Tanaka, 2001). As such, we consider that these linear ridges are most likely the result of sedimentary and/or magmatic volcanism. Either process, however would have involved high heat flow at regional scales during the Early Amazonian, perhaps driven by

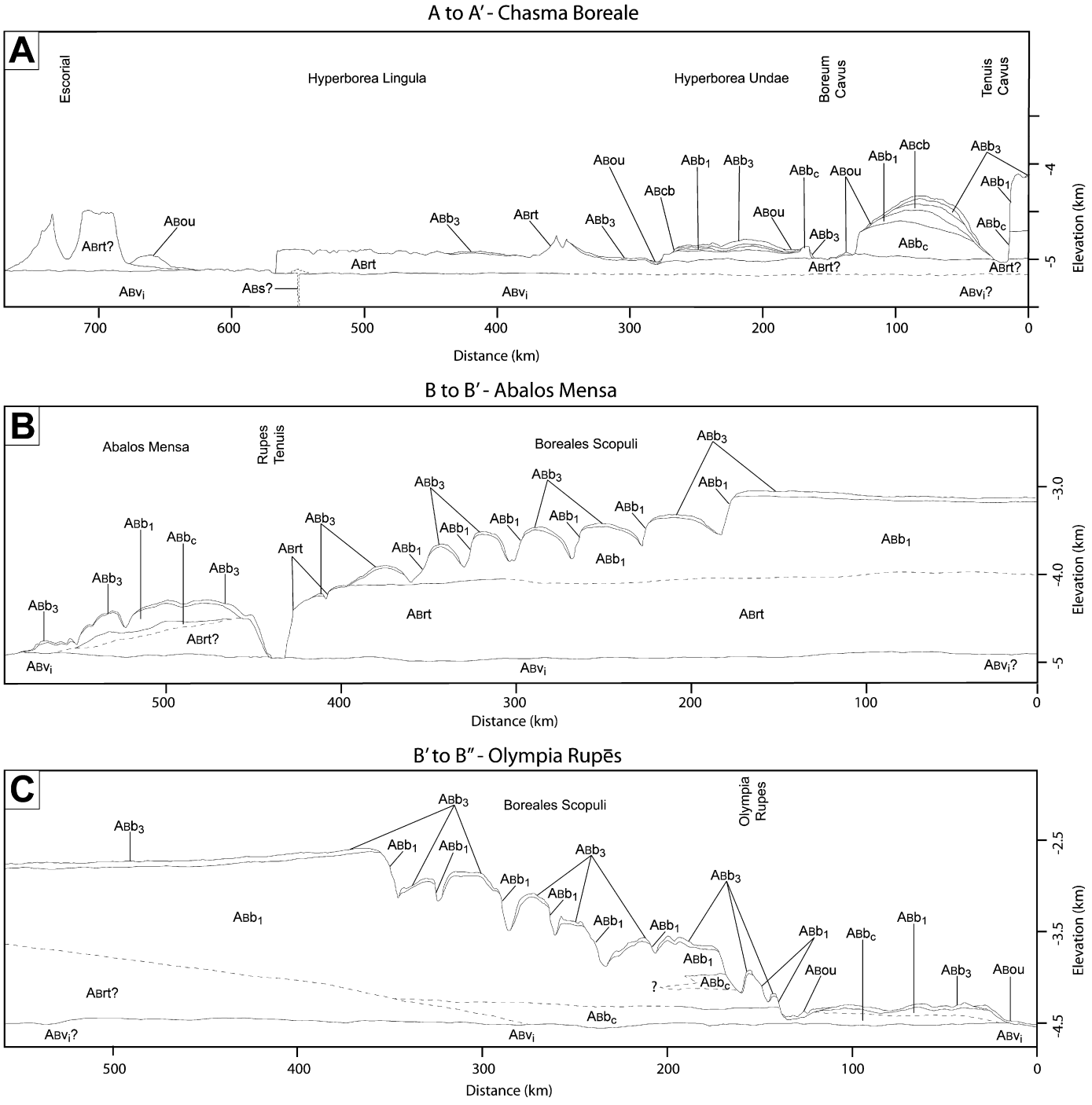

Fig. 4. Schematic topographic profiles and cross-sections depicting mapped and interpreted lateral and vertical stratigraphic relationships between geologic units as mapped in Fig. 3A, which also shows profile locations. Surface topography partly derived from MOLA DEM but local variations were exaggerated (between 50 and 75×) for emphasis and to most aptly illustrate uppermost sections of stratigraphy. As a result, vertical scales are approximate. (A) Profile A–A′ along axis of Chasma Boreale showing relationship of Rupes Tenuis (ABrt) and Planum Boreum cavi (ABb_c) units with overlying units southwest of Tenuis and Boreum Cavi. (B) Profile B–B′ across Abalos Mensa and Rupes Tenuis showing interpreted pinching-out of units ABrt and ABb_c at the margins of Planum Boreum. (C) Profile B′–B″ across Boreales Scopuli and Olympia Rupēs showing how unit ABb_c may onlap unit ABrt beneath Planum Boreum. Also, note lens of unit ABb_c within Olympia Rupēs (see Fig. 11). (D) Profile C–B′ across Olympia Planum showing possible extent of ABrt and ABb_c units beneath Olympia Planum. (E) Profile B′–C′ across Gemina Lingula showing possible transgressive contact between units ABb_c and ABb_1 in northern Gemina Lingula as inferred from stratigraphic relations in Boreum Cavus to the west (Fig. 10).

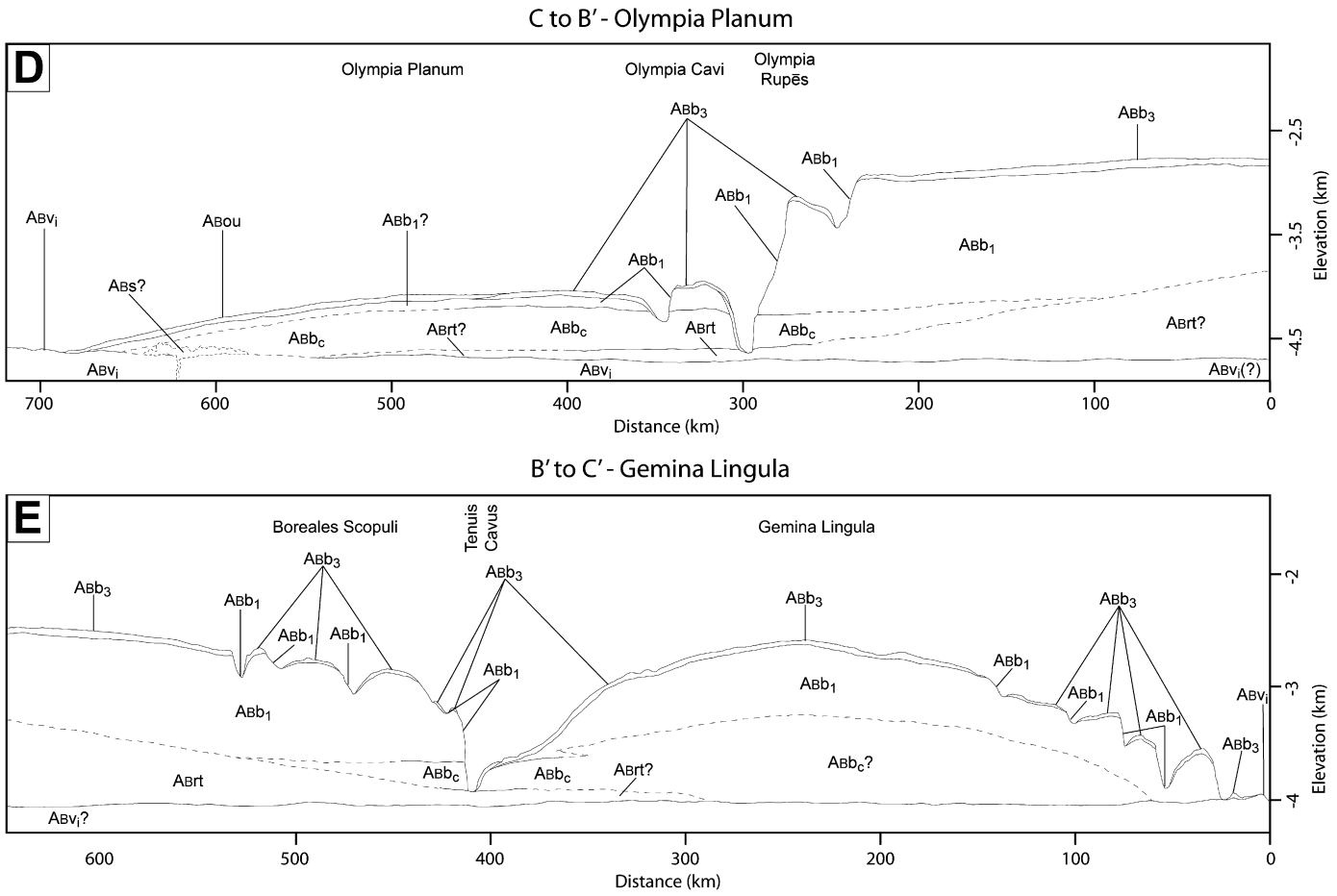

Fig. 4. (*continued*)

Alba Patera magmatism. We thus consider that these features may be geographically-related to the development of the Scandia region unit (ABs), in agreement with the interpretive scenario for this unit proposed by Tanaka et al. (2003).

Overall, the Scandia region unit (ABs) is comprised of relatively high-standing landforms that rise above and overlie the Vastitas Borealis interior unit (ABv_i). These features may be the result of deformational uplifting and/or accumulation of sedimentary and/or volcanic deposits. Their degraded, knobby forms and the absence of clear depositional landforms suggest that the Scandia region unit (ABs) was highly eroded, such that the uplift and subsequent removal of binding volatiles and/or volatile-related minerals may have freed large amounts of sediment that were then transported and deposited elsewhere within the circum-polar region.

4.1.3. Rupes Tenuis unit (ABrt)

The layers of this unit drape over the surface of the Vastitas Borealis interior unit (ABv_i), forming a parallel unconformity (Fig. 6). A hiatus between the units is suggested by a major discontinuity that separates the units (for example, along eroded margins of the ABrt unit, the ABv_i unit does not appear eroded at all). This hiatus is also implied by a 2-km-diameter, exhumed impact crater that lies between the two units (at 81.4° N, 245.2° E; THEMIS V13610006). The Rupes Tenuis unit (ABrt) forms the bulk of materials exposed along Rupes Tenuis and in Hyperborea Lingula, as well as the lowest parts of Olympia Cavi and Rupēs (Figs. 2–5). We count 7 craters ⩾5 km on the unit (including areas buried <100 m by younger materials) on a collection of outcrops totaling $\sim 4.9 \times 10^4$ km^2. These craters yield a density of 143 ± 54 per 10^6 km^2, indicative of a Hesperian age (Tanaka, 1986). However, most of the craters rest on pedestals (Fig. 2) and appear to have armored the subjacent ABv_i unit from erosion, so that outcrops without larger craters may have been preferentially obliterated. This preferential removal of impact craters would apparently lead to a higher-than-original crater density for the extant outcrops. If this effect increased the crater density by a liberal factor of 2, then the original density would be near the beginning of the Early Amazonian. Regardless, superposition of the impacted Rupes Tenuis unit on unit ABv_i (which has tightly-controlled crater counts based on its large regional expanse; Tanaka et al., 2005) indicates that unit ABrt cannot be older than Early Amazonian. As such, we infer that unit ABrt unit formed during the Early Amazonian, after the regional emplaced of unit ABv_i.

The Rupes Tenuis unit (ABrt) locally consists of ∼20 layers, each tens to ∼100 m in thickness (Figs. 6A and 6B). Additional, stratigraphically-higher layered outcrops occur

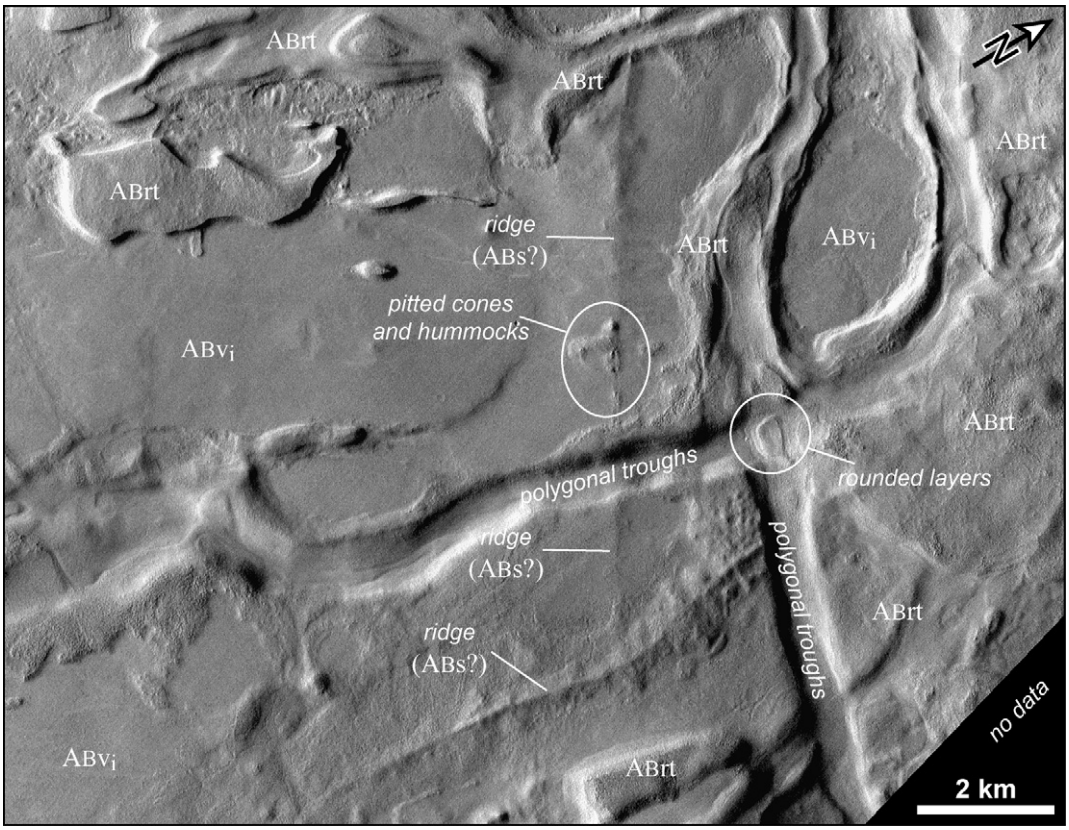

Fig. 5. Close-up view of part of Hyperboreus Labyrinthus. Lowermost layers of the Rupes Tenuis unit (ABrt) superposed on relatively smooth plains made up of Vastitas Borealis interior unit (ABv_i). Note ridges possibly made up of Scandia region unit (ABs), which includes elongated pitted cones and hummocks of inferred mud volcanic or hydromagmatic origin. Polygonal troughs cut all units and contributed to eroded, rounded layer forms. (Part of CTX P01_001600_2605; illumination from left; scale bar is approximate; see Fig. 2 for location.)

above the Rupes Tenuis scarp north and northwest of Crotone crater, where they display lobate ridges. These may be remnants of debris-flow margins, as well as knobby and bumpy surfaces, which may represent zones of volatile deflation (Rodriguez et al., 2007a). These features are partly buried by Planum Boreum 1 and 3 units (ABb_1 and ABb_3, respectively; Figs. 6C and 6D) described below (see also MOC R0-200446). Along Rupes Tenuis, some eroded layers form irregularly-shaped, rounded concave slabs having ridged margins (see CTX P02_0022654_2605). A few rounded lobes of material at the base of Rupes Tenuis that partly bury local spur-and-gully topography may be landslide deposits sourced from within over-steepened exposures of this unit and/or mantles (e.g., MOC R20-00130 at 81.7° N, 276.0° E).

Hyperborea Lingula (Fig. 2) forms a platform of the Rupes Tenuis unit (ABrt) in which as much as 1000 m of the upper part of the unit has been removed, when compared with the maximum unit thickness above Rupes Tenuis. This section includes ~10 layers, each 20 to 30 m thick on average (Tanaka, 2005). Some of the lowermost layers south of Hyperborea Lingula are preserved in polygonal troughs of Hyperboreus Labyrinthus, where they include rounded, dish-shaped forms (Fig. 5). By extension, we suggest that deformation and structurally-controlled erosion may account for the similar, dish-shaped layer outcrops mentioned previously along Rupes Tenuis.

As suggested by Tanaka et al. (2003, 2005) (but with different unit names), the ABrt unit likely forms the Escorial crater plateau (Fig. 4A) as the surface elevation of this plateau (~ −4450 m) is midway between that of Hyperborea Lingula (~ −4850 m) and the top of eastern Rupes Tenuis (~ −4050 m). Similarly, Abalos Colles, which consist of pitted cones, rise to −4800 to −4500 m and may represent remnants of highly-eroded impact craters that perhaps formed within a "paleo-plateau" made up of unit ABrt (Figs. 2 and 4A and 4B). Although Abalos Colles have also been interpreted to be volcanic (Garvin et al., 2000b), closely-associated lava flows or other volcanic morphologies and structures have not been discovered to bolster this interpretation.

An outcrop of the ABrt unit making up the lowermost layers within a depression of Olympia Cavi reveals details about the unit and how it appears to differ from the overlying Planum Boreum cavi unit (ABb_c) (Fig. 7). The outcrop consists of several relatively high-albedo, laterally-continuous, densely-fractured terraces having rounded margins that may represent evenly-bedded layers (Fig. 7B). The distinct terraces suggest differential erosion of the layers. The terraces distinguish these layers from a steeper section of alternating light and dark beds mapped as the ABb_c unit (see also Fishbaugh and Head, 2005; Fig. 6); the dark beds are the sources of locally-rippled, dark sedimentary deposits. The ABrt unit layers are thinner at this outcrop in Olympia Cavi than along Rupes Tenuis. They are

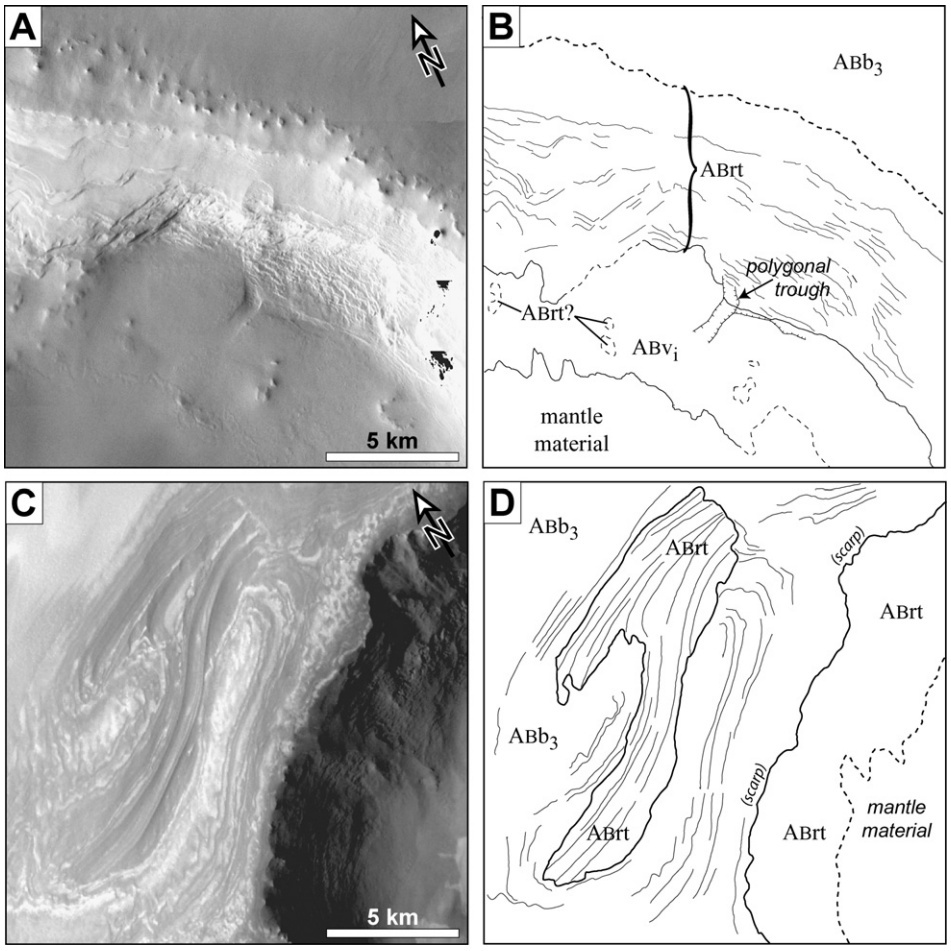

Fig. 6. Image panels and interpretive sketches of parts of Rupes Tenuis scarp along margin of Planum Boreum. (A and B) Approximately 20 topographic terraces delineate lower layers of Rupes Tenuis unit (ABrt), which buries plains surface (with polygonal troughs) of the Vastitas Borealis interior unit (ABv_i) that is partly obscured by mantle material. Plateau surface covered by Planum Boreum 3 unit (ABb_3). (Excerpt of THEMIS V1122500; illumination from lower left; scale bar is approximate.) (C and D) Outcrop near western margin of Chasma Boreale shows window of evenly-layered Rupes Tenuis unit (ABrt) beneath unconformably draping, relatively bright layers of Planum Boreum 3 unit (ABb_3) (and possibly Planum Boreum 1 unit (ABb_1)). Here, ABrt unit is marked by tall benches and arcuate scarps. (Excerpt from THEMIS V13197002; illumination from lower left; scale bar is approximate.)

also relatively few, suggesting that the unit may be less well-developed and/or more deeply eroded in Olympia Cavi than along Rupes Tenuis.

Layering in the Rupes Tenuis unit (ABrt) appears to be predominantly horizontal to sub-horizontal and thus far lacks observed erosional contacts such as cross-bedding (Fig. 6). These observations are indicative of predominantly vertical construction and of an overall absence of horizontal mobilization of the accumulated sediments (which would have produced migrating dunes). Thus, the unit's even-layering and polar location suggest that precipitation and cold-trapping of dust-laden volatiles could have played a dominant role in the unit's accumulation (Kolb and Tanaka, 2001). In addition, the unit may also contain loess deposits formed by blown-in silt-size sediments. Tanaka (2005) indicates that development of mesas, knobs, and depressions by erosion of the nearby, extensive Scandia region unit (as mapped by Tanaka et al., 2005) may have provided the source material for the ABrt unit. The extent and relief of the unit's erosional surface indicates that the volume of debris eroded from that deposit may be similar to that of the ABrt unit (Tanaka, 2005). In addition, the fine-sized particles eroded off the Vastitas Borealis interior unit (ABv_i) may have also contributed as sources to the ABrt unit. Nevertheless, the presently unknown role of volatiles and/or chemical precipitates (Tanaka, 2006) in the cementing matrix implies that the particle grain size of the materials that presently form this unit cannot be determined based on its geomorphologic and morphometric attributes. For example, dust particles could be bound into sand-sized particles (Herkenhoff and Vasavada, 1999), or the effects of alteration and abrasion may have assisted in the comminution of basaltic and gypsum sands into finer particles.

We interpret that each layer of the Rupes Tenuis unit (ABrt) represents a stage of "significant" deposition. Such stages could result from pulses of formation and/or erosion of the Scandia region unit (ABs). Thus far, it is difficult to determine if layer truncations and unconformities occur within the ABrt that would document interruptions in local to regional deposition.

Previous work did not distinguish two different basal units for Planum Boreum below the "classical" polar layered deposits in the fashion that we do herein [our Rupes Tenuis (ABrt) and

Planum Boreum cavi (ABb_c) units]. Herkenhoff (2003) recognized a lower unit of Planum Boreum along Rupes Tenuis where unit ABrt occurs. He mapped it as distinct from overlying layered deposits, based on its rough and knobby appearance in Viking images (layers, however, were not noted) and called it "mantle material." The recognition of platy beds of dark materials for parts of the margins of Planum Boreum in MOC images led to the suggestion that much of the base of Planum Boreum and virtually all of Olympia Planum could be characterized this way (Byrne and Murray, 2002; Edgett et al., 2003; Fishbaugh and Head, 2005). However, evenly-layered sequences making up some partly exposed margins of Planum Boreum (i.e., Rupes Tenuis and Hyperborea Lingula) became evident in MOC and THEMIS VIS images (Fishbaugh and Head, 2005; Tanaka, 2005). These margins were observed to cut into older surfaces superposed by multi-kilometer-diameter craters and were seen to be largely mantled and neither steep nor sourcing dunes. However, initially, there was insufficient high-resolution image data to consistently distinguish and confidently map these outcrops as different from the platy outcrops typically occurring in cavi walls (Tanaka et al., 2005; Tanaka, 2005). THEMIS VIS and CTX images now enable us to do so, and our Rupes Tenuis unit (ABrt) is the older of the two.

4.2. *Middle to Late Amazonian materials (<1.0 Ga)*

4.2.1. *Planum Boreum cavi unit (ABb_c)*

The stratigraphically lowest Middle to Late Amazonian unit (see discussion below on crater age) that we identify herein is the Planum Boreum cavi unit (ABb_c; see Fig. 3). Our mapping indicates that the Rupes Tenuis unit (ABrt) was cratered by large impacts and deeply eroded prior to deposition of the Planum Boreum cavi unit (ABb_c), which contains few superposed impact craters. These observations require a major unconformity having a relief of hundreds of meters between these units (Figs. 3C and 4); however, younger materials generally bury the unconformity. Locally, such as beneath Olympia Planum and perhaps parts of Planum Boreum, unit ABb_c likely rests directly on the Vastitas Borealis interior unit (ABv_i) (Figs. 4C–4E). The upper geologic contact of the cavi unit with unit ABb_1 appears to be time-transgressive in places (see discussion below).

Previous work has suggested the existence of a paleo-erg underlying the dunes of Olympia Undae and thus comprising

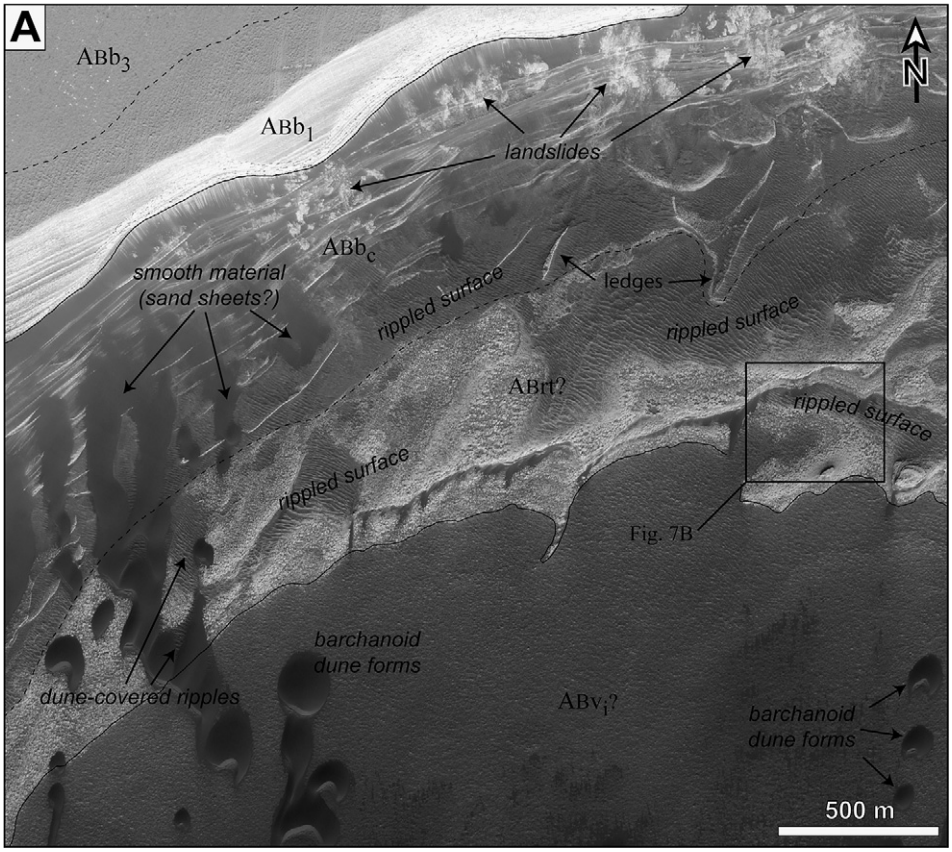

Fig. 7. (A) View of southwest-facing scarp of an Olympia Cavi depression on Olympia Rupēs margin of Planum Boreum. Inferred stratigraphy (from bottom to top) includes Vastitas Borealis interior unit (ABv_i?), Rupes Tenuis unit (ABrt?), and Planum Boreum cavi and 1 units (ABb_c and ABb_1, respectively). Local thickness of inferred unit ABrt is ~50 m. Dark material, mainly rippled or smooth, covers parts of units ABrt and ABb_c, whereas on unit ABv_i it appears as barchanoid dunes. Irregular ledges have apparent concave surfaces and may represent curving lower layers of lower part of unit ABb_c that trap dark material. Location of inset box (B) shown. (Excerpt from HiRISE PSP_001341_2650; illumination from lower left; scale bar is approximate; scene centered near 85.0° N, 150.6° E.) (B) Close-up of scene in (A) showing rounded unit ABrt layer margins (except for one sharp-edged knob); some layer interfaces, cracks, and surfaces buried by smooth and rippled dark material. Closely-spaced layer margins reveal that dark material is superficial and not part of layer sequence.

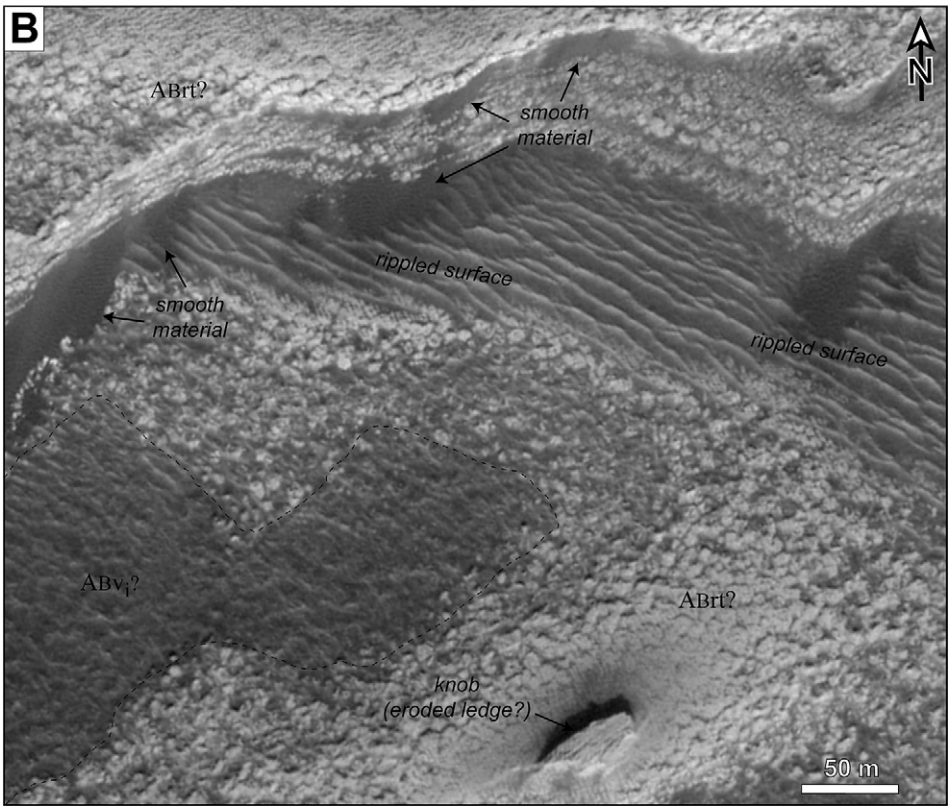

Fig. 7. (*continued*)

the bulk of Olympia Planum, based on the hundreds of meters thickness of the planum and the overlying dunes (Fishbaugh and Head, 2000, 2001, 2005; Byrne and Murray, 2002; Tanaka, 2005). The planum forms a broadly arcuate, half-dome-shaped plateau that extends more than 1000 km from 120° to 240° E and rises approximately 800 m above the circumpolar plains of Vastitas Borealis. We have been able to identify and trace the cavi unit along scarps that cut northern parts of Olympia Planum (Fig. 8). Generally, the geologic materials that overlie the cavi unit within the Olympia Cavi are several tens to >100 m thick and generally appear to thin toward the south. Based on the gently sloping surface of Olympia Planum and the thin covering of overlying materials, we suggest that the cavi unit likely follows the shape of the planum toward the south and that the majority of the volume of Olympia Planum is likely made up of the cavi unit (ABb$_c$) (Fig. 4D). In particular, beneath eastern Olympia Undae, the cavi unit (ABb$_c$) may directly underpin the polar erg as seen where an outer scarp of the Planum Boreum 1 unit (ABb$_1$) meets the Olympia Undae and is underlain by the ABb$_c$ unit (Figs. 8A and 8B). Thus, the underlying cavi unit (ABb$_c$) may provide much of the source materials for Olympia Undae.

An approximate crater density can be obtained for the Planum Boreum cavi unit based on the number of obvious as well as candidate impact craters on the western surface of Olympia Planum, where we interpret that the cavi unit (ABb$_c$) is thinly buried. We find two well-preserved impact craters that are ⩾5 km in diameter (19-km-diameter Jojutla crater (Fig. 1) and a 6.8-km-diameter unnamed crater at 81.2° N, 161.5° E). However, there appears to be a dearth of 1- to 5-km-diameter craters (perhaps two at 80.7° N, 188.3° E and 81.7° N, 175.7° E) on Olympia Planum with respect to the dozens that would be expected from an extrapolation based on the number of 5-km-diameter craters given a ~ -2 power law distribution (e.g., Tanaka, 1986). We attribute this lack of smaller impact craters to tens of meters of resurfacing of the upper part of the cavi unit (typical rim heights for north polar region craters ⩾10 km in diameter are ⩾100 m according to Garvin et al., 2000a), perhaps by cavi unit (ABb$_c$) accumulation, loosing and subsequent removal of sand-sized particles by weathering and saltation, or other resurfacing processes.

As such, we can only obtain an *approximate* measure of relative age for the ABb$_c$ unit based on the two larger, relatively well-preserved impact craters. Not only is the statistical sample lacking, but the area that it covers is unclear. Western Olympia Planum, which covers $\sim 7 \times 10^4$ km^2, may be less modified; however, it is unclear whether eastern Olympia Planum should also be included, because it may be more heavily modified. Given the plausible range of area based on this uncertainty results in a maximum ⩾5 km diameter crater density of $\sim 30 \pm 20$ per 10^6 km^2 (equivalent to ⩾1 km diameter crater density of $\sim 720 \pm 480$ per 10^6 km^2) and a minimum density of about half that value. The one-sigma range in the maximum and minimum crater densities bracket the surface age of the ABb$_c$ unit between the middle of the Early Amazonian and the early part of the Late Amazonian (Fig. 3B) (Tanaka, 1986). Given the uncertainty in crater age, as well as the uncertainty in Amazonian cratering rates (Hartmann, 2005), means that the age of the cavi

unit is poorly constrained and could fall within the range of ~100 million to ~2 billion years. Thus our assignment of the cavi unit to the Middle Amazonian (Figs. 3B and 3C) is approximate.

The Planum Boreum cavi unit (ABb_c) was first recognized as part of a low-albedo "platy unit" (Byrne and Murray, 2002) consisting of light-toned layers within dark material in the lower layered sequences of Planum Boreum, where it is particularly well exposed in the Olympia Cavi walls. Subsequent observations of these layered sequences showed that they actually form lateral patches within steep-walled cavi and lower parts of mostly west- and south-facing scarps of Planum Boreum, Chasma Boreale, and Abalos Mensa from which dark sand dunes originate (Edgett et al., 2003; Fishbaugh and Head, 2005; Tanaka, 2005; Byrne et al., 2007; Herkenhoff et al., 2007). The light-toned layers of the cavi unit (ABb_c) have approximately decimeter- to meter-scale thickness (determined from both local slope exposures of the layers in HiRISE images (e.g., Fig. 9A) and broad relief from MOLA data).

Light-toned layers may form singly or in sequences. They form benches in outcrops, suggesting that they are more resistant than the intervening dark-toned layers. An enhanced-color HiRISE sub-frame (Fig. 9A) shows that the ABb_c unit includes laterally-extensive packets of bright, tan or grayish-tan layers alternating with variably thick lenses of dark material mostly covered by dark ripples. The bright layers also display a characteristic polygonal fracture pattern consisting of joints spaced meters apart (Fig. 9A inset). Where terraces are well-developed in the cavi unit (ABb_c), erosion may include disaggregation of the dark layers by sublimation of interstitial ice cement and removal of fines by wind. Overlying light-toned layers display increased fracturing on terrace margins, where undermining of dark material may cause the light-toned layers to fall apart and where exposure to wind and Sun may increase sublimation. The paucity of boulders on the terraced scarps indicates that sublimation and wind erosion are more effective than rock avalanches in causing scarp retreat. In steeper slopes, where ledges are less developed, the light-toned layers display scour marks apparently produced by rock avalanches sourced from bright layers, which have resulted in landslide deposits and boulder fields along and near the base of scarp walls (Herkenhoff et al., 2007). Landslide deposits, including blocks, may then be removed by sublimation and wind (Edgett et al., 2003; Herkenhoff et al., 2007).

Clear examples of cross-bedding in which beds of opposing dips truncate one another appear locally in the cavi unit (ABb_c) (Fishbaugh and Head, 2005; Herkenhoff et al., 2007). These tend to occur where the light-toned layers (or layer se-

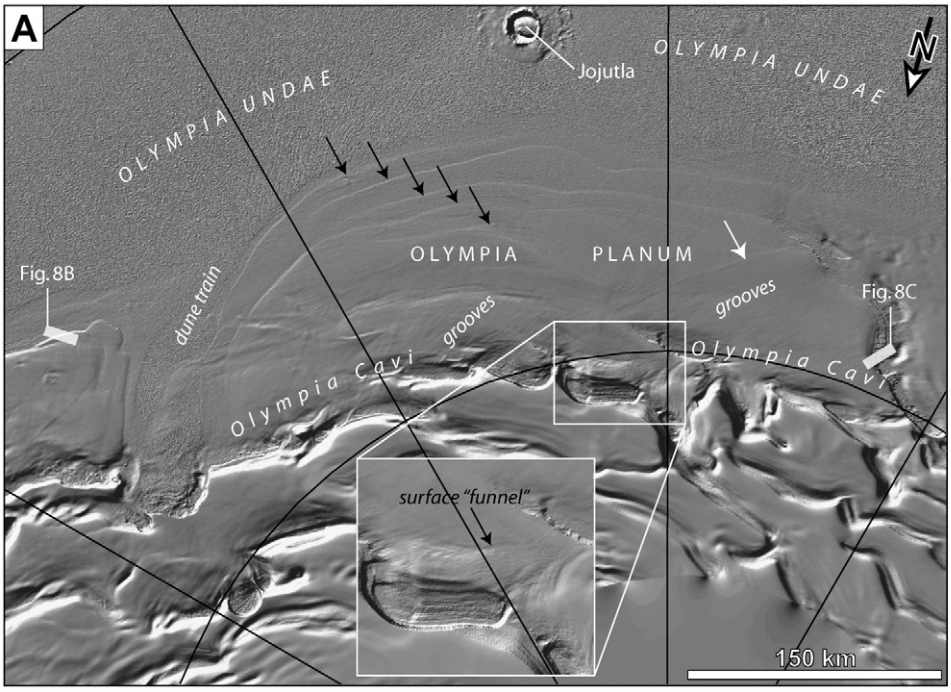

Fig. 8. Images showing details of Olympia Planum. (A) Topographic hillshade showing subtle, arcuate topographic benches (black arrows) on Olympia Planum, which are bordered on south by Olympia Undae dune sea. A broad dune train, a surface "funnel," a long bench (white arrow), and a series of grooves trend southwestward from Olympia Cavi; these features may reflect sand abrasion of Planum Boreum 1 unit (ABb_1) material. Their common orientation reflects a dominant wind direction along the Planum Boreum margin. (MOLA ~115 m/pixel DEM; artificial illumination from southeast; north pole toward bottom.) (B) View of bench scarp in eastern Olympia Planum consisting of layered Planum Boreum 1 unit (ABb_1) overlain by Planum Boreum 3 and 4 units ($ABb_{3,4}$—uppermost layers and residual ice, respectively). These units in turn overlie lower, moderately dark, hummocky surface made up of Planum Boreum cavi unit (ABb_c). Scattered dark dunes and mantle of Olympia Undae unit (ABou) overlie lower surface. (Excerpt from MOC E02-01976 image; illumination from the bottom; 4.84 m/pixel.) (C) View of scarp in northwestern Olympia Planum made up of thick sequence of pronounced layers of Planum Boreum cavi unit (ABb_c) unconformably overlain by subdued layers of Planum Boreum 1 unit (ABb_1) and thick layers and residual ice of the Planum Boreum 3 and 4 units ($ABb_{3,4}$). (Excerpt from MOC R18-02325; illumination from right; 3.39 m/pixel.)

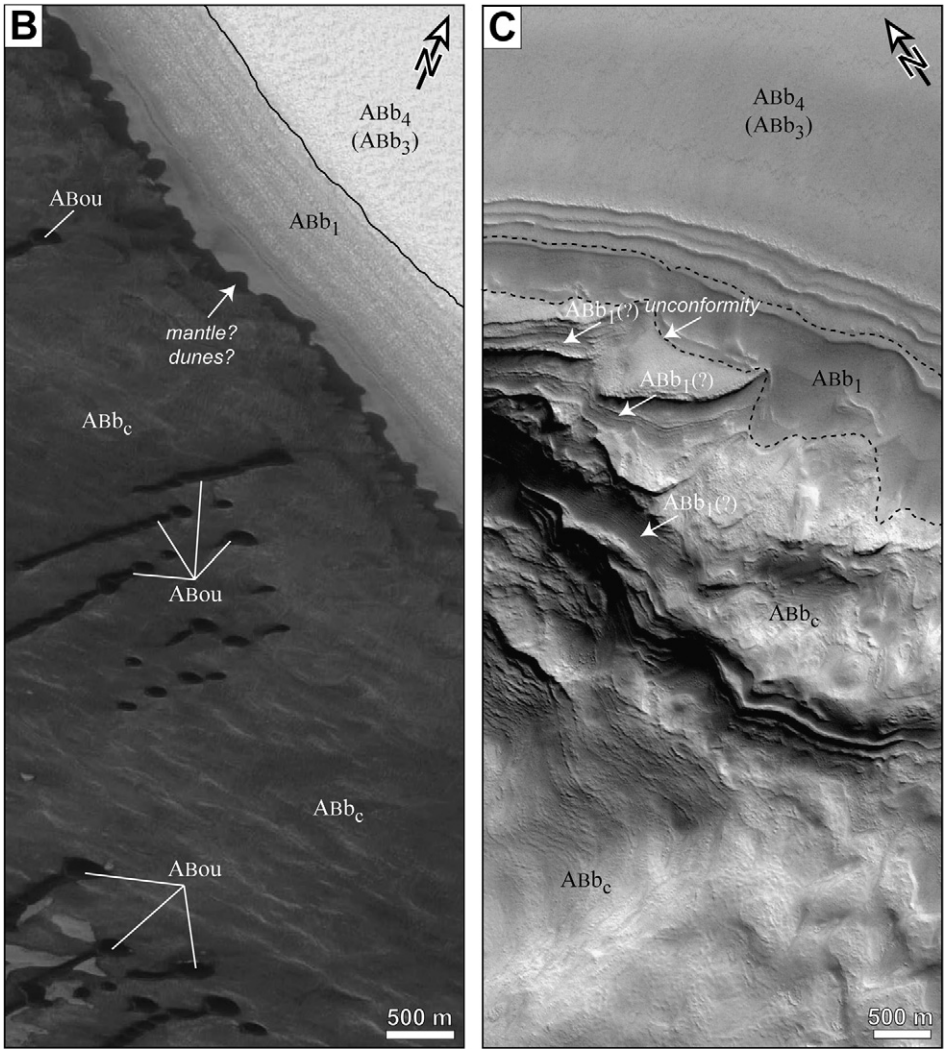

Fig. 8. (*continued*)

quences) are thin and traceable only for tens to hundreds of meters and are separated by relatively-thick dark layers. In these cases, the unit may result from the stacking of dunes. We also suggest that the intermittent deposition of resistant, relatively-bright interbeds sequestered underlying sandy material, which could also have become indurated by the accumulation of interstitial ice. Such processes are termed "niveo-aeolian" and have been documented both on Earth as well as elsewhere on Mars (e.g., Selby et al., 1974; Bourke, 2004), and we suggest that it applies to the overall accumulation of light- and dark-toned beds in the cavi unit (ABb_c).

Light-toned layer sequences in the cavi unit can extend horizontally for kilometers, as in Boreum Cavus (e.g., Fig. 10; see also Fishbaugh and Head, 2005). In close-up view, these sets of layers undulate in thickness and appear to be steeply dipping where they fan and pinch out (e.g., Fig. 9A inset). This bedding pattern is indicative of low-relief variability in the depositional surface caused by horizontally variable rates in accumulation in both the light- and dark-toned beds. Thus where layers pinch out, accumulation temporarily did not occur or layers were eroded away before superposed layers were emplaced. The relief of these pinch outs is uncertain without detailed topographic data, but may commonly be on the order of meters given that they generally involve only one set of layers at a given location, whereas subsequent layer sets infill the resulting gap (e.g., Fig. 9A inset). These relations indicate that the accumulating unit surfaces were undulating at horizontal scales of hundreds of maters. This paleo-landscape is reflected in the elongate, oriented hollows that have developed in part of the eroding scarp of Boreum Cavus (Fig. 9A). We propose that this laterally-variable accumulation pattern resulted from uneven accumulation of the light- and dark-toned layers, facilitated by repeated mantling by sand sheets, much like those that coat the surfaces of Boreum Cavus and the plateau surface east of it (Fig. 10).

Understanding the layering character of the cavi unit (ABb_1) as above is helpful for mapping it. Where evenly-layered, the ABb_c unit is difficult to discriminate from the Rupes Tenuis unit (ABrt). We suggest that the ABrt unit does not have dark, sandy interbeds (see Fig. 7), but this suggestion needs further testing. The overlying Planum Boreum 1 unit (ABb_1) has variable contact relations with the ABb_c unit, as follows. (1) In most places,

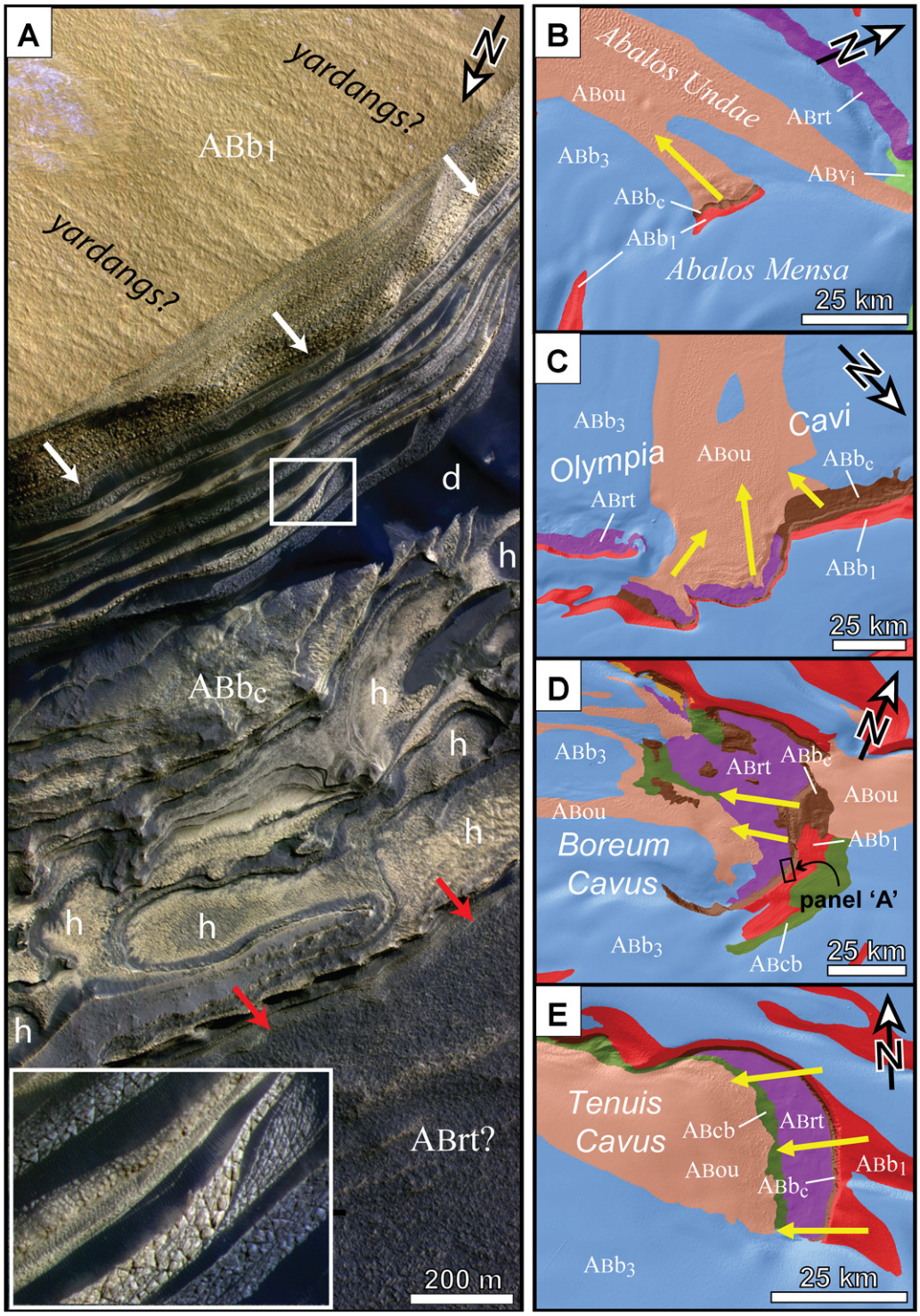

Fig. 9. Image and geologic map excerpts showing the Planum Boreum cavi unit ($A\text{Bb}_c$) and its stratigraphic relationships with adjacent units. (A) Color-enhanced view of west-facing scarp wall and adjacent floor of Tenuis Cavus [see (D) for location]. Planum Boreum 1 unit ($A\text{Bb}_1$) unit forms orange-yellow surface sculpted into rugged, linear grooves that may be yardangs. Plateau surface and upper part of scarp consists of Planum Boreum 1 unit ($A\text{Bb}_1$), which gradationally overlies (along white arrows) alternating bright and dark layers of Planum Boreum cavi unit ($A\text{Bb}_c$). Hummocky surface and subtle topographic benches (below red arrows) may be layers of Rupes Tenuis unit (ABrt?) (or, alternatively, Vastitas Borealis interior unit, $A\text{Bv}_i$), perhaps thinly veneered with dark fines. Inset at lower left (blow-up of smaller box) shows detail of light-toned fanning beds of $A\text{Bb}_c$, which exhibit polygonal fracturing and occur in packages of similar color and texture. These beds indicate pockets of beds of uneven thickness separated by lenses of dark-toned, sandy material. Erosion of such lenses and overlying deposits may lead to formation of elongate hollows (h) hundreds of meters across in the broader scene. Note thick accumulation of dune sand (d) along base of steeper part of scarp, which includes meter-scale ripples (seen in inset), perhaps indicative of cross-slope winds mobilizing sand-sized particles. (Excerpt from HiRISE PSP_1334_2645; illumination from upper right; scale bar is approximate.) (B–E) Geologic maps of areas of unit $A\text{Bb}_c$ exposures (dark brown unit) in lower parts of cavi walls. Yellow arrows indicate dominantly southwestward transport pathways of sand based on dune-train orientations; the cavi sand sources feed vast circum-polar dune seas mapped as Olympia Undae unit (ABou) (see Fig. 3A).

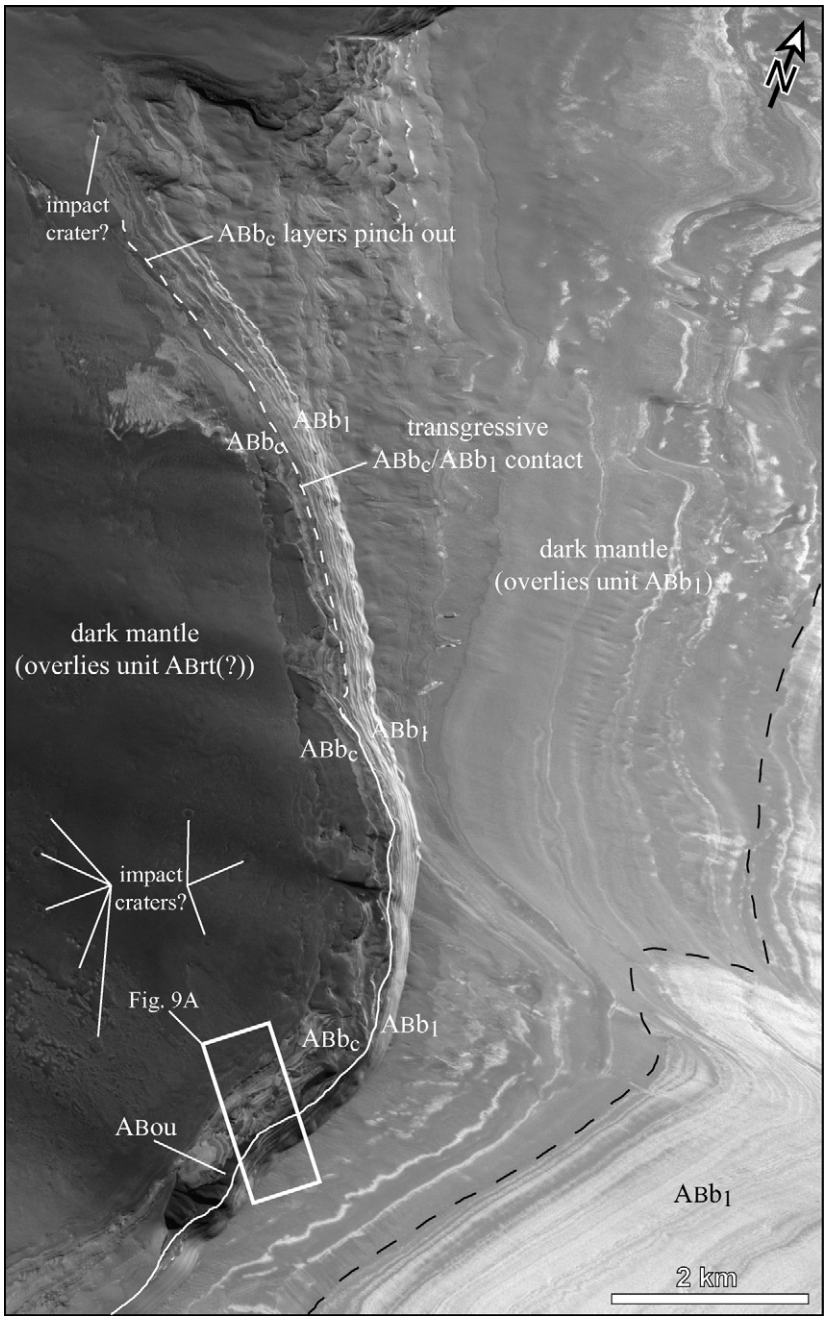

Fig. 10. View of eastern Boreum Cavus at head of Chasma Boreale, flanked by Planum Boreum. Inferred stratigraphy bottom to top includes cratered Rupes Tenuis unit (ABrt?), multi-layered Planum Boreum cavi and 1 units (ABb_c and ABb_1, respectively) and patch of dunes on scarp making up Olympia Undae unit (ABou). Dark mantles cover most of scene left of dashed black line. Note ABb_c/ABb_1 contact (white line) becomes transgressive (dashed white line) and lower layers of ABb_c unit pinch out along northwestern part of scarp. Location of Fig. 9A shown. (Excerpt from CTX P01_001334_2644; illumination from lower left; scale bar is approximate; see Fig. 1 for location.)

the units are conformable and gradational across several layer sequences based on transitions in layer albedo and morphology (e.g., Fig. 9A). (2) In Olympia Cavi, the contact at least locally forms an abrupt, irregular unconformity, and thus is distinctive (e.g., Fig. 8C). (3) In the wall of Boreum Cavus, a transgressive relation is indicated as darks layers in the top part of the ABb_c unit gradually pinch out to the south such that the sequence transitions laterally into the ABb_1 unit (Figs. 9A and 10).

We also find that layers of the cavi unit (ABb_c) pinch out northward below the transgressive contact in Boreum Cavus (Fig. 10), such that the unit thickens toward and perhaps beneath northern Gemina Lingula, as portrayed in Fig. 4E. These relations suggest that accumulation of the cavi unit in this area began beneath northern Gemina Lingula then shifted toward northern Boreum Cavus, where sand sheets presently prevail (Fig. 10). These younger sequences appear to form the northern walls of upper Chasma Boreale, where the cavi unit apparently onlaps unit ABrt and pinches out somewhere northwest of the chasma (Fig. 4E), as it is not observed in the vicinity of Crotone crater.

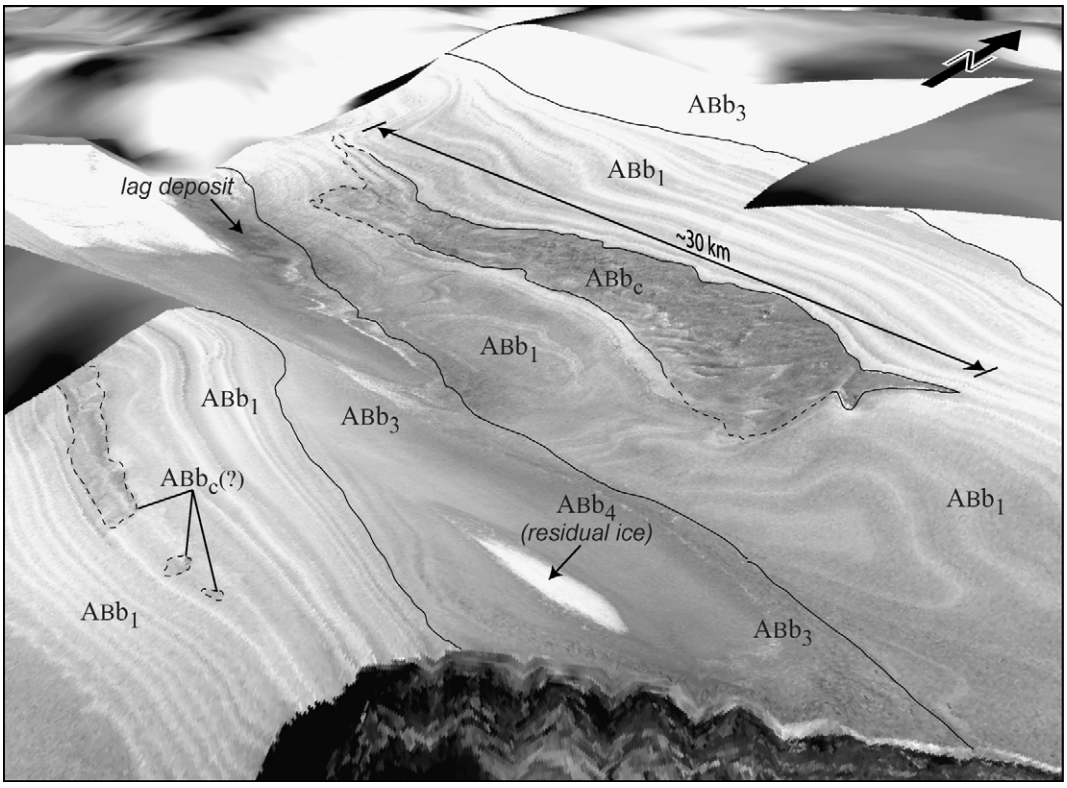

Fig. 11. Oblique view directed to the northwest of Boreales Scopuli trough system of Planum Boreum above scarp of western Olympia Rupēs (foreground). An outcrop ~30 km long made up of several layers of Planum Boreum cavi unit (ABb_c) in lower part of 400-m-high, south-facing trough wall occurs within and interfingers westward with Planum Boreum 1 unit (ABb_1) (see schematic profile in Fig. 3C). Note possible additional, smaller outcrops of the cavi unit (ABb_c?) in the adjacent, south-facing trough wall at left. Planum Boreum 3 unit (ABb_3) caps plateau and north-facing trough surfaces. Dark material interpreted to be lag deposit covers part of western trough floor. Image composed of parts of two CTX frames (P01_001593_2635 and P01_001646_2639; illumination from south) draped over a 3D surface constructed from MOLA using ~7× vertical exaggeration.

Another possible outcrop of the Planum Boreum cavi unit (ABb_c) forms an elongate (~3 × 30 km in size) bench of dark layered material in a Boreales Scopuli trough above western Olympia Rupēs (Fig. 11). The dark layers grade laterally on the western end of the outcrop into typical layers of unit ABb_1. The eastern end of the outcrop pinches out farther east in the ABb_1 unit. The surface of the outcrop has a rippled texture, including cuspate scarps at hundreds-of-meters length scales common in other exposures of the cavi unit (ABb_c). This outcrop is the basis for showing a lens of the cavi unit within unit ABb_1 in a cross-section (Fig. 4C) and in the stratigraphic column (Fig. 3C). The appearance of this lens is similar to thick bench-forming layers previously noted as possible marker beds in north polar layered deposits (e.g., Kolb and Tanaka, 2001; Malin and Edgett, 2001; Herkenhoff et al., 2007). We interpret this outcrop of unit ABb_c and its observed lateral transgression into unit ABb_1 as indicative of episodes of local deposition of sandy, cavi-unit type layers during accumulation of unit ABb_1. If the marker beds formed the same way, then regional episodes of sandy material deposition are indicated as well.

A mound-shaped outcrop of the cavi unit (ABb_c) on the west flank of Abalos Mensa (81.7° N, 282.7° E; THEMIS VIS V13459003) crests at ~ −4500 m and descends down to ~ −4600 m. The depression in which this outcrop is located extends to < −4800 m in places, whereas local Vastitas Borealis surfaces extend < −5000 m. These elevation observations indicate that below the depression and above Vastitas Borealis, the rock sequence may accommodate more of unit ABb_c and/or the Rupes Tenuis unit (ABrt) (Fig. 4B). Thus far, the cavi unit has not been observed in lower parts of Tenuis Mensa or in other, low-relief outliers of north polar layered deposits

Overall, it appears that the Planum Boreum cavi unit (ABb_c) was emplaced surrounding and up against lower flanks of parts of the Rupes Tenuis unit (ABrt). The unit accounts for the half-dome shape of Olympia Planum, which raises the possibility that the buried cavi unit beneath Planum Boreum forms a similar, partial apron around the eroded surface of the Rupes Tenuis unit (ABrt) beneath Gemini Scopuli and perhaps a tongue beneath and forming an inner core of Gemina Lingula (Figs. 1, 4C–4E). Erosion has removed some of the unit in Olympia Cavi, most of it within Chasma Boreale, and nearly all of it along the Rupes Tenuis scarp (assuming it was formerly extensive here, except where protected within Abalos Mensa).

4.2.2. Planum Boreum 1 unit (ABb_1)

This finely-layered unit overlies the Vastitas Borealis interior (ABv_i), Rupes Tenuis (ABrt), and Planum Boreum cavi (ABb_c) units. Its basal layers disconformably overlie those of the former two units where their buried surfaces are flat, whereas contact relations with the cavi unit (ABb_c) are complex (see Section 4.2.1). In Planum Boreum above Rupes Tenuis and along

margins of outer Chasma Boreale, the Planum Boreum 1 unit (ABb_1) forms layered sequences tens to a few hundred meters thick and is draped over the irregularly-shaped, eroded topography of unit ABrt [see also equivalent units of Herkenhoff (2003), Fishbaugh and Head (2005), and Tanaka (2005) in Table 1].

The Planum Boreum 1 unit (ABb_1) consists of horizontally-extensive layers and dozens of local unconformities primarily exposed in extensive systems of troughs and scarps of Boreales and Gemini Scopuli (Fig. 1) and local outcrops perched on the surrounding plains, including Abalos, Tenuis, and Olympia Mensae and Olympia Planum, and perhaps in local depressions and craters (such as Korolev at 73° N, 164° E) (Fig. 3A; e.g., Garvin et al., 2000a; Malin and Edgett, 2001; Milkovich and Head, 2005, 2006; Tanaka, 2005; Tanaka et al., 2005). The uneven surface of this unit and large relief of its base on top of the ABv_i, ABrt, and ABb_c units indicate that the thickness of this unit is highly variable. The ABb_1 unit likely exceeds 1500 m in thickness in the vicinity of the north pole (primarily >86°–87° N) and in the central part of Gemina Lingula, based on the thickness of outcrops within regional spiral troughs. In HiRISE and MOC images, distinct layers can be resolved at approximately decimeter to meter thicknesses based on their widths in images and mean slopes in MOLA data (e.g., Tanaka, 2005; Herkenhoff et al., 2007). As such, the number of layers in a 500-m-thick deposit may range from hundreds to thousands.

Within the north-central crescent of Olympia Planum that is not obscured by the Olympia Undae dunes, five distinct, concentric scarps can be identified in the 115-m/pixel resolution MOLA DEM (Fig. 8A). These scarps delineate platforms or terraces that are several kilometers wide, ~10 m high, and as much as >300 km long. They gently peak in elevation above central Olympia Planum. The platforms behind each scarp in some cases dip gently northward-opposite the regional slope. We interpret these benches as made up chiefly of layer sequences of Planum Boreum 1 unit (ABb_1), based on their broad continuity, flatness, and layering where exposed in scarps. The northward dip of the benches may actually represent not the bedding attitude but instead enhanced erosion along below inter-bench scarps. In addition, the series of westward-progressing depressions that comprise Olympia Cavi are connected by surface scours, grooves, and "funnels" that trend southwestward, paralleling local dune patterns (Fig. 8A). We suggest that the saltation of sand removed from Olympia Cavi provide a scouring mechanism that may have aided in the exposure and sculpting of the subtle topographic platforms of northern Olympia Planum.

A few additional, lower-elevation platforms occur within and are buried by the northern Olympia Undae where they are relatively short and discontinuous. However, parts of the southwestern margins of Olympia Planum (e.g., at 80.6° N, 160° E and 81.3° N, 138° E) display scarps bounding smooth benches <160 m high and mostly clear of dunes. These outcrops may be made up of unit ABb_1, as eroded remnants of formerly-continuous deposits perhaps extending southwestward to Olympia Mensae, which display outcrop margins of similar height and form. In the depression partly shown in Fig. 8C, the ABb_1 unit is several tens to >100 m thick. Overall, the ABb_1 unit seems to thinly cover northern Olympia Planum north of Olympia Undae and at least parts of south-central and southwestern Olympia Planum beneath Olympia Undae. However, it is at least locally (Fig. 8B) and perhaps broadly absent beneath eastern Olympia Undae.

The layers that comprise unit ABb_1 appear alternately light and dark, and the direct tonal contrast between the layers is likely to depend on vertical variations in albedo and texture as well as on illumination conditions. The albedo of the layers varies significantly in HiRISE images (e.g., Fishbaugh et al., 2007; Herkenhoff et al., 2007; Tanaka, 2007) and may reflect in many cases the colors of surficial deposits rather than that of the unit itself. Bright surfaces may include CO_2 frost, while dark surfaces may include recent dust lags that preferentially collect on broader and/or coarsely-textured layer and unconformity surfaces of the Planum Boreum 1 unit (ABb_1) as seen in some HiRISE images (Fig. 12).

CRISM observations indicate that the Planum Boreum 1 unit (ABb_1) exposes generally intermediate concentrations of water ice in the cliff faces of Chasma Boreale and adjacent troughs. An ice-poor signature occurs where the unit forms broad grooves in the plateau surface east of Tenuis Cavus (84.6° N, 4.6° E and 84.4° N, 3.6° E; Seelos et al., 2007); here, the unit may be mantled (see Section 5).

Dozens of unconformities in unit ABb_1 have been identified in Viking and MOC images (Fig. 12; e.g., Howard et al., 1982; Malin and Edgett, 2001; Tanaka, 2005; Fortezzo and Tanaka, 2006). The lateral traceability of the unconformities can help reveal significant stoppages in material accumulation of local to regional extent. Eastern Gemini Scopuli, where troughs and scarps are largely interconnected, is an optimal site to map the horizontal extents of unconformities in the ABb_1 unit. In this region, angular unconformities are mostly present on and confined within equator-facing slopes within troughs as observed in THEMIS VIS images. These unconformities range from ~2 to 20 km in length. Notably, the majority of truncated layers are found near the margins of the north polar plateau where size and depth of the troughs (compared to those at higher latitudes) expose thick sequences of layered deposits. Typically, troughs have no more than one identifiable unconformity. However, there are instances of multiple angular unconformities within a single trough. Multiple, stacked, angular unconformities in some troughs suggest localized, episodic erosion and deposition (e.g., Tanaka, 2005). Rarely, multiple angular unconformities are linked by what we interpret as a disconformity (or parallel unconformity, where the layers above and below the unconformity are parallel and appear conformable). Tracing apparent disconformities is facilitated when (1) there are multiple angular unconformities that pinch out against it, but elsewhere the overlying and underlying beds appear to be conformable, and/or (2) a unique-appearing marker bed or set of beds (as characterized by apparent thickness, color, or texture) is identified in the superposed layers and in association with layer truncations at other locations. Such relations are locally observable in MOC, HiRISE, and CTX images

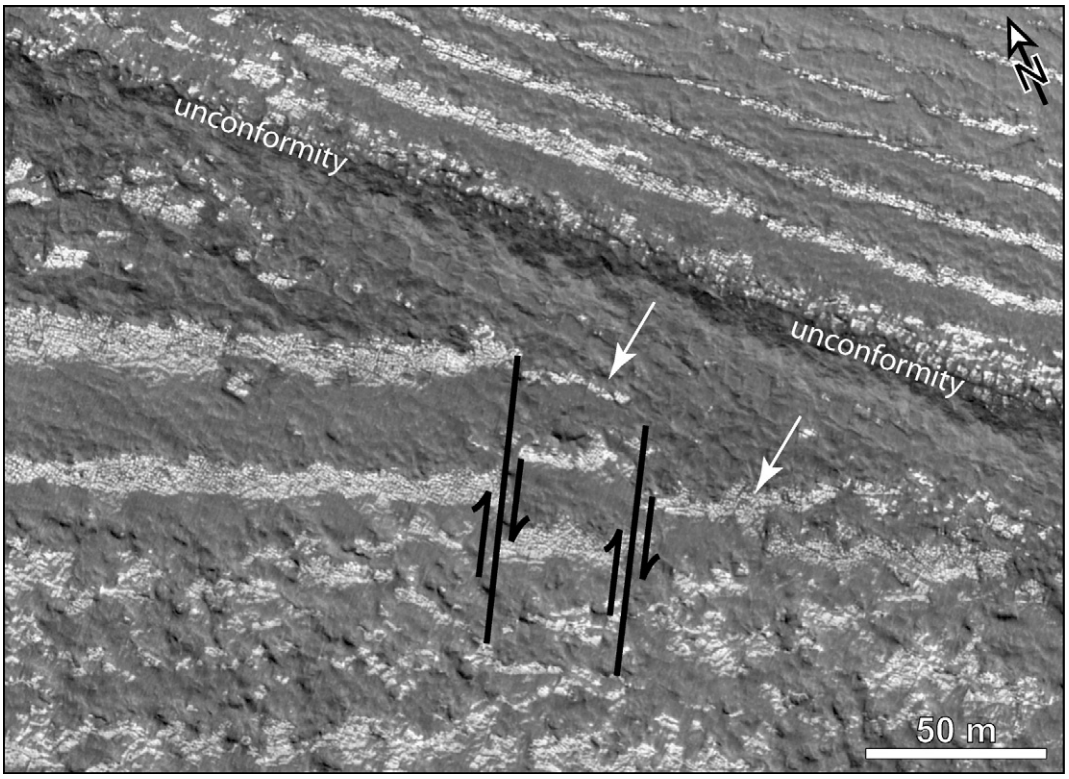

Fig. 12. View of steep scarp (nearly 30° slope in MOLA data) of eastern Gemini Scopuli made up of Planum Boreum 1 unit (ABb_1). Note unconformity, which consists of a hummocky terrace covered by dark material. Layers above the unconformity appear rather uniform, whereas lower layers (white arrows) show offsets as indicated. (Excerpt of HiRISE PSP_001398_2615; centered near 81.5° N, 47.3° E; illumination from lower left.)

Thus far, we have not found evidence for regional inter-trough and perhaps Planum Boreum-wide erosion. This may in part be due to the difficulty in tracing unconformities in THEMIS VIS images. In addition, regional erosional events may have been more severe in some troughs than others, such that correlating unconformities may be particularly challenging. Furthermore, the elevations of mapped unconformities are variable (between ~ -3500 and -5000 m) and tend to be higher the farther north they occur. This relation may indicate that past erosion followed the dome-like profile of the polar plateau existing at the times when unconformities were produced.

A study of unconformity dip directions near the margin of Planum Boreum using THEMIS VIS images and MOLA topography indicates a dominant east–southeast trend of unconformities in mostly equator-facing walls (Fortezzo and Tanaka, 2006). This dip trend is inconsistent with the insolation-induced ablation model for trough formation and migration (Howard, 1978; Howard et al., 1982). Instead, the trends are generally near perpendicular to the trend of the troughs, which are consistent with their marking major stages in trough formation during accumulation of the ABb_1 unit, perhaps in association with retreat of the planum margin (Fortezzo and Tanaka, 2006).

Some steep scarps of the Planum Boreum 1 unit (ABb_1) display layer offsets of less than a few tens of meters along the plane of the outcrop surface. In one location, the offsets occur immediately below an unconformity surface (Fig. 12), suggesting that offsets formed prior to the unconformity and were not subsequently active.

HiRISE images indicate that most light-toned layers in Planum Boreum 1 unit (ABb_1) exposed in cliff faces contain extensive cracks (e.g., Fig. 9A); each are several to a few tens of meters long and spaced a few meters (or less) apart (Byrne et al., 2007; Herkenhoff et al., 2007; Tanaka, 2007). As in the case of the cavi unit described previously, fractures may be instrumental in facilitating erosion of the ABb_1 unit. Locally, meter-wide ridges occur in the bright layers that may be veins of relatively resistant material filling the cracks (HiRISE PSP_001398_2615). They may represent hardening of material along fractures due to chemical alteration or recrystallization.

4.2.3. *Planum Boreum 2 unit (ABb_2)*

This unit overlies units ABb_1, ABb_c, ABrt, and ABv_i. In particular, the unit unconformably overlies the ABb_1 unit along the latter's uppermost slopes and south-facing margins, where it is interpreted to form modest angular unconformities or parallel unconformities. Unit ABb_2 is overlain by units ABcb, ABb_3, and ABb_4 (see below) in many areas.

This unit was first sub-divided from the "classical" layered deposits by Rodriguez et al. (2006b) as low-albedo materials that form layers and interior deposits in numerous polar troughs. These materials are locally eroded into grooves and pit chains and form the initiation zones of extensive systems of veneers, suggesting that they form a poorly-consolidated deposit (Rodriguez et al., 2007b). The observation that the materials

that form the Planum Boreum 2 unit (ABb_2) appear to be easily mobilized by wind, and that the perennial ice that surrounds their outcrops appears to have undergone retreat, suggests that these materials contain sand-sized particles (Rodriguez and Tanaka, 2007). In addition, correlations between image data and OMEGA water-ice maps reveal that this unit is free of water ice and thus likely consists primarily of lithic particles (Rodriguez et al., 2007b). In these occurrences, the deposit appears to be meters to tens of meters thick, displays no clear layering, and appears to be readily eroded and mobilized into veneers. Along the tops of most equator-facing scarps of Planum Boreum, the unit is not apparent in available images. This may indicate either that the unit is either absent or obscured in such locations.

We recognize outcrops of similar appearance and stratigraphic position elsewhere within Planum Boreum. As such, we include these outcrops as part of the Planum Boreum 2 unit (ABb_2). However, we note that this does not mean that they are remnants of a formerly continuous deposit that covered most of Planum Boreum or that they all formed synchronously. Outcrops of similar appearance and stratigraphic position occur: (1) in some troughs of Boreales and Gemini Scopuli, where the unit may reach 100 m in thickness (Rodriguez et al., 2007b); (2) in northwestern Chasma Boreale, where the unit coats layers made up of the ABb_2 and ABb_1 units (Fig. 13B) and has a water-poor signature in CRISM data (Seelos et al., 2007); and (3) as small, dark, isolated, locally-layered patches around Planum Boreum including east of Chasma Boreale, where it reaches 50–60 m in thickness (e.g., MOC E23-0811, R23-01073, and R22-00901) and in impact craters and their ejecta blankets [e.g., Jojutla crater (HiRISE TRA_000865_2615) and a 7.5-km-diameter crater at 79.2° N, 323.7° E (MOC E01-01028)].

4.2.4. *Chasma Boreale unit (ABcb)*

This unit (ABcb) locally exhibits up to 40 layers, which are exposed in parts of Chasma Boreale, including Tenuis and Boreum Cavi, as seen in MOC and CTX images (Fig. 13). In northern Tenuis Cavus, the unit overlies embays units ABb_c and ABb_1 (Fig. 13A) and what appears to be eroded ridges and mesas of unit ABrt (CTX P01_001346_2647). In southern Tenuis Cavus (84.4° N, 1.8° E; MOC R23-00158 and S01-00925), the ABcb unit is overlain by dunes and a coarsely-textured (possibly eroded) part of the ABb_3 unit, which extends from the surface of Planum Boreum down onto the southern wall of Tenuis Cavus. Small patches of the unit appear to cover the ABb_2 unit in Chasma Boreale, but this relation requires further scrutiny as the ABb_c and ABb_2 have similar dark, layered appearances. The ABcb unit layers are wind-sculpted and show little development of layer-controlled terraces, unlike those commonly observed in nearby exposures of units ABb_1 and ABb_3. This may indicate that the unit is relatively friable and poorly consolidated. Unit ABcb may include local unconformable sequences, as displayed in northern Tenuis Cavus. The unit also may form much of the buried part of the broad, layered elongate mound that covers the southwestern part of Boreum Cavus and much of eastern Chasma Boreale (Fig. 4A). Here, it is overlain by the Hyperborea Undae dune field and its rippled sand sheet (unit Abou), by unit ABb_3, and by a band of residual ice (unit ABb_4). The unit displays moderate water-ice content in CRISM data (Seelos et al., 2007).

We interpret the unit to mark a period of first deposition and then erosion (accounting for the unit's patchy, draped appearance on subjacent units), which we have not recognized elsewhere around Planum Boreum. Although the ABcb unit is only of local extent, the unit's stratigraphic position and morphologic character leads us to suggest that the contact between units ABb_2 and ABb_3 represents a hiatus in the accumulation of layered sequences of sufficient duration to accommodate possible erosion of the ABb_2 unit followed by local deposition and erosion of the ABcb unit.

4.2.5. *Planum Boreum 3 unit (ABb_3)*

This unit forms a sequence of several, commonly ill-defined layers that overlie units ABb_c, ABb_1, ABb_2, ABcb, and parts of Abou. It forms most of what was previously described as "banded terrain" (Howard et al., 1982) and mapped as "Planum Boreum 2 unit" (Tanaka et al., 2005) and "upper layered deposits" (Tanaka, 2005). In this paper, we divide the latter into units ABb_2 and ABb_3. The ABb_3 unit has a maximum thickness of a few tens of meters near its margins and occurs over much of Planum Boreum on plateau surfaces and north-facing scarps and trough walls cut into the ABb_1 unit (e.g., Figs. 3, 4, 6, 8, 9B–9E, 11, 13). Locally, the unit occurs as relatively bright material covering rippled, interdune surfaces, such as in northwestern Olympia Undae, and thus largely postdates the Abou unit (HiRISE PSP_001593_2635 at 83.5° N, 118.8° E). It has variable albedo that may largely be due to surficial coatings of water ice, CO_2 frost, and lithic veneers (see Section 5). Thus far, we have found few contacts of the unit with the middle- to high-latitude mantle material described by Mustard et al. (2001), which also embays dunes and infills inter-dune lows of the Olympia Undae unit. East of Chasma Boreale, the mantle appears to embay and overlie the ABb_3 unit (MOC R23-01073). Craters are sparse on unit ABb_3; two craters <100 m in diameter in MOC images indicate a surface age of <15 ka (Tanaka, 2005). However, since this age is inferred from just a couple, small craters, the age and its implications should be viewed with caution.

4.2.6. *Planum Boreum 4 unit (ABb_4)*

The high-albedo, texturally-distinct Planum Boreum 4 unit (ABb_4) caps the bulk of the polar plateau and buries the underlying layered sequences. The unit is mostly underlain by unit ABb_3. It forms the residual ice cap, as mapped previously by Tanaka and Scott (1987) and Tanaka et al. (2005). The distribution of the unit based on its bright albedo in MARCI color data (Fig. 14) matches closely with high surface water-ice concentrations mapped by CRISM data in the Chasma Boreale region (see Fig. 2 in Seelos et al., 2007). In MOC (Thomas et al., 2000) and HiRISE images (e.g., Byrne et al., 2007), the unit displays pitted, cracked, and ridged textures at meter to decameter scales that may result from redistribution of material due to aeolian processes (as in formation of small dunes of granular ice) and sublimation. HiRISE color data in late summer shows that the material in the floors of the pits is the same

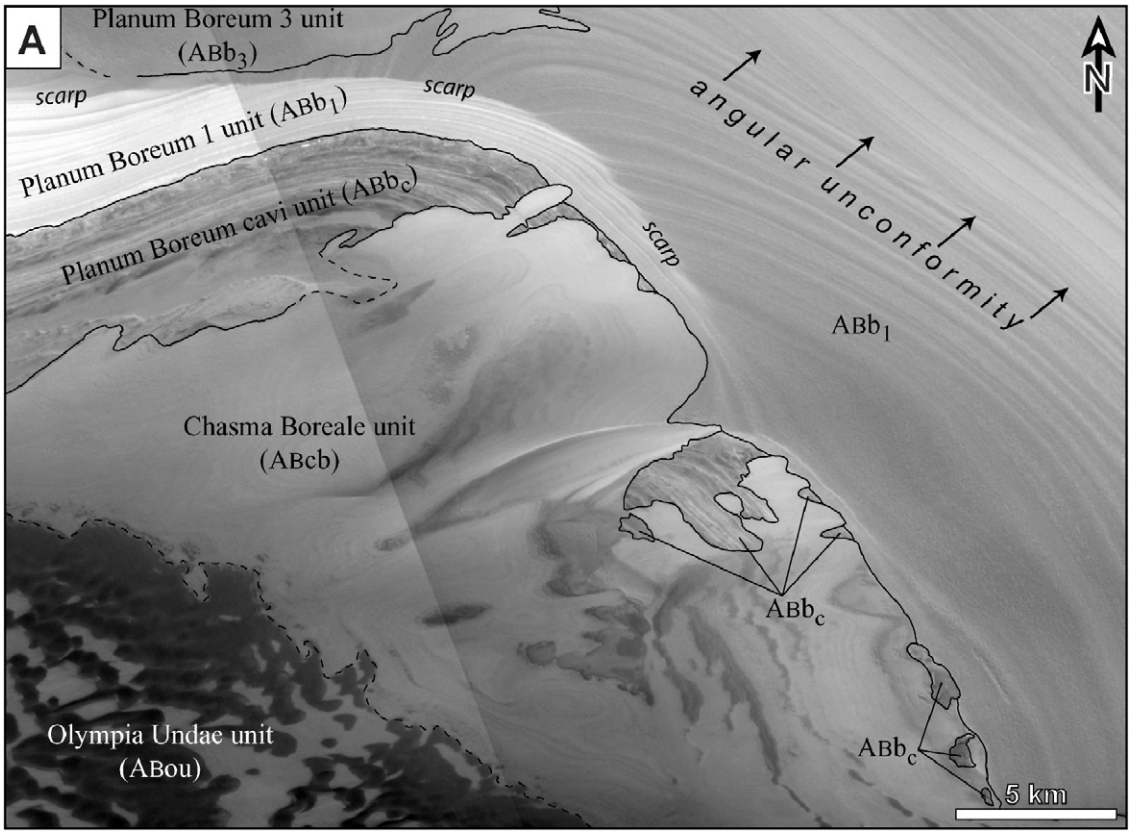

Fig. 13. Views of Chasma Boreale walls showing stratigraphic relations among map units. (A) Northeastern corner of Tenuis Cavus shows inferred stratigraphy from oldest to youngest: Planum Boreum cavi unit (ABb_c; dark, rugged layers), Planum Boreum 1 unit (ABb_1, bright, even layers with unconformity), Chasma Boreale unit (ABcb, bright layers overlapping ABb_c and ABb_1 units), Planum Boreum 3 unit (ABb_3), and dunes of the Olympia Undae unit (ABou). (Excerpt from a mosaic of CTX T01_000885_2645 and P01_001703_2645; illumination from bottom; scale bar is approximate.) (B) Part of northwestern Chasma Boreale shows inferred stratigraphy from oldest to youngest: Planum Boreum cavi (ABb_c; dark, rugged layers on chasma floor), Planum Boreum 1 unit (ABb_1, even layers in chasma wall), Planum Boreum 2 unit (ABb_2, dark layers coating chasma wall), Chasma Boreale unit (ABcb, bright layers overlapping ABb_c unit), Planum Boreum 3 and 4 units ($ABb_{3,4}$, uppermost layers and residual ice on upper and lower plateau surfaces), and dark dunes of Olympia Undae unit (ABou). (Excerpt from CTX T01_000807_2638; illumination from left; scale bar is approximate.)

color as the underlying Planum Boreum materials (Byrne et al., 2007), which indicates that the thickness of the ice may be the same as the relief of these features, previously measured to be ~20 cm in one MOC image (Herkenhoff et al., 2002). Furthermore, features overlain by unit ABb_4 are not obscured (e.g., Figs. 15B and 15C), also indicating that the unit is thin. A dark lag may also occur between the Planum Boreum 3 and 4 units (Fig. 15B). Along the tops of scarps in Planum Boreum, the ABb_4 unit is seen to unconformably overlie the ABb_2 and ABb_3 units. Impact craters observed beneath the thin ABb_4 unit yields an age of <15 ka for the surface of the ABb_3 (Tanaka, 2005), suggesting that the unit ABb_4 residual ice has accumulated over this period. This duration is consistent with its formation during the decline in north polar insolation since 21.5 ka (Montmessin et al., 2007).

4.3. Materials throughout Amazonian (< ~3 Ga)

4.3.1. Crater material

Impact craters occur throughout the martian stratigraphic record. In the north polar region, most impact craters reside on Early Amazonian materials, including the Vastitas Borealis interior (ABv_i), Scandia region (ABs), and Rupes Tenuis (ABrt) units. Given that the Early Amazonian crater population by definition is made up of ~63% of all Amazonian craters ⩾5 km in diameter (Tanaka, 1986), then a majority of craters in the northern circum-polar plains are likely to be Early Amazonian.

Many of these impact craters have ejecta deposits and crater interiors that are elevated tens to hundreds of meters above adjacent plains (units ABv_i and ABs) (Mouginis-Mark, 1979; Tanaka et al., 2005; Tanaka, 2005; Skinner et al., 2006). These raised craterforms are also referred to as "pedestal craters." Geologic relations at Planum Boreum may elucidate what the material is that makes up the majority of the pedestals. On Planum Boreum, several craters ⩾5 km in diameter that are superposed on unit ABrt form pedestal craters and rounded margins (e.g., Boola crater) of the Rupes Tenuis scarp (Figs. 1 and 2). Unit ABrt itself shows extensive backwasting that has resulted in scarps hundreds of meters high. This unit appears to be the only reasonable candidate to make up the 700-m-high plateau upon which Escorial crater rests. Abalos Colles

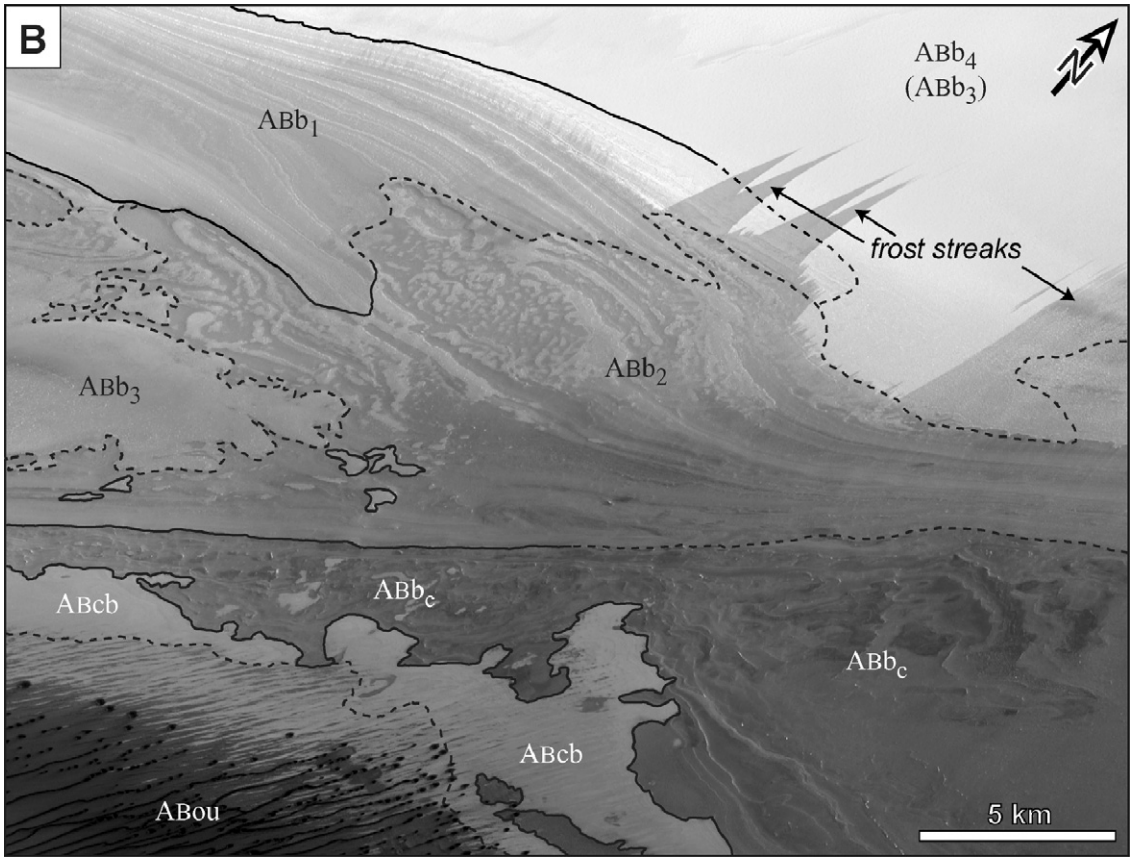

Fig. 13. (*continued*)

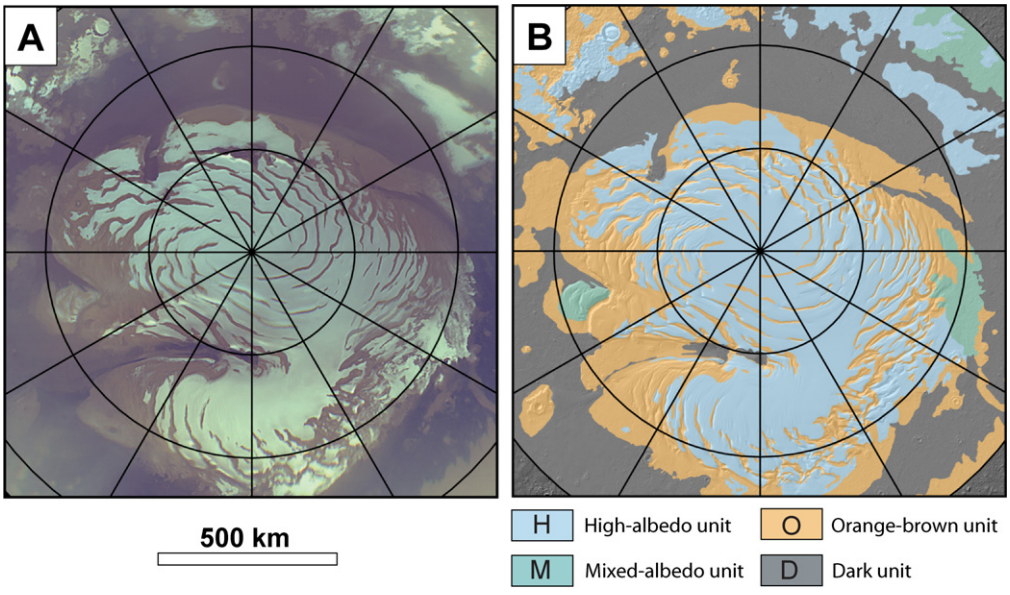

Fig. 14. View and map of Planum Boreum region, Mars (polar stereographic projection centered at north pole). (A) MARCI color image mosaic (~900 m/pixel) acquired during northern summer. (B) Color and albedo unit map based on (A). Unit interpretations include: H, residual ice/Planum Boreum 4 unit (ABb_4); O, on Planum Boreum, mostly Planum Boreum 1 and 3 units ($ABb_{1,3}$) and in Vastitas Borealis, mostly ice-rich soil; M, mixture of H and O units; and D, sand sheets and dunes, including Olympia Undae unit (ABou).

(Fig. 2) have been interpreted to be volcanic cones (Garvin et al., 2000b) or pedestal craters in which the flanks beyond the crater rims have been eroded, as an extension of the ABrt unit (Tanaka et al., 2003). Pedestal craters are also common at lower latitudes of the northern plains (Mouginis-Mark, 1979; Tanaka et al., 2005). Possibly the pedestal material is also the

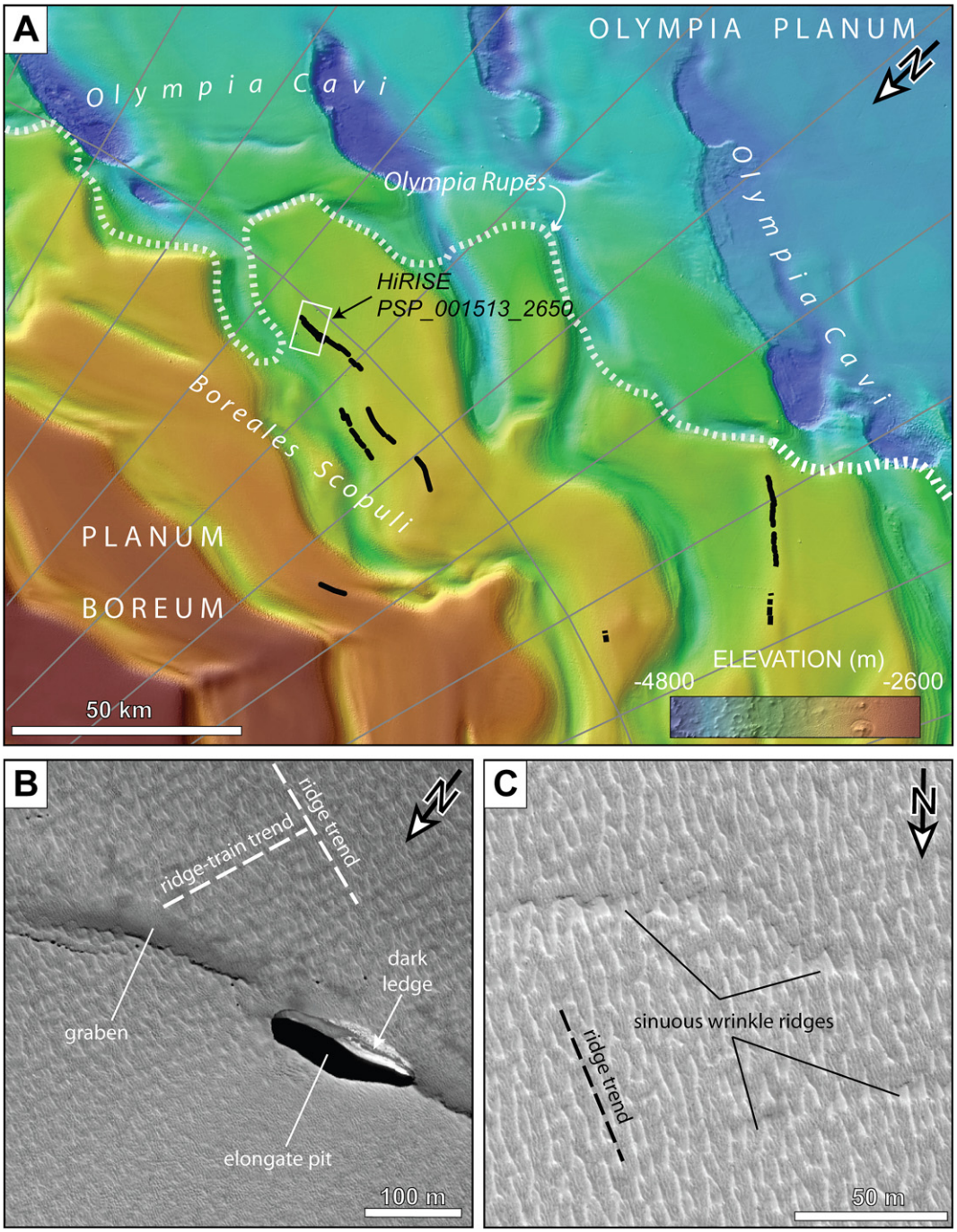

Fig. 15. Graben systems in part of Boreales Scopuli region of Planum Boreum. (A) Grabens (black lines) occur on ridge crests and flanks between Boreales Scopuli troughs, which align with depressions of Olympia Cavi below Olympia Cavi and Rupēs. Location shown of HiRISE image partly displayed in (B) and (C). (MOLA DEM, 5° grid, polar stereographic projection, north at lower left.) (B) Part of WNW-trending graben on broad ridge in middle of HiRISE image with 60 × 160 m elongate depression along the steeper, southern wall. Note dark material exposed on ledge in pit; bright material in pit made up of Planum Boreum 3 unit (A_{Bb_3}). Residual ice (Planum Boreum 4 unit, A_{Bb_4}) forms northwest-trending ridges meters to tens of meters long and grouped into northeast-trending ridge trains. Illumination from lower left. (C) Sinuous, west-trending wrinkle ridges interpreted to be contractional structures occur in north part of HiRISE image near base of trough [see (A)] and trend parallel to grabens in (B), deforming Planum Boreum 3 unit (A_{Bb_3}). Also note extensive, bright, relatively large, widely-spaced and intervening small, closely-spaced ridges of residual ice (Planum Boreum 4 unit, A_{Bb_4}), which are not organized into trains in this area. Illumination from lower left.

A_{Brt} unit or some stratigraphic equivalent, but their distance of hundreds to thousands of kilometers from Planum Boreum make this suggestion highly conjectural. Interestingly, some of the pedestals at lower latitudes, where not thickly mantled, consist of layered material, exposed both within the crater's interior (e.g., THEMIS V19110010 and MOC e17-01205) and along its platform margin (e.g., THEMIS V13602003 and MOC fha01129). This suggests that not only has much of the Vastitas

Borealis undergone episodic burial and exhumation during the Amazonian (e.g., Skinner et al., 2006), but also that there may be an underappreciated dynamic link between how the lowlands and polar plateau are affected by geologic processes of deposition and exhumation. At higher latitudes around Planum Boreum, the formation of pedestal-type craters by deflation of the underlying ABrt unit could have continued until emplacement of the Planum Boreum 1 unit (ABb_1), as most large craters on the ABrt unit are on pedestals but locally are partly buried by unit ABb_1.

Pedestal craters are commonly interpreted to form through the armoring of once-extensive mantle deposits by impact ejecta followed by the stripping of unarmored mantle extents (e.g., Mouginis-Mark, 1979). However, the manner in which ejecta material inhibits the erosion of the underlying materials has not been well established. It is not uncommon in terrains that have undergone substantial vertical deflation (such as many regions of the Vastitas Borealis) for the ejecta materials to be completely removed, buried, or altered. One possibility is that the interior deposits of impact craters are largely compacted (and possibly cemented) dust and/or silt-sized particles (Rodriguez et al., 2007a). This material in the impact crater interior may act as an impermeable seal, either hindering volatile migration or diverting groundwater migration toward the crater periphery. As such, erosional activity may be focused along an impact crater's outer margin leaving resistant material as the high-standing pedestal. To use a region-specific example, if Abalos Colles are the interiors of eroded craterforms, they would suggest greater induration of the pedestal material immediately beneath the crater rims and interiors.

4.3.2. Olympia Undae unit (ABou)

We collectively mapped the extensive, dark circum-polar dune fields and spatially-associated sand sheets as the Olympia Undae unit (ABou), the extent and character of which were previously delineated by other workers (e.g., Tsoar et al., 1979; Ward et al., 1985; Tanaka and Scott, 1987; Tanaka et al., 2005). The geologic map in Fig. 3A shows the unit where it is expressed as distinct morphologic textures based on the 115 m/pixel MOLA DEM. This version of mapping delineates the unit's margin based on the occurrence and density of closely-spaced irregular ridges and bumps that resolve larger dune forms as well as the underlying and surrounding sand sheets to the extent where they morphologically subdue underlying surfaces. The larger dune fields are named Olympia, Abalos, Hyperboreae, and Siton Undae (see Fig. 1).

This unit is transient in that its materials likely have episodically formed, migrated, and disappeared for much of the Amazonian Period. The Planum Boreum cavi unit (ABb_c) contains the oldest confirmed record of sand accumulation associated with Planum Boreum (Byrne and Murray, 2002), including dune-like cross-bedding (Herkenhoff et al., 2007). Given the evidence for erosion described previously for the Scandia region (ABs) and Rupes Tenuis (ABrt) units, the earliest dunes and sand sheets of the Olympia Undae unit (ABou) may have accumulated beginning in the Early Amazonian (Figs. 3B and 3C). Layer morphology of the ABrt unit in places is similar to that of the ABb_c unit (e.g., Fishbaugh and Head, 2005; Fig. 12), and thus unit ABrt may include sandy deposits as well.

The dunes of the Olympia Undae unit (ABou) are perched on a variety of older units and appear to have carved yardangs into the ABb_1, ABb_2, and ABcb units. Many of the dunes appear to have been largely inactive since emplacement of unit ABb_3 and the circum-polar, stratigraphically-similar, mantle material (however, MOC R23-00615 shows local traces of dune movements of hundreds of meters across mantle material). The dunes commonly have muted forms and most do not show signs of recent movement. Possible exceptions include the head of Abalos Undae (e.g., MOC R01-00728 at 81.7° N, 282.6° E) and parts of the central floor area of Chasma Boreale: (1) where two sets (southwest- and south-southwest-trending) of linear dunes and yardangs mark a bright layered deposit that may be unit ABb_3 (e.g., MOC M02-00815 at 83.2° N, 314.0° E) as it appears to bury the head of Hyperboreae Undae 25 km to the south-southeast, and (2) southwest of Boreum Cavus, where a field of barchan and linear dunes appears to be perched on either a sand sheet or the ABb_3 unit and where oval, flat-floored depressions within the sheet may be the footprints of exhumed dunes (MOC S01-00668 at 84.5° N, 335.9° E; Mullins et al., 2006).

Image analysis (e.g., Byrne and Murray, 2002; Edgett et al., 2003; Fishbaugh and Head, 2005) and geologic mapping (Fig. 3; also Tanaka, 2005) show that some of the dune fields originate from exposures of the ABb_c unit within Abalos Mensa, Olympia Cavi, Boreum Cavus, Tenuis Cavus, parts of Chasma Boreale, and Olympia Planum (Figs. 9B–9E, 8A and 8B). The eastern terminus of Hyperboreae Undae appears buried by the ABb_3 unit. Some of the dunes have dark, downwind streaks associated with them (e.g., MOC image E04-00846) that may indicate movement of sand sufficiently recent to be preserved and not dispersed, as most north polar dunes do not display such streaks. Bourke et al. (2008) have shown that two 20-m-wide dome dunes recently shrank and then disappeared over ~3 Mars years in the north polar area. Locally, dunes overlie irregular, eroded surfaces of Planum Boreum units, including possible yardangs suggestive of varying wind direction (e.g., MOC images R19-01291 and R20-00214). The dunes are commonly surrounded by rippled material that likely constitutes a thin sand sheet that noticeably subdues underlying landforms in the 115 m/pixel MOLA DEM shaded relief image (e.g., Fig. 7). Thus, mapping of the unit based on color information in the MARCI color mosaic of the polar plateau and surrounding plains (Fig. 14) shows more fully the apparent distribution of dark sand, including where it may only be a few grains think. The dark deposits of the northern circum-polar plains also include some of the strongest signatures of TES Surface Type 2, which Wyatt et al. (2004) interpreted to be weathered basaltic sand due to their spatial association with and possible derivation from northern plains materials.

CRISM data covering Hyperboreae Undae indicate that the dune materials (i.e., the Olympia Undae unit, ABou) display the weakest signature of surface ice within Chasma Boreale (Seelos et al., 2007). OMEGA data show a strong signature of gypsum in eastern Olympia Undae (Langevin et al., 2005), and CRISM data indicate that the gypsum occurs on dune crests

and may originate from underlying bedrock, which appears to be exposed as bright fractured material in HiRISE images (Roach et al., 2007). This conclusion is consistent with formation of the gypsum during the Early Amazonian, perhaps in association with formation of the Scandia region unit (ABs) as discussed previously, which (along with unit ABv_i) occurs just east of Olympia Undae (Fig. 3A; Tanaka, 2007). Alternatively, Fishbaugh et al. (2007) suggested that the gypsum resulted from subglacial flooding from Chasma Boreale.

5. Color and albedo units

Surfaces of the north polar region can be divided into units by their color and albedo. Such color units relate to the visual-range albedo and spectral properties of surface materials, which vary according to their lithic and ice composition. Based on an MRO Mars Color Imager (MARCI) Mars' summertime color image mosaic (Fig. 14), when CO_2 frost was largely absent, we define 4 color units, as follows: (1) a high-albedo unit for much of Planum Boreum, (2) a dark unit surrounding Planum Boreum, (3) an orange-brown unit for margins of Planum Boreum and plains south of the dark unit, and (4) a mixed unit comprised of the high-albedo and orange-brown units in close spatial association. North polar THEMIS day-time infrared image mosaics obtained during martian summer were used to investigate surface albedo due to their nearly complete coverage and their close relation to albedo (Christensen et al., 2003). These data show that the orange-brown unit has a low surface albedo and forms three extensive zones in Planum Boreum, whereas the mixed unit, which occurs both on and off of Planum Boreum (Fig. 14), has intermediate surface albedo (Rodriguez et al., 2007b).

The high-albedo unit corresponds closely to the thin, residual water-ice cap mapped as unit ABb_4. It covers most upper plateau surfaces free of dunes of Planum Boreum, Olympia Planum, Olympia Mensae as well as floors of depressions and craters in the Scandia Cavi region and some nearby plains (Figs. 1 and 14). The other color units consist of combinations of the mapped stratigraphic units shown in Fig. 3 and of surficial (generally meters thick or less), poorly consolidated and relatively transient ice and loose materials. We discuss further the latter color units and their significance below.

The dark unit corresponds to surfaces having strong TES Surface Type 2 signatures, which have been interpreted to have basaltic andesite or weathered basalt compositions (Bandfield et al., 2000; Wyatt et al., 2004). The dark unit notably encompasses (and is significantly more extensive) than the Olympia Undae unit that forms dunes and a sheet of material thick enough to subdue underlying polygonal troughs of the Vastitas Borealis interior unit as currently mapped from MOLA data (Fig. 3; Tanaka et al., 2005). The areas of difference occur mainly outside of Olympia and Abalos Undae and the collective dune fields south and southeast of the mouth of Chasma Boreale. The areas of dark surface that have a paucity of dunes and thick sand sheets are composed of relatively thin sheets of sand or finer materials produced by comminution of dark sand, perhaps a few meters thick or less, and/or unmantled bedrock material (e.g., CTX image P01_001506_2600). These dark, dune-free surfaces also are generally farthest removed from cavi dune sources following mapped dune migration paths (Tsoar et al., 1979). We therefore suggest that these areas are mostly covered by dark aeolian fines that represent distal accumulations far dispersed from now-stagnant dunes. This interpretation is consistent with dark wind streaks observed downwind from dark polar dunes in summertime images (e.g., THEMIS VIS V12883002 at 78.6° N, 330.9° E).

The orange-brown color unit of Planum Boreum and of parts of the Vastitas Borealis and Scandia regions is similar in color to much of the material making up the surface of Mars. The material may include oxidized iron-rich dust and duricrust that gives it its color, as previously observed from Earth and various spacecraft (e.g., Soderblom, 1992), and near-surface water ice as detected by the ODY Gamma Ray Spectrometer (Feldman et al., 2004). In Vastitas Borealis, the surface has the texture and likely consists of the geologically recent, meters-thick mantle described by Mustard et al. (2001) that extends from middle to higher latitudes; this mantle overlies unit ABv_i. On Planum Boreum, the orange-brown unit covers most of the marginal surface not covered by the high-albedo unit as well as trough walls (Fig. 14). These zones correspond to low-albedo surface sedimentary mantles that suppress the underlying water-ice signature (Rodriguez et al., 2007b). These mantles consist, at least in part, of dense systems of veneers that typically spread from units ABb_c and ABb_2. Erosion of the materials that form these two units and their subsequent re-deposition across parts of Planum Boreum is likely to be the primary emplacement mechanism of the low-albedo surfaces that correspond to the orange-brown color unit of Planum Boreum.

Erosional lag deposits derived from removal of ice from underlying units as well as material deposited from atmospheric suspension may have also contributed, or perhaps dominated, the emplacement of the orange-brown color unit (e.g., Murray et al., 1972; Kieffer et al., 1976). Evidence for recent accumulations of dust occurs along the east rim of Boreum Cavus, where fractures within unit ABb_1 are subdued and where low, streamlined, rippled mounds are found (Figs. 9A and 16). Where they abut the lip of Boreum Cavus, the mounds display scarp-facing cavities that may reflect erosion. In these cavities, the mound material does not display any layering, as eroded surfaces of other Planum Boreum units generally show. Also, the mounds occur above the scarps, which is where aeolian fines might collect from winds that flowed in the up-scarp direction. In addition, their streamlined forms suggest that they are controlled by wind. We thus interpret the mounds to be dust to silt-size loess transported by wind during a period of upslope wind flow (reverse of the present direction as indicated by dune orientations), and their rippled surfaces may result from modification by wind. Other lags may occur on terraces associated with pronounced layers and unconformities (e.g., Fig. 12).

Other areas display intermediate and/or mixed color signatures, which may correspond to complex surficial geologic processes. For example, north polar THEMIS day-time infrared image mosaics obtained during martian summer shows three low-albedo zones and one zone of mixed high and low albedo

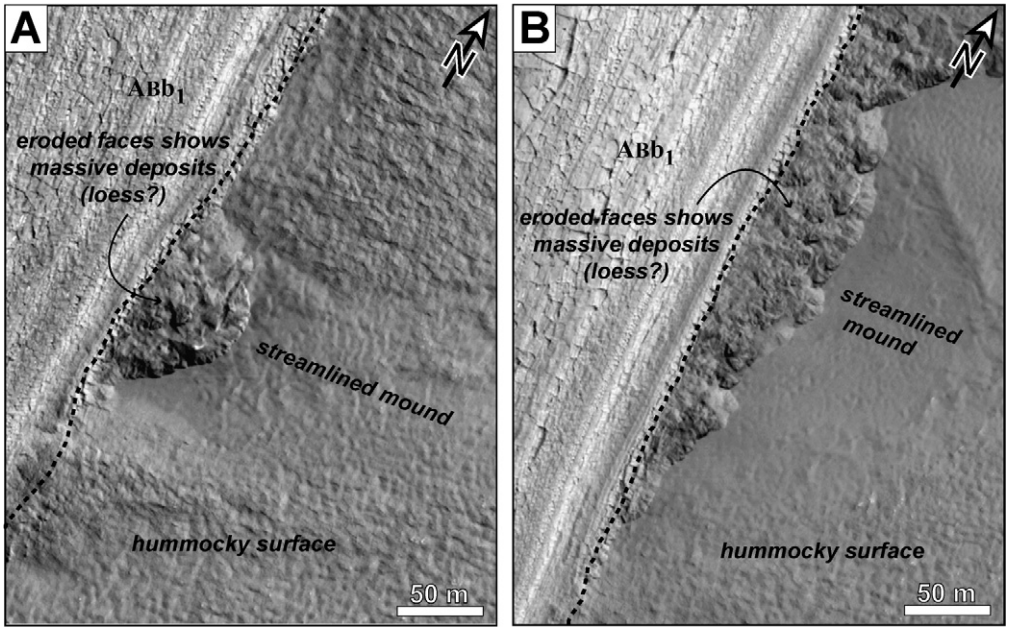

Fig. 16. (A, B) Two views of edge of Planum Boreum above east wall of Boreum Cavus. Steep wall consists of fractured layers of Planum Boreum 1 unit (ABb_1). In contrast, plateau surface has hummocky texture and streamlined mounds that appear eroded along the lip of the cavus head scarp (dashed line). Eroded mound material appears to be unlayered or poorly layered. Mounds and hummocky material may be loess deposits. (Parts of HiRISE image PSC_001334_2645, illumination from lower left.)

with a combined area of ∼16% of the total surface area of the northern polar plateau. The occurrence of the dark ABb_2 unit and veneers within polar troughs is associated with significant erosion and preferential retreat of the ABb_3 unit, which may have led to the exhumation of buried sections of some polar troughs (Rodriguez and Tanaka, 2007).

6. Fault structures

Previous workers did not recognize any major or extensive mappable fault structures in most of Planum Boreum using Viking data at local to regional scales (Dial, 1984; Dial and Dohm, 1994; Herkenhoff, 2003). Overall evidence from the geologic record for faulting and folding in Planum Boreum based on currently available data is, to the best of our knowledge, limited to minor faulting and perhaps folding as revealed in THEMIS VIS, MOC, and HiRISE images (e.g., Malin and Edgett, 2001; Milkovich and Head, 2006; Nunes et al., 2006, 2007; Pais et al., 2006; Tanaka, 2007). Glacial flow of north polar deposits, as predicted by ice-deformation modeling studies (e.g., Fisher, 2000; Pathare and Paige, 2005), is not detected given the paucity of deformation structures within the stratigraphy. Also, aligned sets of scarps along particular layers of the ABb_1 unit that have the appearance of potential thrust faults when observed in MOC images (Milkovich and Head, 2006) lack offsets where observed in HiRISE images (e.g. HiRISE PSP_001462_2630 at 83.0° N, 94.9° E) and instead may result from aeolian processes such as cross-bedding or erosional fluting. The tectonic history of Planum Boreum may have mainly involved small-scale faulting produced by minor compaction of the materials forming Planum Boreum due to processes such as sedimentary deposition and loading, surface erosion, and volatile deflation, similar to the cause suggested for local faults observed in the south polar plateau (Murray et al., 2001).

6.1. Polygonal troughs in the Rupes Tenuis unit (ABrt)

At Hyperborea Lingula in the floor of the mouth of Chasma Boreale and at the adjacent Hyperboreus Labyrinthus in the lowest part of the Vastitas Borealis plain (Figs. 2 and 5), extensive polygonal troughs dissect the Rupes Tenuis (ABrt) and Vastitas Borealis interior (ABb_1) units. The troughs could have formed by desiccation and compaction of volatile-rich materials during the Early Amazonian. At Hyperboreus Labyrinthus, the ABrt unit is eroded below the surface level of Hyperborea Lingula, and erosion of the trough walls has resulted in ridges where the trough-bounding faults should have been (Fig. 5). This indicates some sort of hardening process has occurred in materials along the fault structures, such as salt cementation or freezing of liquid volatile phases. The polygonal troughs progress down into the ABb_1 unit and may relate to long-lived desiccation of volatile-rich materials during the Early Amazonian. Polygonal troughs are not evident elsewhere in exposures of the ABrt unit. However, rounded and dish-shaped eroded layer outcrops evident within the troughs of Hyperboreus Labyrinthus (Fig. 5) are similar in form to layer outcrops of unit ABrt in parts of Rupes Tenuis (e.g., CTX P02_001654_2605); one possibility is that they also relate at least in part to trough deformation.

6.2. Conjugate faults near Udzha crater

Local, conjugate fault systems occur in the ABb_1 unit near Udzha crater (Fig. 1; Tanaka, 2005). These faults have modest,

tens of meters displacements and may have been generated by the Udzha impact.

6.3. Grabens, pits, and sinuous ridges above western Olympia Cavi

We have detected 8 systems of ~100-m-wide troughs on Planum Boreum as seen in MOLA, THEMIS VIS and HiRISE data, all within the same region above western Olympia Cavi (Figs. 3A and 15A; 83°–86° N, 107°–138° E). They all occur along or parallel with gentle ridge crests and range from 2.6 to 23 km long (Fig. 15A). In some cases, MOC and HiRISE images provide sufficient resolution to confirm the morphology of the troughs. One example includes a series of echelon, linear troughs aligned along the crest of a broad ridge (Figs. 15A and 15B). These troughs are tens to >100 m wide, with individual segments that are as much as a few kilometers long. We interpret these troughs to be grabens based on the linear bounding scarps and their echelon arrangement—the scarps are the surface expressions of the bounding normal faults. The entire graben system extends for ~20 km. The grabens underlie meter- to decameter-scale ridges (trends marked in Fig. 15B) made up of residual ice (unit ABb_4), which appear to deform unit ABb_3 (and perhaps underlying ABb_1 and ABb_2 units, though these are unseen). These grabens are asymmetric. Analyses of terrestrial examples show that asymmetric grabens are bounded by a master and an antithetic fault, with greater offset along the master fault (e.g., Schultz et al., 2007). Thus, the graben-bounding faults may extend through the decameters-thick ABb_3 unit and into the ABb_1 unit (locally estimated to be ~800 m thick).

Circular pits mostly 2–6 m wide occur along the steeper wall of the graben; an exceptionally large pit forms an elongate (60 × 160 m) depression at the end of one graben (Fig. 15B). The lack of apparent raised rims is consistent with the collapse of surficial materials into subsurface voids (Okubo and Martel, 1998) that have developed along dilational sections of the graben-bounding faults (Martel and Langley, 2006). Such pits form ahead of upward-propagating normal faults due to the concentration of near-tip tensile stress (Martel and Langley, 2006). This results in the formation of pits along the trace of, and along the up-thrown side of the underlying normal fault, as observed here (Fig. 15B). This interpretation is the most consistent with terrestrial experience, given the location of the pits along the graben-bounding normal faults. Furthermore, the lack of raised rims surrounding the pits indicates that impact and explosive volcanic origins that would result in annular, raised rims of ejecta are not favored.

The development of the underlying normal faults indicates the presence of differential stress within Planum Boreum. Viscous flow of the Planum Boreum materials in response to the topography of the adjacent trough can result in a concentration of differential stress in the area of these pits and graben (Nunes et al., 2006, 2007), though predicted magnitudes of differential stress are smaller than that required for faulting (Nunes et al., 2006, 2007). However, brittle failure in the form of deformation bands and related granular deformation structures can occur at magnitudes of stress that are insufficient for Coulomb slip (Okubo and Schultz, 2006; Schultz and Siddharthan, 2005). In this way, normal faults may nucleate at depth and propagate to the surface in response to these lower magnitudes of differential stresses induced by viscous flow. Thus, if large-scale viscous flow in the Planum Boreum materials were commonplace because of an ice-rich composition, then widespread graben formation can be predicted on the planum. Since this is not the case, it appears that another process or geologic control may be operative. In this region, Olympia Cavi depressions extend to the margin of Planum Boreum and are aligned with and connected to the troughs of Boreales Scopuli (Fig. 15A). It may be that scarps had initially developed in the Planum Boreum cavi unit (ABb_c) and then were buried by the Planum Boreum 1 and 3 units (ABb_1 and ABb_3). Thus the buried features may lead to differential compaction and shear stress in the Planum Boreum units above them.

Parallel with these troughs are low, sinuous ridges <25 m wide and <700 m long and spaced ~100 m apart (Fig. 15C). Actual displacements of the constituent material cannot be observed. Thus our interpretation of the features as contractional ridges arises from their similar morphology to subdued wrinkle ridges (crenulations and other secondary features are not detected) and their occurrence and alignment with the troughs, which would be consistent with modest, gravity-driven relaxation of the broad ridge. The slope of the ridge flank is a mere 1°, so the resulting shear stress is modest. Compressional stresses due to growth of the adjacent graben (e.g., Martel and Langley, 2006) may have also contributed to the formation of these contractional ridges.

6.4. Tenuis Cavus south rim structure

We observe three nested systems of arcuate grooves and scarps extending ~15 km from the south rim of Tenuis Cavus that appear to outline now-buried, former margins of the cavus. The grooves locally have multiple anastomosing branches or echelon segments and scattered circular pits <20 m across (e.g., CTX T01_000885_2645 and MOC R23-00158 and M20-00416). The structures cut unit ABb_3 and likely result from differential settling of that unit and perhaps underlying materials across what may be steep, buried scarps.

7. Geologic evolution of Planum Boreum

Here, we present a synthesis of geologic evolution of the Planum Boreum region throughout the Amazonian Period, based on our geologic mapping results presented in previous sections (Figs. 3 and 4).

7.1. Early Amazonian

The beginning of the Amazonian in the northern lowlands of Mars marks the cessation of the catastrophic discharges that carved the outflow channels of Xanthe Terra and Chryse Planitia and delivered huge amounts of erosional debris and volatiles therein (e.g., Baker et al., 1991; Parker et al., 1989, 1993;

Head et al., 1999; Clifford and Parker, 2001; Tanaka et al., 2001, 2003, 2005; Kreslavsky and Head, 2002; Rodriguez et al., 2006a). The formation of the Vastitas Borealis interior unit ($A\text{Bv}_i$), which covers the martian northern plains, has been attributed to extensive resurfacing due to the mobilization and release of volatiles within the outflow-channel-discharged sedimentary materials (Tanaka et al., 2003, 2005). Thus the Vastitas Borealis interior unit ($A\text{Bv}_i$) is interpreted to be ubiquitous beneath Planum Boreum and Olympia Planum (Fig. 4). Some of the processes that may have contributed to the resurfacing history of the northern plains include sediment compaction and increase in pore fluid pressure, contractional deformation and extensive polygonal fracturing, and/or density inversions produced by variations in substrate density and/or by magmatism (Tanaka et al., 2003; Skinner and Tanaka, 2007).

A regional thermal anomaly associated with magmatic activity in Alba Patera may have resulted in regional resurfacing within the Vastitas Borealis interior unit ($A\text{Bv}_i$), producing the Scandia region unit (ABs), which may have originally extended across much of Vastitas Borealis north of Alba Patera, covering some 1.5×10^6 km^2 (Tanaka, 2005). Geologic mapping indicates that the Scandia region unit (ABs) extends as scattered outcrops beneath eastern Olympia Planum and Planum Boreum along Rupes Tenuis (especially near Boola crater) and perhaps Hyperborea Lingula (Figs. 3A, 4A, 4D, and 5).

Wind erosion of the ABs unit may have produced extensive migratory dunes, sand sheets, and loess deposits in the north polar region, leading to the formation of the Rupes Tenuis unit (ABrt). However, the absence of cross-beds within the ABrt unit suggests that any dunes that formed must have accumulated somewhere else, most likely around the periphery of Planum Boreum. The present topography of unit ABrt varies dramatically and abruptly among exposed outcrops along Rupes Tenuis, Olympia Rupēs, and Hyperborea Lingula (Figs. 4A and 4B). These observations indicate that the unit has undergone episodic retreat or truncation that modified extensive paleo-plateau surfaces. The scarp along Rupes Tenuis displays laterally-extensive horizontal to sub-horizontal layering. These layers may represent discreet episodes of deposition, variability in the types of sedimentary deposits, and/or they may have resulted from diagenetic processes. In any case, their shallow dips indicate that these layers have undergone significant retreat and likely formed part of a large, paleo-plateau that extended hundreds of kilometers farther south.

It appears that the lower layers of the ABrt unit associated with the ridge-flanked troughs of Hyperboreus Labyrinthus that rim most of the southern plateau margin of the lingula may be preserved here (and not elsewhere) because they are more erosionally resistant. This resistance may result from cementation and alteration along fracture and fault systems related to volatile-migration through these materials prior to erosion. The processes of weathering and ablation of the unit may have included sublimation of ice cement and matrix and aeolian erosion.

Remnants of the putative unit ABrt paleo-plateau include the Escorial crater plateau and potentially Abalos Colles and numerous pedestal impact craters located between 40° and 50° N (Tanaka et al., 2005). In particular, impact craters such as Boola and those northwest of Chasma Boreale appear to have played a major role in defining the preserved topography of the paleo-plateau. However, where buried beneath Planum Boreum and Olympia Planum, the extent and topography of the ABrt unit are uncertain (Fig. 4). Retreat processes may have involved widespread collapse driven by volatile removal from the unit and erosion of unconsolidated materials. Erosion progressed and then largely waned sometime during the Early Amazonian, resulting in the present surface of the unit, though largely buried.

7.2. Middle to Late Amazonian

The Planum Boreum cavi unit ($A\text{Bb}_c$) was emplaced on top of the Rupes Tenuis unit (ABrt) in upper Chasma Boreale and along Olympia Rupēs. It also forms an isolated outcrop in a depression in western Abalos Mensa, in which the presence of unit ABrt is uncertain (Fig. 4A). However, it is absent along Rupes Tenuis, above Hyperborea Lingula, and along the margins of Gemina Lingula and thus either has been removed from those locations or never was emplaced there. It also forms the base of the eastern walls of Boreum and Tenuis Cavi, where the floor material is made up of either the $A\text{Bv}_i$ or the ABrt unit (Figs. 9D and 9E). South of the cavi, the $A\text{Bb}_c$ unit may thicken somewhat within inner Gemini Lingula, as indicated in the eastern wall of Boreum Cavus (Fig. 10). It may be that the preserved occurrences of the unit represent the types of depositional sinks where the unit primarily formed. If so, the depositional controls may have been (1) the topography, as sands may have accumulated preferentially along the lower margins of the then circum-polar plateau, and (2) low-insolation conditions that led to precipitation of the icy layers that confined that sandy material. After each icy layer or layer sequence was deposited, a return to sand migration would have brought in a new supply of sand. Eventually, sand supply would have been largely sequestered in the deposit. The cavi unit ($A\text{Bb}_c$), being multilayered and interbedded, may represent dozens or hundreds of climate oscillations spanning potentially millions of years. It also is the earliest stratigraphic evidence that a large circumpolar erg had developed, which would have supplied sand to the accumulating unit. Variations in sand supply and other factors may have dictated where dunes collected, as indicated by cross-beds, versus where sand sheets were deposited in layers and lenses without associated cross-beds.

When the sand supply largely ran out, migrated elsewhere, and/or decreased due to changes in atmospheric density and wind patterns, the even, parallel layers of the Planum Boreum 1 unit ($A\text{Bb}_1$) began to be deposited on Planum Boreum, Olympia Planum, and surrounding plains (forming Tenuis and Olympia Mensae) and some crater floors (e.g., Korolev). These surfaces include all of the aforementioned geologic units. In most exposures, the basal layers of the $A\text{Bb}_1$ unit rest conformably on the cavi unit ($A\text{Bb}_c$) (e.g., Fig. 9A). Locally, however, the contact is irregular and unconformable (in Olympia Planum, Fig. 8C) or laterally transgressive (in Boreum Cavus, Fig. 10). Thus the contact relation is spatially variable, indicating a complex episode at the end of most $A\text{Bb}_c$ unit development, ranging

from a simple cessation of sandy layer emplacement, to local enrichment of dark layers, to considerable erosion prior to unit $A\mathrm{Bb}_1$ deposition. This indicates regionally variable sand supply and deposition of ice-rich layers during the transitional period.

Angular unconformities in the Planum Boreum 1 unit ($A\mathrm{Bb}_1$) indicate episodes of at least local erosion or non-deposition, perhaps controlled by pre-existing topographic irregularities on both underlying materials as well as the $A\mathrm{Bb}_1$ unit itself (Tanaka, 2005; Fortezzo and Tanaka, 2006; Kolb and Tanaka, 2006, 2008a). We find one lens of the Planum Boreum cavi unit ($A\mathrm{Bb}_c$) that appears partly bounded at its base by an unconformity, which may have resulted from enhanced erosion of the $A\mathrm{Bb}_1$ unit by sand associated with the lens. We do not, however, see evidence for patterns of unconformities indicative of widespread, insolation-driven trough migration in this unit, as proposed by Howard et al. (1982). Also, given that layer sequences appear to be continuous across broad regions of Planum Boreum (e.g., Milkovich and Head, 2005; Fishbaugh and Hvidberg, 2006) and that faults and folding in the unit appear to be rare, we do not see evidence for any significant glacial-like, soft-sediment, or ice-relaxation flow, as has been proposed (e.g., Weijermars, 1986; Clifford, 1987; Fisher, 2000; Pathare and Paige, 2005), nor other substantial tectonic deformation of the unit, though gentle bending and thinning may not be easily recognized. However, the layers commonly appear laterally-disrupted at meter scales (e.g., Fig. 9A), which may indicate that minor degradation due to surficial processes (e.g., thermokarst development and slope failures) affected the unit during its accumulation and perhaps during and after its erosion. Deformation is also absent in the head scarps of Chasma Boreale, where fracturing might be expected if polar melt-water discharges (as proposed by Dial and Dohm, 1994; Benito et al., 1997; Fishbaugh and Head, 2002) had led to collapse of overlying strata into subsurface voids. In addition, the lack of outflow channels in Chasma Boreale, particularly on the ancient cratered floors of Tenuis and Boreum Cavi, argues against such discharges.

Prior to the emplacement of subsequent units, the Planum Boreum cavi ($A\mathrm{Bb}_c$) and 1 ($A\mathrm{Bb}_1$) units underwent considerable erosion, resulting in Chasma Boreale, the arcuate troughs and marginal scarps of Gemini and Boreales Scopuli, the depressions of Olympia, Boreum, and Tenuis Cavi, and the relatively modest undulations on western Gemina Lingula. We suggest that the erosion was mainly due to ice sublimation, wind scouring, and local avalanching, as erosional hollows, landslides, frost streaks, aeolian veneers, yardangs, and dunes are prevalent on many of the surfaces on and adjacent to the margins of Planum Boreum and within Chasma Boreale (Fig. 9; see also Howard, 2000; Byrne and Murray, 2002; Edgett et al., 2003; Fishbaugh and Head, 2005; Rodriguez et al., 2007b; Herkenhoff et al., 2007). On the other hand, the Rupes Tenuis (ABrt) and Vastitas Borealis interior ($A\mathrm{Bv}_i$) units do not display any clear indications of any significant, further erosion. A few troughs and some of the Olympia Cavi depressions expose terraces in the ABrt unit that are aligned with the long axis of the troughs and scarps. If at these sites the ABrt unit also has not undergone erosion during this episode, then the substrate topography likely affected surface topography, leading to preferential erosion of those overlying units along persistent scarps. Such sustained topographic/stratigraphic control on erosion has been implicated for south polar chasmata based on inward dipping beds and stacked unconformities in multiple sequences of layered deposits in chasmata walls (Kolb and Tanaka, 2006, 2008a).

Polar troughs are arranged along spiral trends that extend from the center to the periphery of Planum Boreum but are absent across upper Gemini Lingula. Most interior troughs form topographically enclosed depressions, whereas most marginal troughs open out into Vastitas Borealis or, locally, onto the surface of the ABrt unit. Most troughs form concentric to one another, except for much of southern Gemini Scopuli, where troughs and scarps commonly cross-cut one another. Also, trough sections along the periphery of Planum Boreum are wider, deeper and generally more complex and would suggest that in these regions the top of the Planum Boreum 1 unit has been eroded away as troughs enlarged by headward erosion.

Chasma Boreale may have been particularly susceptible to aeolian erosion, perhaps by down-slope katabatic winds (Howard, 2000), particularly if the surface topography of the Planum Boreum 1 unit ($A\mathrm{Bb}_1$) retained the scarps in the Rupes Tenuis unit (ABrt) now exposed in the margins of Chasma Boreale. Additionally, or alternatively, once the scarps were exhumed they may have provided topographic control to wind erosion. The deep grooves in the unit above the east margins of Boreum and Tenuis Cavi (Figs. 9D–9E) and the dune orientations within the chasma attest to the strong topographic control exerted on local wind patterns.

The duration of this major phase of erosion of the Planum Boreum 1 ($A\mathrm{Bb}_1$) unit is not well constrained. Possibly, the unit was largely emplaced as early as the Middle Amazonian, roughly a billion years ago. The present crater age of the eroded surface is on order of a few million years (Tanaka, 2005). So the erosion could have taken much of or some relatively brief episode of this period.

Following that major period of erosion, dark material of Planum Boreum 2 unit ($A\mathrm{Bb}_2$) was emplaced in northwestern Chasma Boreale and in the troughs of and on the plains adjacent to Planum Boreum. Possibly, the unit was more widespread but is not recognized in most places now due to erosion and burial. The $A\mathrm{Bb}_2$ unit was then eroded, resulting in yardangs in the unit that generally follow current wind patterns (down Chasma Boreale and concentric to the margin of Planum Boreum). However, the yardangs do not extend into the $A\mathrm{Bb}_1$ unit, which must have been established moderate resistance to aeolian erosion by that point in time. Within Chasma Boreale, bright layered deposits were emplaced to form the Chasma Boreale unit (ABcb), indicating that the chasma may have served as a shelter that led to local deposition of bright layered deposits. Alternatively, the unit could have been more regional in extent but preferentially preserved in the chasma. Next, renewed erosion of the Planum Boreum cavi unit ($A\mathrm{Bb}_c$) yielded dunes of the Olympia Undae unit (ABou) in the vicinity of the cavi. Distal dune fields, including Siton, Aspledon, and much of Olympia Undae may have originated during earlier erosional episodes of the cavi

unit and include former sources along the margins of Planum Boreum, such as Rupes Tenuis, that are now depleted.

Planum Boreum 3 unit (ABb_3) then was emplaced over much of the flat topography and pole-facing slopes of Planum Boreum and the plains surrounding the planum. The unit is not preserved on most equator-facing slopes and on dunes, perhaps due to wind, slope, textural, and insolation effects that inhibited deposition and/or promoted erosion. The margins of the unit are commonly eroded in the floors of troughs and include pits and knobs. On the Planum Boreum surface, the unit shows extensive, parallel, meter-scale ridge forms that may be yardangs. Where the unit is draped over scarps and ridges above western Olympia Cavi (Fig. 15) and the south rim of Tenuis Cavus, modest extension and perhaps contraction of the unit and underlying materials ensued.

Most recently, the residual ice cap, mapped as the Planum Boreum 4 unit (ABb_4), was formed as a thin, widespread deposit. Due to its thinness and its interannual variability in areal coverage, the residual ice may be an ephemeral unit over timescales of centuries to millennia, depending on climate oscillations. Its role (or the role of a similar unit throughout the Amazonian) in the overall accumulation of the layered deposits of Planum Boreum is not entirely understood.

Overall, our picture of the evolution of Planum Boreum suggests an extended history dating back some 3 billion years. If the majority of the exposed layering record extends back at least several hundred million years, it would suggest that much of the climate history recorded in the north polar region predates the past 20 million years when reliable determination of the orbital parameters can be calculated (Laskar et al., 2004). The uncertainty in the timing and duration of the erosional period following deposition of the Planum Boreum 1 unit (ABb_1) makes detailed comparison between the orbitally-driven climate history and the layering record poorly constrained, thus making previous attempts to do so questionable (e.g., Laskar et al., 2002; Milkovich and Head, 2005; Tanaka, 2005).

Furthermore, we find that the majority of Planum Boreum construction occurred during two major stages. The first stage was the emplacement of the Rupes Tenuis unit (ABrt) during the Early Amazonian, which originally may have extended far into the northern plains. The unit locally exceeds ~1300 m in thickness and its original maximum thickness is unknown. Erosion of the unit apparently was protracted, permitting the development of pedestal craters and of irregularly-shaped platforms and scarps that define its present margins and surfaces. These include Hyperborea Lingula and Rupes Tenuis. The second major stage of construction involved emplacement of the Planum Boreum cavi (ABb_c) and 1 (ABb_1) units, which covered the present Planum Boreum to depths of as much as 1500 m and extended hundreds of kilometers outward where only scattered remnants occur today. These units were then intensely dissected, forming the spiral troughs, Chasma Boreale, and the marginal scarps of Planum Boreum. Since then, three minor episodes of deposition may have been extensive but deposited at most a few hundred meters of material; these depositional episodes constrain two more episodes of wind-driven erosion.

8. A common north–south polar geologic evolution?

The north and south poles of Mars are both covered by plateaus (Planum Boreum and Planum Australe) each made up of horizontally layered deposits of similar area, thickness, and overall geomorphic expression (e.g., Tanaka and Scott, 1987; Fishbaugh and Head, 2001; Kolb and Tanaka, 2001). Such deposits are interpreted to form partly by precipitation of ice mixed with some dust from the atmosphere and thus should be sensitive and responsive to the global climate and atmospheric volatile budget history. However, other units and surfaces relate to local aeolian deposition and sediment sources. Because of this, we expect that the correlation of the two sets of polar deposits may be complicated and include both global and regional resurfacing records. Another apparent obstacle to intercorrelation of the two sets of polar deposits has been the much older mean surface age of Planum Australe (<100 Ma) materials vs that of Planum Boreum (<5 Ma) deposits as reflected by their crater densities (Herkenhoff and Plaut, 2000; Koutnik et al., 2002; Tanaka, 2005). However, crater densities for these surfaces as determinants of unit ages are highly suspect due to their dependence on the timing and rate of post-depositional erosion. For example, the evidence for recent dark veneer formation and migration on Planum Boreum argues for recent erosion of this plateau's surface (Rodriguez et al., 2007b). Because of such resurfacing, stratigraphic correlation between the north and south polar deposits based on the comparison of their crater populations cannot be achieved.

Nevertheless, the plausibility of similar geologic histories between the two sets of polar materials can be assessed, which is what we attempt here by developing a scenario in which depositional and erosional episodes at each pole may correlate. The south polar geology is described in more detail in a geologic map of the south polar region chiefly based on MOLA, MOC, THEMIS, and HRSC data (Kolb and Tanaka, 2008b) and in topical, mapping based studies (Kolb and Tanaka, 2001, 2006, 2008b). We use that work and our stratigraphic results herein to build the case for the following scenario.

8.1. Early Amazonian

The south polar Richardson unit forms deposits as much as 1500 m thick centered within impact craters and depressions south of 60° S. The Richardson unit is Early to Late Amazonian as it is superposed on Dorsa Argentea units and is locally overlain by Planum Australe materials (Kolb and Tanaka, 2008b). The unit is topped by dune fields. Overall, the Richardson unit appears to be a friable material and forms the oldest deposit in the south polar region that may reflect depositional activity related to the polar location (e.g., cold-trapping of ice and atmospheric dust). Because the age of the unit is poorly constrained, the part of it underlying the dunes may be stratigraphically equivalent to the Rupes Tenuis unit (ABrt).

A possible local source for the Richardson unit is the Cavi Angusti unit of the Dorsa Argentea province. It is deeply eroded to form large depressions (cavi). This unit is evenly bedded and began forming in the middle Late Hesperian, accumulat-

ing to form the >2-km thick dome-shaped Planum Angustum centered at 75° S. As with other units of the Dorsa Argentea province as well as the north polar Scandia region unit (ABs), the Cavi Angusti unit may result from local, sedimentary diapiric and volcanic processes (Tanaka and Kolb, 2001). Alternatively, the Dorsa Argentea province materials have been interpreted as to result from glaciation (Head and Pratt, 2001). In either case, these processes may have produced loose fines of rock and ice at the surface. Finally, if the Rupes Tenuis (ABrt) and Richardson units, which may have local sources for their lithic components, are to be correlated, their formation must be related to a global climate episode that produced ice cement; otherwise, any temporal correlation would be just coincidental.

8.2. Middle to Late Amazonian

The earliest dune activity recorded at the north pole is the Planum Boreum cavi unit (ABb_c). It lies on top of the Early Amazonian Rupes Tenuis unit (ABrt) and grades into the Planum Boreum 1 unit (ABb_1), as bright layers are interbedded into its upper parts. Given our assessment that the latter unit may be Middle to Late Amazonian, the cavi unit (ABb_c) also seems most likely to occur in this same time frame. Its stratigraphic position could coincide with the dune forms at the top of the south polar Richardson unit that locally underlie the Planum Australe 1 unit (THEMIS VIS V08771001 and V08746001). The lower age of those dunes is loosely constrained; they generally form within deep craters (possibly of late Noachian to Hesperian age as they have relatively pristine to moderately degraded rims). The source of the Richardson unit dune sand may be the eroded Cavi Angusti unit or other local materials.

The Planum Boreum 1 (ABb_1) and Planum Australe 1 units form similar-appearing finely layered deposits. In the south, a regional unconformity in the bottom third of the Planum Australe 1 unit stratigraphy divides the unit into the lower and upper members. This unconformity marks an intensive erosional period that initiated chasmata and curvilinear canyon formation in Promethei Lingula and Australe Scopuli and likely other canyons and troughs throughout the plateau. In Planum Boreum, recognition of most unconformities generally requires the image resolution of MOC narrow-angle images (<10 m/pixel), which only provide scattered coverage of Planum Boreum, whereas the more extensive THEMIS VIS images (18–40 m/pixel) do not reveal most unconformities. Thus, with current data, we cannot properly evaluate whether or not a regional unconformity exists within the ABb_1 unit. Although the Planum Australe 1 unit has a much higher crater density than the ABb_1 unit, the erosional histories of the units may have been dissimilar. The ABb_1 unit may have a widely varying surface age, given the putative, cratered and partly buried outcrop of the unit in Olympia Planum. The variable surface age of the unit may result from long-lived aeolian scouring, which may be orders of magnitude more effective in the north pole than in the south due to the north's much greater sand supply as well as wind stresses generated by the much higher atmospheric densities at its lower elevations. Thus it is plausible to suggest that these units at both poles may be similar in age.

At both poles, the chasmata occur where the polar plateau units bury high-standing sections of substrate. In the south, the substrate structures control the location and formation of the chasmata; in the north, the Rupes Tenuis unit (ABrt) forming the western wall of Chasma Boreale likely controls the location of the canyon. As well, headward erosional retreat can explain why curvilinear canyon sections at both poles are wider, deeper, and generally more complex along the plateau margins. In Planum Australe, the headward erosion appears to have occurred step-wise during erosional or non-depositional periods.

The major erosion features (chasmata, curvilinear canyons, and plateau margins) were formed prior to emplacement of the Planum Boreum 2 (ABb_2) and 3 (ABb_3) units in the north and the ~300-m-thick unconformable, widespread sequence of Planum Australe 2 unit in the south. The equivalent of the ABb_2 unit—dark, thickly bedded material tens-of-meters thick—does not appear in the south polar region. This may be related to the paucity of dark fines in Planum Australe. However, the extensive AAa_2 unit could be correlative to accumulation of relatively bright layers of the Chasma Boreale unit (ABcb), although the latter unit is not widely distributed. Both units formed after extensive erosion of thick layered deposits (Planum Australe 1 unit in the south and ABb_1 and ABb_2 units in the north). The Planum Australe 3 unit (AAa_3) is limited to the highest part of Planum Australe, which is Australe Mensa. That unit is made of 6 or 7 layers and is ~300 m thick. It could be correlative to the Planum Boreum 3 unit, which may have a similar number of layers (Tanaka, 2005). Finally, at both poles, the high-albedo deposits that comprise the residual ice caps unconformably overlies all older plateau units, forming the water-ice dominated Planum Boreum 4 unit (ABb_4) in the north and the CO_2-dominated Planum Australe 4 unit in the south that may be underlain by a layer of water ice (Titus et al., 2003).

In summary, this scenario permits all episodes of Middle to Late Amazonian south polar aeolian deposition to correlate with all but one Planum Boreum unit (north polar unit ABb_c with south polar Richardson unit, ABb_1 with Planum Australe 1 unit, ABcb with Planum Australe 2 unit, ABb_3 with Planum Australe 3 unit, and ABb_4 with Planum Australe 4 unit) along with common episodes of erosion between each period of deposition. The Planum Boreum 2 unit (ABb_2) is the only unit of Planum Boreum not having a recognized, possibly correlative south polar unit. If the ABb_2 unit is largely derived from dark fines of the Olympia Undae unit (ABou), it may be that a similar south polar source, such as the dunes of the Richardson unit, was of insufficient volume and/or friability to yield a substantial equivalent deposit, assuming that the unit would otherwise form.

9. Conclusions

The wealth of previous work and new observations has provided a basis for us to ascertain an updated history of the north polar region of Mars. We find that geologic mapping of this complex and fascinating region of Mars has greatly enriched

our understanding of bedrock, surficial materials, and landforms produced by depositional, erosional, deformational, and other modificational processes. Observed intimate temporal and spatial associations have led to important inferences related to the geologic and climatic histories of the materials that form Planum Boreum. We consider the following to be the most significant findings and interpretations of this study:

(1) There are two, not one, major "basal units" of Planum Boreum, which we map as the Rupes Tenuis (ABrt) and Planum Boreum cavi (ABb_c) units. We infer that the ABrt unit formed during the Early Amazonian based on its relatively high density of craters $\geqslant$5 km in diameter. In contrast, the Planum Boreum cavi unit (ABb_c) superposes the ABrt unit, has a different geologic character, a most likely Middle to early Late Amazonian crater age, and gradational and time-transgressive relations with the overlying Planum Boreum 1 unit (ABb_1).

(2) The Rupes Tenuis (ABrt) likely arose as a depositional sink for the lithic fines eroded primarily from the Scandia region unit (ABs) due to resurfacing driven by a possible thermal anomaly in the Scandia region at that time, perhaps related to Alba Patera magmatism. The unit appears to have formed by the episodic accumulation of air-fall and wind-blown deposits, possibly as a result of sedimentary cycles involving the volcanic (magmatic/sedimentary) expulsion of volatiles and sediments from the Scandia region and their precipitation and migration into cooler and atmospherically calmer polar latitudes.

(3) We confirm that the Olympia Planum is largely a frozen paleo erg (as suggested by Byrne and Murray, 2002) made up of the Planum Boreum cavi unit (ABb_c) and partly veneered by the finely-layered deposits of the Planum Boreum 1 and 3 units ($ABb_{1,3}$). The zone of Olympia Planum covered by Olympia Undae is the only part of the polar plateau that shows no trough incision or marginal scarp retreat.

(4) Sand dunes, sheets, and surficial veneers, which are identified by their dark color, rippled surfaces, serrated margins, and/or irregular- to cross-bedded outcrops, have played major depositional and erosional roles throughout the geologic evolution of Planum Boreum. When entrapped by ice-rich layers and/or topographic features, they can form thick deposits, possibly including much of the Rupes Tenuis (ABrt) unit during the Early Amazonian and the overlying Planum Boreum cavi and 2 units (ABb_c and ABb_2, respectively) during the Middle to Late Amazonian. Following emplacement of the Planum Boreum 1 unit (ABb_1), the Planum Boreum cavi unit (ABb_c) has been particularly susceptible to erosion by southwest-trending, down-slope and circumpolar winds where exposed in steep, marginal scarps along the periphery of Planum Boreum, leading to dune fields of the Olympia Undae unit (ABou). At the head of Chasma Boreale, sustained activity of sand sheets is evident in both the preserved stratigraphic record as well as the exposed surficial materials (Fig. 10). This association, along with the recognition of the cavi (ABb_c) and dark Planum Boreum 2 (ABb_2) units in parts of upper Chasma Boreale, indicate that the chasma was a major topographic feature through the Middle to Late Amazonian, perhaps sustained by the erosional and ablational effects of surficial fines and their interstitial components.

(5) The Rupes Tenuis (ABrt) and Planum Boreum cavi (ABb_c) units, which form the base of Planum Boreum, include high proportions of poorly-consolidated fines, making them susceptible to erosion. Their preservation appears strongly controlled by the local aeolian environment, post-depositional hardening processes, and burial and protection by younger deposits. Much of the Rupes Tenuis unit (ABrt) appears to be buttressed by local outcrops within it that were perhaps hardened by impact-related activity (e.g., at Boola crater) and/or by local, subsurface heating events (Hyperboreus Labyrinthus) (Figs. 2 and 5). Although younger Planum Boreum units largely bury and protect the cavi unit (ABb_c), exposures of the unit along scarps of Chasma Boreale, Olympia Rupēs, and Abalos Mensa have likely been eroded due to strong katabatic and circum-polar winds, leading to exhumation of steep-walled cavi depressions. The Olympia Undae erg particularly appears to be mainly sourced from southeastern Olympia Planum, including the Planum Boreum cavi unit (ABb_c) as well as a source of gypsum in the substrate below the eastern tip of Olympia Undae. The gypsum may be related to distal hydromagmatic activity of Alba Patera in association with development of the Scandia region unit (ABs).

(6) Timing relations are complex and poorly constrained for the "classical" polar layered deposits, which we divide into the Planum Boreum 1 to 4 ($ABb_{1–4}$) and Chasma Boreale (ABcb) units. The sequences of the Planum Boreum 1 unit (ABb_1) are the ones most studied for possible correlation with orbitally-induced climate oscillations. This unit's age relations, which can be constrained based on its stratigraphic associations with the Planum Boreum cavi unit (ABb_c) and, to a lesser degree, based on impact craters preserved in Olympia Planum, indicate that the Planum Boreum 1 unit (ABb_1) may be as much as hundreds of millions to a billion years old. Crater dating based on the troughs cut into the ABb_1 unit points to the most recent age of resurfacing and not to the emplacement age of the unit, whose layered exposures therein are clearly eroded. Because the Planum Boreum 2 and 3 units ($ABb_{2,3}$) overlap that surface, they are likely younger than that surface's age, which is crater-dated at about a few million years (Tanaka, 2005). However, those units also display partly-eroded margins and thus that "few million years" inference should be viewed as a minimum age. Therefore, these units cannot be clearly tied to the confidently-calculated part of the orbitally-driven insolation history that can be determined for the past ~20 million years on Mars (Laskar et al., 2004). The residual ice, or Planum Boreum 4 unit (ABb_4), is the only unit that has a constrained crater age (<15 ka; Tanaka, 2005) that closely coincides with a climatic signature, as defined by a decline in north polar summer insolation since 21.5 ka (Montmessin et al., 2007).

(7) Numerous unconformities are documented in troughs and scarps of the Planum Boreum 1 unit (ABb_1), particularly in its lower parts. They mostly appear to be of local extent, and their orientations indicate that they relate to the local topography, including the troughs. Thus the troughs of Planum Boreum may be long-lived and evolve in their geometry over time. Troughs along Olympia Rupēs extend into the Planum Boreum cavi unit (ABb_c), which suggests that they formed by excavation and widening. For fine-grained materials emplaced by air-fall, volatile precipitation, and aeolian deposition, erosion may have proceeded by sublimation and aeolian removal of unconsolidated fines.

(8) Documentable deformation of the north polar layered deposits of Planum Boreum is minor and involves local development of grabens and thrusts (wrinkle ridges) and associated features. The structures may be due to local stresses involved in the uneven mass distribution of Planum Boreum materials and consequent compaction of buried material. Glacial flow, basal thrusting, and subglacial flood discharges are not evident in the layered stratigraphy and structure and geomorphology of Planum Boreum.

(9) We find a potential coincidence in the number, sequence, and character of major stages of deposition and erosion in the geologic records at both the north and south poles, with some apparent minor discrepancies. If this intercorrelation is largely correct, then the polar geologic records are indeed signatures of global climate. They track the activity of volatiles and lithic fines, including periods when volatiles are supplied to the poles and times when more desert-like conditions dominate, leading to migration of dunes and ablation of the polar deposits.

10. Unanswered questions

Many of our conclusions require further testing, which can be accomplished with the continued analysis of recent and new data of current and possibly future Mars orbiters. We fully expect refinements and corrections to our hypotheses. Among the more important issues and questions that remain unresolved yet tractable for further research include:

(1) The thick accumulation of the basal Rupes Tenuis (ABrt) and Planum Boreum cavi (ABb_c) units indicates that the north pole is not just a cold trap for ices, but also an aeolian trap for lithic fines. Why is this? Is the north polar region a long-term aeolian sink? Are there climatic periods such as during higher obliquity when the aeolian region is more energetic, leading to erosion?

(2) Origin and development of the spiral troughs, eroded margins, and unconformities of Planum Boreum remain unclear. However, since some of these features extend into the Planum Boreum cavi unit (ABb_c), might it be that the troughs dominantly form by aeolian erosion?

(3) Considering that north and south polar plateau history spans the entire Amazonian Period, is it therefore possible to correlate major episodes of volatile accumulations at both poles to major outflow-channel discharges that flooded the northern plains in association with volcanic activity at the Tharsis and Elysium rises?

Acknowledgments

We wish to thank Shane Byrne, Kathryn Fishbaugh, Sarah Milkovich, and Daniel Nunes for helpful discussions, comments, and suggestions as well as acknowledge the detailed comments by two anonymous reviewers that led to substantial improvements. We also wish to congratulate and give credit to the instrument teams that produced and made available the Mars spacecraft data products used in this paper. This work was support by a grant from NASA's Planetary Geology and Geophysics Program.

References

Baker, V., Strom, R., Gulick, V., Kargel, J., Komatsu, G., Kale, V., 1991. Ancient oceans, ice sheets, and the hydrological cycle on Mars. Nature 352, 589–594.

Bandfield, J., Hamilton, V., Christensen, P., 2000. A global view of martian surface compositions from MGS-TES. Science 287, 1626–1630.

Benito, G., Mediavilla, F., Fernandez, M., Marquez, A., Martinez, J., Anguita, F., 1997. Chasma Boreale, Mars: A sapping and outflow channel with a tectono-thermal origin. Icarus 129, 528–538.

Blasius, K., Cutts, J., Howard, A., 1982. Topography and stratigraphy of martian polar layered deposits. Icarus 50, 140–160.

Bourke, M., 2004. Niveo-aeolian and denivation deposits on Mars. Eos (Fall Suppl.) 85 (46). Abstract P21B-01.

Bourke, M.C., Edgett, K.S., Cantor, B.A., 2008. Recent aeolian dune change on Mars. Geomorphology 94, 247–255.

Buczkowski, D.L., Cooke, M.L., 2004. Formation of double-ring circular grabens due to volumetric compaction over buried impact craters: Implications for thickness and nature of cover material in Utopia Planitia, Mars. J. Geophys. Res. 109, doi:10.1029/2004GL014100. E02006.

Buczkowski, D.L., Frey, H.V., Roark, J.H., McGill, G.E., 2005. Buried impact craters: A topographic analysis of quasi-circular depressions, Utopia Basin, Mars. J. Geophys. Res. 110, doi:10.1029/2004JE002324. E03007.

Byrne, S., Murray, B., 2002. North polar stratigraphy and the paleo-erg of Mars. J. Geophys. Res. 107 (E6), doi:10.1029/2001JE001615.

Byrne, S., Herkenhoff, K., Russell, P., Hansen, C., McEwen, A., The HiRISE Team, 2007. Preliminary HiRISE polar geology results. Lunar Planet. Sci. 38. Abstract 1930 [CD-ROM].

Carr, M., 1982. Periodic climate change on Mars: Review of evidence and effects on distribution of volatiles. Icarus 50, 129–139.

Chapman, M.G., 1994. Evidence, age, and thickness of a frozen paleolake in Utopia Planitia, Mars. Icarus 109, 393–406.

Christensen, P.R., and 21 colleagues, 2003. Morphology and composition of the surface of Mars: Mars Odyssey THEMIS results. Science 300, 2056–2061.

Clifford, S., 1987. Polar basal melting on Mars. J. Geophys. Res. 92, 9135–9152.

Clifford, S., Parker, T., 2001. The evolution of the martian hydrosphere: Implications for the fate of a potential ocean and the current state of the northern plains. Icarus 154, 40–79.

Cutts, J., 1973. Nature and origin of layered deposits of the martian polar regions. J. Geophys. Res. 78, 4231–4249.

Cutts, J., Blasius, K., Briggs, G., Carr, M., Greeley, R., Masursky, H., 1976. North polar region of Mars: Imaging results from Viking 2. Science 194, 1329–1337.

Cutts, J., Blasius, K., Roberts, W., 1979. Evolution of martian polar landscapes: Interplay of long-term variations in perennial ice cover and dust storm intensity. J. Geophys. Res. 84, 2975–2994.

Dial, A., 1984. Geologic map of the Mare Boreum area of Mars. US Geol. Surv. Misc. Invest. Ser. Map I-1640.

Dial, A., Dohm, J., 1994. Geologic map of science study area 4, Chasma Boreale region of Mars. US Geol. Surv. Misc. Invest. Ser. Map I-2357.
Edgett, K., Williams, R., Malin, M., Cantor, B., Thomas, P., 2003. Mars landscape evolution: Influence of stratigraphy on geomorphology in the north polar region. Geomorphology 52, 289–297.
Feldman, W., Prettyman, T., Maurice, S., Plaut, J., Bish, D., Vaniman, D., Mellon, M., Metzger, A., Squyres, S., Karunatillake, S., Boynton, W., Elphic, R., Funsten, H., Lawrence, D., Tokar, R., 2004. Global distribution of near-surface hydrogen on Mars. J. Geophys. Res. 109, doi:10.1029/2003JE002160.
Fishbaugh, K., Head, J., 2000. North polar region of Mars: Topography of circumpolar deposits from Mars Orbiter Laser Altimeter (MOLA) data and evidence for asymmetric retreat of the polar cap. J. Geophys. Res. 105, 22455–22486.
Fishbaugh, K., Head, J., 2001. Comparison of the north and south polar caps of Mars: New observations from MOLA data and discussion of some outstanding questions. Icarus 154, 145–161.
Fishbaugh, K., Head, J., 2002. Chasma Boreale, Mars: Topographic characterization from Mars Orbiter Laser Altimeter data and implications for mechanisms of formation. J. Geophys. Res. 107 (E3), doi:10.1029/1999JE001230. 2-1–2-29.
Fishbaugh, K., Head, J., 2005. Origin and characteristics of the Mars north polar basal unit and implications for polar geologic history. Icarus 174, 444–474.
Fishbaugh, K., Hvidberg, C., 2006. Martian north polar layered deposits stratigraphy: Implications for accumulation rates and flow. J. Geophys. Res. 111. E06012.
Fishbaugh, K.E., Herkenhoff, K., Byrne, S., Russell, P., McEwen, A., Hansen, C., HiRISE Team, 2007. HiRISE observations of north polar stratigraphy and implications for geologic history. In: 7th Int. Conf. on Mars. Abstract 3194 [CD-ROM].
Fishbaugh, K.E., Hvidberg, C.S., Beaty, D., Clifford, S., Fisher, D., Haldemann, A., Head, J.W., Hecht, M., Koutnik, M., Tanaka, K., 2008. Introduction to the 4th Mars Polar Science and Exploration Conference special issue: Five top questions in Mars polar science. Icarus 196, 305–317.
Fisher, D., 2000. Internal layers in an "accublation" ice cap—A test for flow. Icarus 144, 289–294.
Fortezzo, C.M., Tanaka, K.L., 2006. Unconformity and bedding orientations in Planum Boreum, Mars: Preliminary results and discussion. In: 4th Int. Conf. on Mars Polar Sci. Explor. Abstract 8079 [CD-ROM].
Frey, H.V., Roark, J.H., Shockey, K.M., Frey, E.L., Sakimoto, S.E.H., 2002. Ancient lowlands on Mars. Geophys. Res. Lett. 29, doi:10.1029/2001GL013832. 1384.
Garvin, J., Sakimoto, S., Frawley, J., Schnetzler, C., 2000a. North polar region craterforms on Mars: Geometric characteristics from the Mars Orbiter Laser Altimeter. Icarus 144, 329–352.
Garvin, J., Sakimoto, S., Frawley, J., Schnetzler, C., Wright, H.M., 2000b. Topographic evidence for geologically recent near-polar volcanism on Mars. Icarus 145, 648–652.
Hartmann, W., 2005. Martian cratering. 8. Isochron refinement and the chronology of Mars. Icarus 174, 294–320.
Head, J., Pratt, S., 2001. Extensive Hesperian-aged south polar ice cap on Mars: Evidence for massive melting and retreat, and lateral flow and ponding of meltwater. J. Geophys. Res. 106, 10075–10085.
Head, J., Hiesinger, H., Ivanov, M., Kreslavsky, M., Pratt, S., Thomson, B., 1999. Possible ancient oceans on Mars: Evidence from Mars Orbiter Laser Altimeter data. Science 286, 2134–2137.
Head, J., Kreslavsky, M., Pratt, S., 2002. Northern lowlands of Mars: Evidence for widespread volcanic flooding and tectonic deformation in the Hesperian Period. J. Geophys. Res. 107 (E1).
Herkenhoff, K., 2003. Geologic map of the MTM 85080 quadrangle, Chasma Boreale region of Mars. US Geol. Surv. Geol. Invest. Ser. Map I-2753.
Herkenhoff, K., Plaut, J., 2000. Surface ages and resurfacing rates of the polar layered deposits on Mars. Icarus 144, 243–253.
Herkenhoff, K., Vasavada, A., 1999. Dark material in the polar layered deposits and dunes on Mars. J. Geophys. Res. 104 (E7), 16487–16500.
Herkenhoff, K., Soderblom, L., Kirk, R., 2002. MOC photoclinometry of the north polar residual cap on Mars. Lunar Planet. Sci. 33. Abstract 1714 [CD-ROM].
Herkenhoff, K., Byrne, S., Tanaka, K.L., 2006. Mars polar geologic nomenclature: What are the caps? In: 4th Mars Polar Sci. Conf. Abstract 8034 [CD-ROM].
Herkenhoff, K., Byrne, S., Russell, P.S., Fishbaugh, K.E., McEwen, A.S., 2007. Meter-scale morphology of the north polar region of Mars. Science 317, 1711–1715.
Howard, A., 1978. Origin of the stepped topography of the martian poles. Icarus 34, 581–599.
Howard, A., 2000. The role of eolian processes in forming surface features of the martian polar layered deposits. Icarus 144, 267–288.
Howard, A., Cutts, J., Blasius, K., 1982. Stratigraphic relationships within martian polar cap deposits. Icarus 50, 161–215.
International Astronomical Union, 1960. Transactions of the International Astronomical Union, Moscow, August 12–20, 1958, vol. 10. Cambridge Univ. Press, pl. 1, p. 262.
Kieffer, H., Chase, S., Martin, T., Miner, E., Palluconi, F., 1976. Martian north pole summer temperatures: Dirty water ice. Science 194, 1341–1344.
Kieffer, H., Jakosky, B., Snyder, C., 1992. The planet Mars: From antiquity to present. In: Kieffer, H., Jakosky, B.M., Snyder, C.W., Matthews, M.S. (Eds.), Mars. Univ. of Arizona Press, Tucson, pp. 1–33.
Kolb, E., Tanaka, K., 2001. Geologic history of the polar regions of Mars based on Mars Global Surveyor data. II. Amazonian Period. Icarus 154, 22–39.
Kolb, E., Tanaka, K., 2006. Accumulation and erosion of south polar layered deposits in the Promethei Lingula region, Planum Australe, Mars. Mars 2, 1–9.
Kolb, E., Tanaka, K., 2008a. Accumulation and erosion of south polar layered deposits in the Australe Scopuli region, Planum Australe, Mars. Icarus, in press (this issue).
Kolb, E., Tanaka, K., 2008b. Geologic map of the Planum Australe region of Mars. US Geol. Surv. Sci. Invest. Map, in review.
Koutnik, M., Byrne, S., Murray, B., 2002. South Polar Layered Deposits of Mars: The cratering record. J. Geophys. Res. 107 (E11), doi:10.1029/2001JE001805.
Kreslavsky, M., Head, J., 2000. Kilometer-scale roughness of Mars: Results from MOLA data analysis. J. Geophys. Res. 105, 26695–26711.
Kreslavsky, M., Head, J., 2002. The Fate of outflow channel effluents in the northern lowlands of Mars: The Vastitas Borealis Formation as a sublimation residue from frozen, ponded bodies of water. J. Geophys. Res. 107 (E12), 5121.
Langevin, Y., Poulet, F., Bibring, J., Gondet, B., 2005. Sulfates in the north polar region of Mars detected by OMEGA/Mars Express. Science 307, 1584–1586.
Laskar, J., Levrard, B., Mustard, J., 2002. Orbital forcing of the martian polar layered deposits. Nature 419, 374–377.
Laskar, J., Correia, A., Gastineau, M., Joutel, F., Levrard, B., Robutel, P., 2004. Long term evolution and chaotic diffusion of the insolation quantities of Mars. Icarus 170, 343–364.
Malin, M., Edgett, K., 2001. Mars Global Surveyor Mars Orbiter Camera: Interplanetary cruise through primary mission. J. Geophys. Res. 106 (E10), 23429–23570.
Malin, M.C., Bell III, J.F., Calvin, W.M., Cantor, B.A., Clancy, R.T., Edgett, K.S., Edwards, L., Haberle, R.M., James, P.B., Lee, S.W., Thomas, P.C., Wolff, M.J., 2007. Initial observations by the MRO Mars Color Imager and Context Camera. Lunar Planet. Sci. 38. Abstract 2068 [CD-ROM].
Martel, S., Langley, J., 2006. Propagation of normal faults to the surface in basalt, Koae fault system, Hawaii. J. Struct. Geol. 28, 2123–2143.
Martin, L., James, P., Dollfus, A., Iwasaki, K., Beish, J., 1992. Telescopic observations: Visual, photographic, polarimetric. In: Kieffer, H., Jakosky, B.M., Snyder, C.W., Matthews, M.S. (Eds.), Mars. Univ. of Arizona Press, Tucson, pp. 34–70.
Milkovich, S., Head, J., 2005. North polar cap of Mars: Polar layered deposit characterization and identification of a fundamental climate signal. J. Geophys. Res. 110, doi:10.1029/2004JE002349.
Milkovich, S., Head, J., 2006. Surface textures of Mars' north polar layered deposits: A framework for interpretation and future exploration. Mars 2, 21–45.
Montmessin, F., Haberle, R.M., Forget, F., Langevin, Y., Clancy, R.T., Bibring, J.-P., 2007. On the origin of perennial water ice at the south pole of Mars:

A precession-controlled mechanism? J. Geophys. Res. 112, doi:10.1029/2007JE002902. E08S17.
Mouginis-Mark, P., 1979. Martian fluidized crater morphology: Variations with crater size, latitude, altitude, and target material. J. Geophys. Res. 84, 8011–8022.
Mullins, K., Hayward, R., Tanaka, K., 2006. Dune forms and ages and associated oblate depressions in the Chasma Boreale region of Planum Boreum, Mars. Lunar Planet. Sci. 37. Abstract 1998 [CD-ROM].
Murray, B., Soderblom, L., Cutts, J., Sharp, R., Milton, D., Leighton, R., 1972. Geological framework of the south polar region of Mars. Icarus 17, 328–345.
Murray, B., Koutnik, M., Byrne, S., Soderblom, L., Herkenhoff, K., Tanaka, K., 2001. Preliminary geological assessment of the northern edge of Ultimi Lobe, Mars south polar layered deposits. Icarus 154, 80–97.
Mustard, J., Cooper, C., Rifkin, M., 2001. Evidence for recent climate change on Mars from the identification of youthful near-surface ground ice. Nature 412, 411–414.
Neuendorf, K., Mehl, J., Jackson, J., 2005. Glossary of Geology, fifth ed. Am. Geol. Inst., Alexandria, VA, 779 pp.
Nunes, D., Byrne, S., Hurwitz, D., 2006. Lineaments in northern martian polar layered deposits: Recent faulting? Eos (Fall Suppl.) 87 (52). Abstract P31B-0143.
Nunes, D., Byrne, S., Okubo, C., 2007. Recent deformation in the residual northern polar cap of Mars: A breaking story. Lunar Planet. Sci. 38. Abstract [CD-ROM].
Okubo, C., Martel, S., 1998. Pit crater formation on Kilauea volcano, Hawaii. J. Volcan. Geotherm. Res. 86, 1–18.
Okubo, C., Schultz, R., 2006. Near-tip stress rotation and the development of deformation band stepover geometries in mode II. Geol. Soc. Am. Bull. 118, 343–348.
Pais, D., Murray, B., Pathare, A., Byrne, S., Chomko, R., 2006. The peculiar stratigraphy of offset troughs within the martian north polar layered deposits—Evidence for deformation? Lunar Planet. Sci. 37. Abstract 1042 [CD-ROM].
Parker, T.J., Saunders, R.S., Schneeberger, D.M., 1989. Transitional morphology in west Deuteronilus Mensae, Mars: Implications for modification of the lowland/upland boundary. Icarus 82, 111–145.
Parker, T., Gorsline, D., Saunders, R., Pieri, D., Schneeberger, D., 1993. Coastal geomorphology of the martian northern plains. J. Geophys. Res. 98, 11061–11078.
Pathare, A., Paige, D., 2005. The effects of martian orbital variations upon the sublimation and relaxation of north polar troughs and scarps. Icarus 174, 419–443.
Roach, L., Mustard, J., Murchie, S., Langevin, Y., Bibring, J., Bishop, J., Bridges, N., Brown, A., Byrne, S., Ehlmann, B., Herkenhoff, K., McGuire, P., Milliken, R., Pelkey, S., Poulet, F., Seelos, F., Seelos, K., CRISM team, 2007. CRISM spectral signatures of the north polar gypsum dunes. Lunar Planet. Sci. 38. Abstract 1970 [CD-ROM].
Rodriguez, J., Tanaka, K., 2007. Complexity in the stratigraphic, erosional, and climatic record of the north polar plateau of Mars. Lunar Planet. Sci. 38. Abstract 1808 [CD-ROM].
Rodriguez, J.A.P., Sasaki, S., Miyamoto, H., 2003. Nature and hydrological evidence of the Shalbatana complex underground cavernous system. Geophys. Res. Lett. 30, 1304.
Rodriguez, J.A.P., Tanaka, K.L., Miyamoto, H., Sasaki, S., 2006a. Nature and characteristics of the flows that carved the Simud and Tiu outflow channels, Mars. Geophys. Res. Lett. 33, doi:10.1029/2005GL024320. L08S04.
Rodriguez, J., Tanaka, K., Sasaki, S., 2006b. Sources, sinks and migration patterns of dark veneers in the northern polar deposits of Mars. Lunar Planet. Sci. 37. Abstract 1437 [CD-ROM].
Rodriguez, J., Tanaka, K., Kargel, J., Dohm, J., Kuzmin, R., Fairén, A., Sasaki, S., Komatsu, G., Schulze-Makuch, D., Jianguo, Y., 2007a. Formation and disruption of aquifers in southwestern Chryse Planitia, Mars. Icarus 191, 545–567.
Rodriguez, J.A.P., Tanaka, K.L., Langevin, Y., Bourke, M., Kargel, J., Christensen, P., Sasaki, S., 2007b. Recent aeolian erosion and deposition in the north polar plateau of Mars. Mars 3, 29–41.
Schiaparelli, G., 1879. Osservazioni astronomiche e fisiche sull'asse di rotazione e sulla topografia del pianeta Marte. In: Atti della R. Accademia del Lincei, Memoria della cl. di scienze fisiche. Memoria 2, ser. 3, vol. 10, 1880–1881, pp. 281–387.
Schultz, R., Siddharthan, R., 2005. A general framework for the occurrence and faulting of deformation bands in porous granular rocks. Tectonophysics 411, 1–18.
Schultz, R., Moore, J., Grosfils, E., Tanaka, K., Mége, D., 2007. The Canyonlands model for planetary grabens: Revised physical basis and implications. In: Chapman, M. (Ed.), The Geology of Mars: Evidence from Earth-Based Analogs, pp. 371–399.
Scott, D., Tanaka, K., Greeley, R., Guest, J., 1986–1987. Geologic maps of the western and eastern equatorial and polar regions of Mars. US Geol. Surv. Misc. Invest. Ser. Map I-1802-A, B, C.
Seelos, F., Murchie, S., Pelkey, S., Seelos, K., CRISM Team, 2007. CRISM multispectral survey campaign—Status and initial mosaics. Lunar Planet. Sci. 38. Abstract 2336 [CD-ROM].
Selby, M., Rains, B., Palmer, R., 1974. Eolian deposits of the ice-free Victoria Valley, southern Victoria Land, Antarctica. New Zealand J. Geol. Geophys. 17 (3), 543–562.
Skinner, J., Tanaka, K., Herkenhoff, K., 2006. Inferences of the regional geologic history of Planum Boreum, Mars, based on observations of the uppermost polar layered deposits. In: 4th Mars Polar Sci. Conf. Abstract 8083 [CD-ROM].
Skinner, J.A., Tanaka, K.L., 2003. How should planetary map units be defined? Lunar Planet. Sci. 34. Abstract 2100 [CD-ROM].
Skinner Jr., J.A., Tanaka, K.L., 2007. Evidence for and implications of sedimentary diapirism and mud volcanism in the southern Utopia highland-lowland boundary plain, Mars. Icarus 186, 41–59.
Skinner Jr., J.A., Skinner, L.A., Kargel, J.S., 2007. Re-assessment of hydrovolcanism-based resurfacing within the Galaxias Fossae region of Mars. Lunar Planet. Sci. 38. Abstract 1998 [CD-ROM].
Smith, D., and 23 colleagues, 2001. Mars Orbiter Laser Altimeter: Experiment summary after the first year of global mapping of Mars. J. Geophys. Res. 106, 23689–23722.
Soderblom, L., 1992. The composition and mineralogy of the martian surface from spectroscopic observations: 0.3 μm to 50 μm. In: Kieffer, H., Jakosky, B.M., Snyder, C.W., Matthews, M.S. (Eds.), Mars. Univ. of Arizona Press, Tucson, pp. 557–593.
Tanaka, K., 1986. The stratigraphy of Mars. In: Proc. 17th Lunar Planet. Sci. Conf., Part 1. J. Geophys. Res. 91 (Suppl.) E139–E158.
Tanaka, K., 2005. Geology and insolation-driven climatic history of Amazonian north polar materials on Mars. Nature 437, 991–994.
Tanaka, K., 2006. Mars' north polar gypsum: Possible origin related to Early Amazonian magmatism at Alba Patera and aeolian mining. In: 4th Mars Polar Sci. Conf. Abstract 8024 [CD-ROM].
Tanaka, K., 2007. North polar layered deposits on Mars as revealed by HiRISE images. Lunar Planet. Sci. Abstract 1866 [CD-ROM].
Tanaka, K., Kolb, E., 2001. Geologic history of the polar regions of Mars based on Mars Global Surveyor data. I. Noachian and Hesperian Periods. Icarus 154, 22–39.
Tanaka, K., Scott, D., 1987. Geologic map of the polar regions of Mars. US Geol. Surv. Misc. Invest. Ser. Map I-1802-C.
Tanaka, K.L., Banerdt, W.B., Kargel, J.S., Hoffman, N., 2001. Huge, CO_2-charged debris-flow deposit and tectonic sagging in the northern plains of Mars. Geology 29, 427–430.
Tanaka, K., Skinner, J., Hare, T., Wenker, A., 2003. Resurfacing history of the northern plains of Mars based on geologic mapping of Mars Global Surveyor data. J. Geophys. Res. 108.
Tanaka, K., Skinner, J., Hare, T., 2005. Geologic map of the northern plains of Mars. US Geol. Surv. Sci. Invest. Ser. Map SIM-2888.
Thomas, P., Squyres, S., Herkenhoff, K., Howard, A., Murray, B., 1992. Polar deposits of Mars. In: Kieffer, H., Jakosky, B.M., Snyder, C.W., Matthews, M.S. (Eds.), Mars. Univ. of Arizona Press, Tucson, pp. 767–795.
Thomas, P., Malin, M., Edgett, K., Carr, M., Hartmann, W., Ingersoll, A., James, P., Soderblom, L., Veverka, J., Sullivan, R., 2000. North–south geological differences between the residual polar caps on Mars. Nature 404, 161–164.
Titus, T.N., Kieffer, H.H., Christensen, P.R., 2003. Exposed water ice discovered near the south pole of Mars. Science 299, 1048–1053.

Tsoar, H., Greeley, R., Peterfreund, A., 1979. Mars: The north polar sand sea and related wind patterns. J. Geophys. Res. 84 (B14), 8167–8180.

Ward, A., Doyle, K., Helm, P., Weisman, M., Witbeck, N., 1985. Global map of aeolian features of Mars. J. Geophys. Res. 90, 2038–2056.

Weijermars, R., 1986. The polar spirals of Mars may be due to glacier surges deflected by Coriolis forces. Earth Planet. Sci. Lett. 76, 227–240.

Wyatt, M., McSween, H., Tanaka, K., Head, J., 2004. Global geologic context for rock types and surface alteration on Mars. Geology 32, 645–648.